ACT Data Release 6
(2017-2022)
Thibaut Louis

- 3 dichroic detector arrays for DR6: PA4, PA5 and PA6
- 3750 working detectors (70% yield) at 100 mK
- 3 broad bands: f090 (77 – 112 GHz),
  f150 (124 – 172 GHz) and f220 (182 – 277 GHz)
- Combined sensitivity of 6.2 μK√s,
  and 1.4’ FWHM @ f150

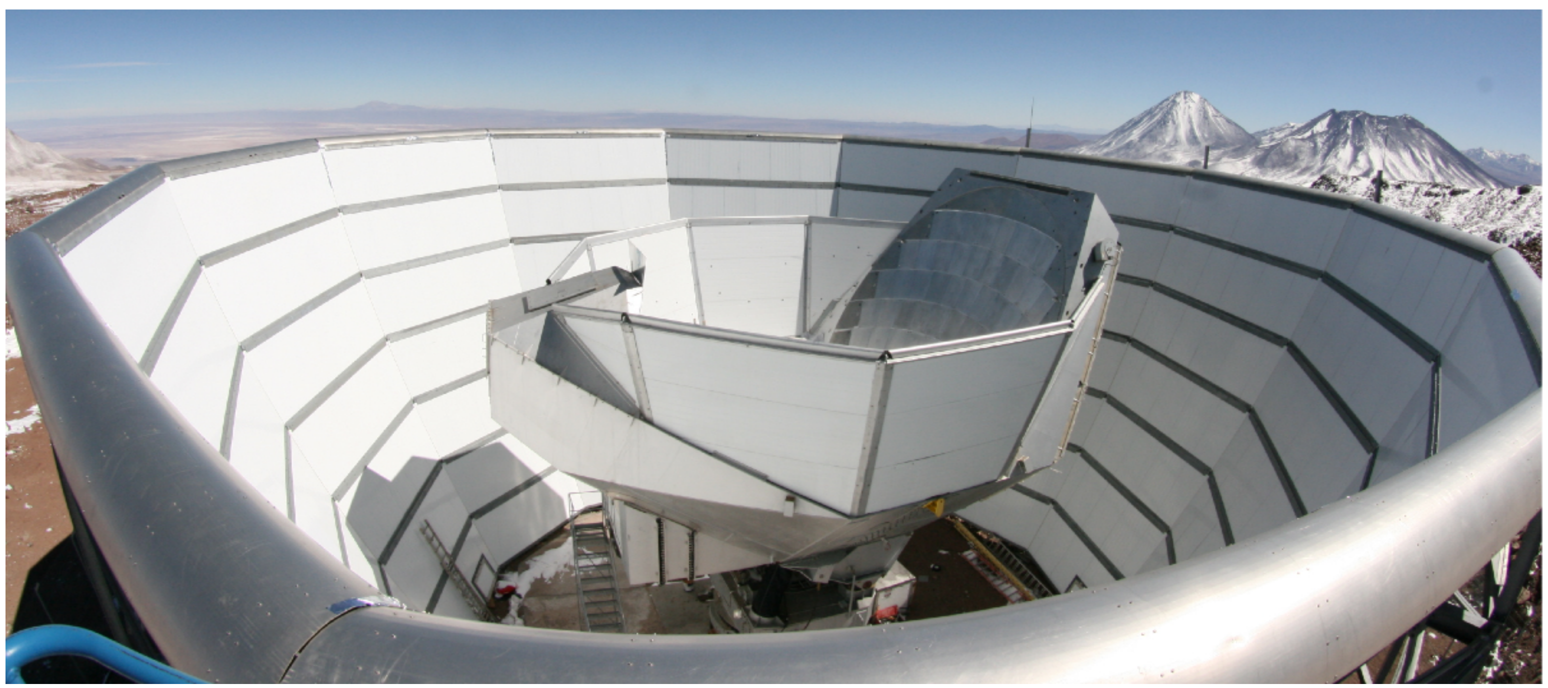

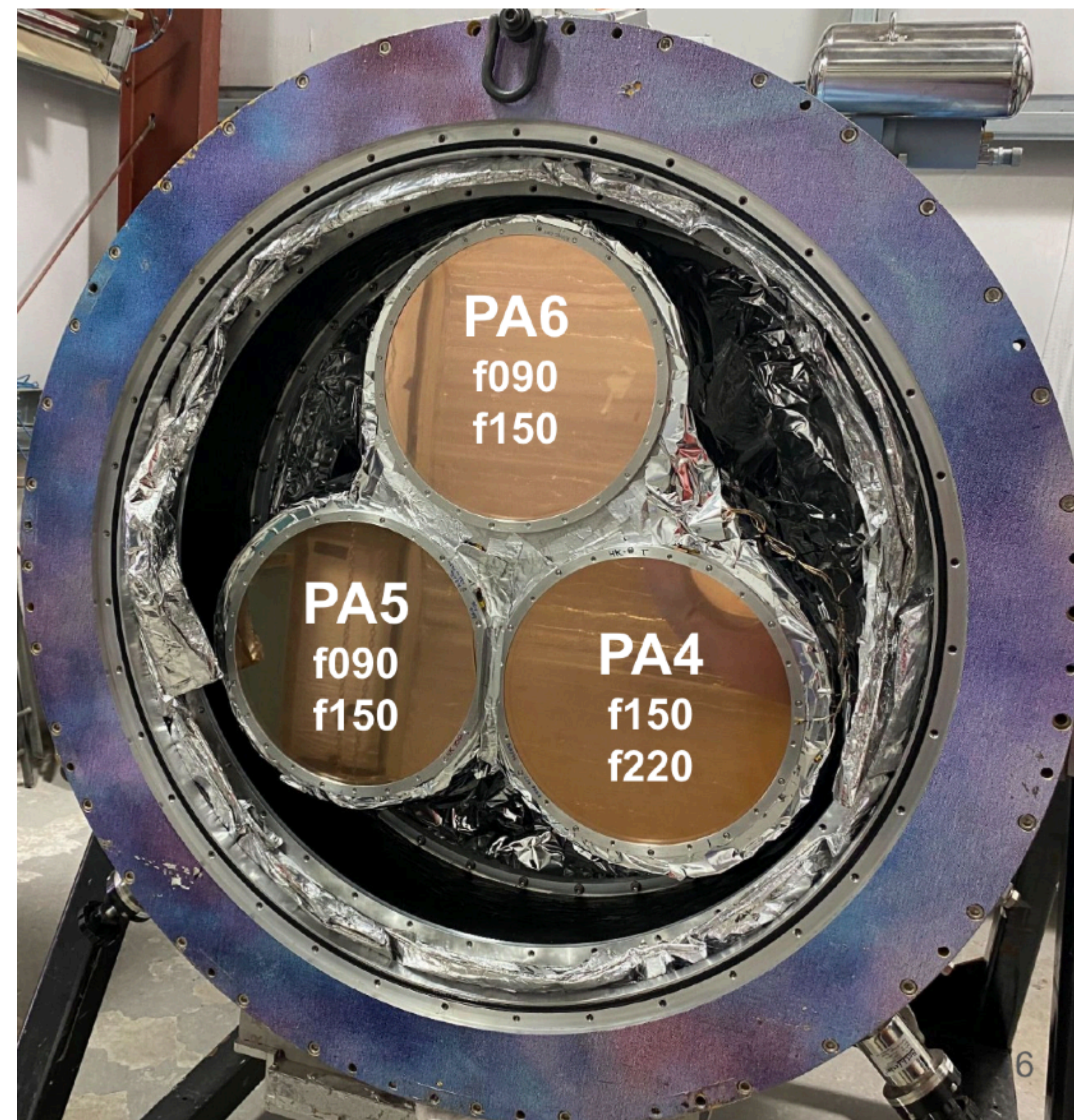

ACT survey: approx. 40% of the sky

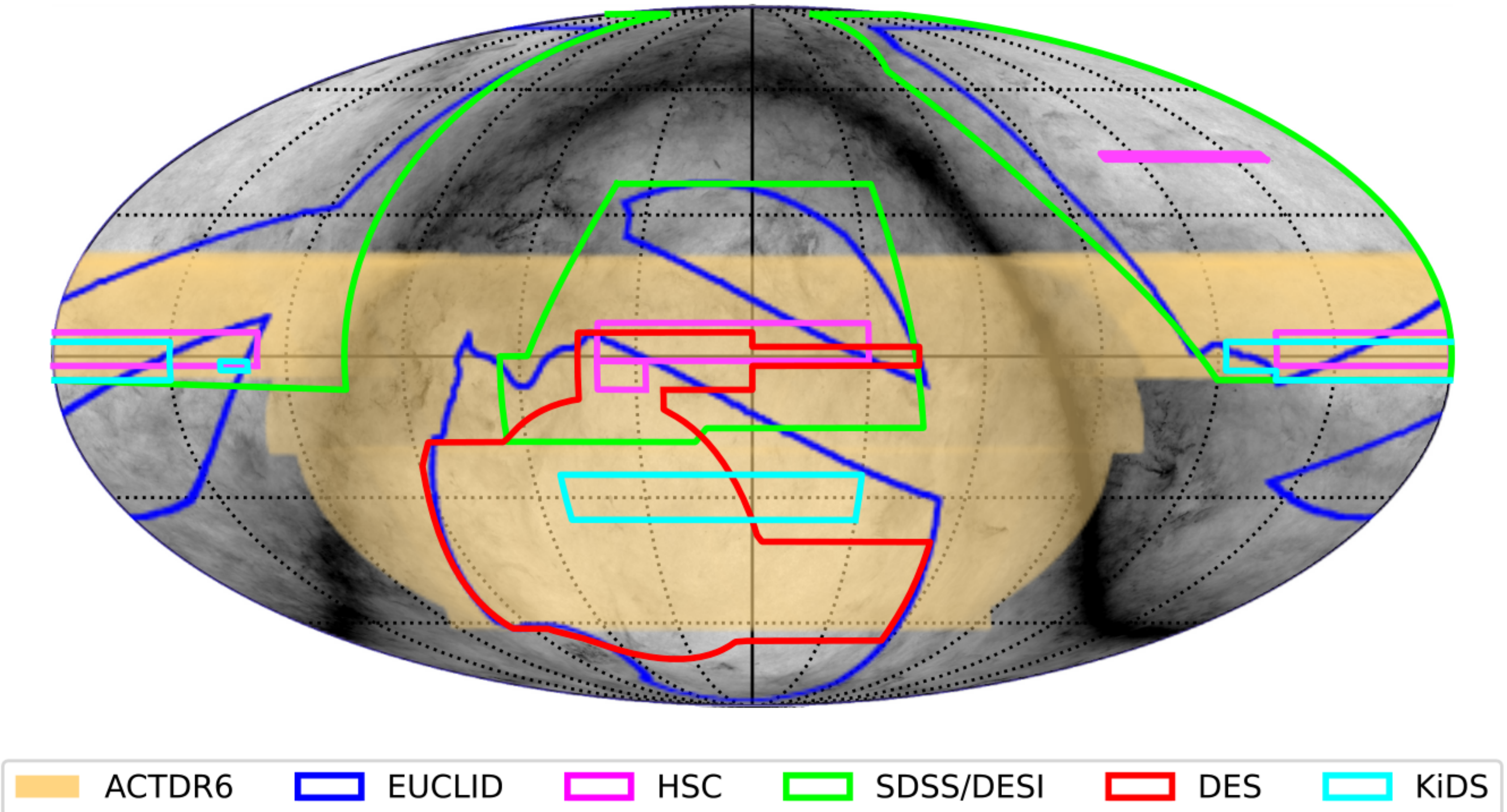

ACT DR6: Three main papers

Draft version January 24, 2025
Typeset using LaTeX **twocolumn** style in AASTeX63

The Atacama Cosmology Telescope: DR6 maps

Sigurd Naess,[1] Yilun Guan,[2] Adriaan J. Duivenvoorden,[3] Matthew Hasselfield,[4] Yuhan Wang,[5] and et al, ACT collaboration

[1] *Institute of Theoretical Astrophysics, University of Oslo, Norway*
[2] *Dunlap Institute for Astronomy and Astrophysics, University of Toronto, 50 St. George Street, Toronto, ON M5S 3H4, Canada*
[3] *Joseph Henry Laboratories of Physics, Jadwin Hall, Princeton University, Princeton, NJ, USA 08544*
[4] *Center for Computational Astrophysics, Flatiron Institute, New York, NY, USA 10010*
[5] *Department of Physics, Cornell University, Ithaca, NY 14853, USA*

The Atacama Cosmology Telescope: DR6 Power spectra, Likelihood and ΛCDM parameters

Thibaut Louis,[1] Adrien La Posta,[2] Zachary Atkins,[3] Hidde T. Jense,[4] and ACT Collaboration

[1] *Université Paris-Saclay, CNRS/IN2P3, IJCLab, 91405 Orsay, France*
[2] *Department of Physics, University of Oxford, Denys Wilkinson Building, Keble Road, Oxford OX1 3RH, United Kingdom*
[3] *Joseph Henry Laboratories of Physics, Jadwin Hall, Princeton University, Princeton, NJ, USA 08544*
[4] *School of Physics and Astronomy, Cardiff University, The Parade, Cardiff, Wales, UK CF24 3AA*

The Atacama Cosmology Telescope: DR6 Constraints on Extended Cosmological Models

Erminia Calabrese,[1] J. Colin Hill,[2] Hidde T. Jense,[1] Adrien La Posta,[3] and ACT Collaboration

[1] *School of Physics and Astronomy, Cardiff University, The Parade, Cardiff, Wales, UK CF24 3AA*
[2] *Department of Physics, Columbia University, New York, NY 10027, USA*
[3] *Department of Physics, University of Oxford, Denys Wilkinson Building, Keble Road, Oxford OX1 3RH, United Kingdom*

Data and code release

Alongside the papers, we release all the data products needed to reproduce our analysis. *For the first time in CMB data analysis, we also provide the complete power spectrum and likelihood pipeline, enabling users to go from public products to cosmological parameters and to reproduce all the figures from the power spectrum paper*.

	Planck	ACT	SPT3G	BICEP/Keck
Likelihood	Yes	Yes	If/once paper is accepted	Yes
Maps	Yes	Yes	No	No
Analysis Codes	Partial release	Full Release	No	No

Data and code release

As we approach percent-level constraints on parameters, signs of tension (or hints of new physics) have emerged

H0 tension

$$H_0^{\rm SH0ES} = 73.17 \pm 0.86 \text{ km/s/Mpc (Breuval et al. 2024)}$$
$$H_0^{\rm Planck} = 67.36 \pm 0.54 \text{ km/s/Mpc (Planck 2018 results. VI)}$$

Planck anomalies

$$A_L = 1.180 \pm 0.065 \text{ (Planck 2018 results. VI)}$$
$$\Omega_k = -0.044 \pm 0.018 \text{ (Planck 2018 results. VI)}$$

DESI equation state of dark energy

$$\left.\begin{aligned} w_0 &= -0.752 \pm 0.057 \\ w_a &= -0.86^{+0.23}_{-0.20} \end{aligned}\right\} \quad \begin{array}{l}\text{DESI+CMB} \\ \text{+DESY5,}\end{array}$$

Planck Birefringence

$$\beta_{\rm biref}^{\rm Planck} = 0.342^{+0.094}_{-0.091} \qquad \text{(Minami \& Komatsu 2020)}$$

(Eskilt & Komatsu 2022)

Data and code release

Given this state of the art, within ACT, we have agreed that the only way to make progress as a community is to strive for maximum transparency and reproducibility

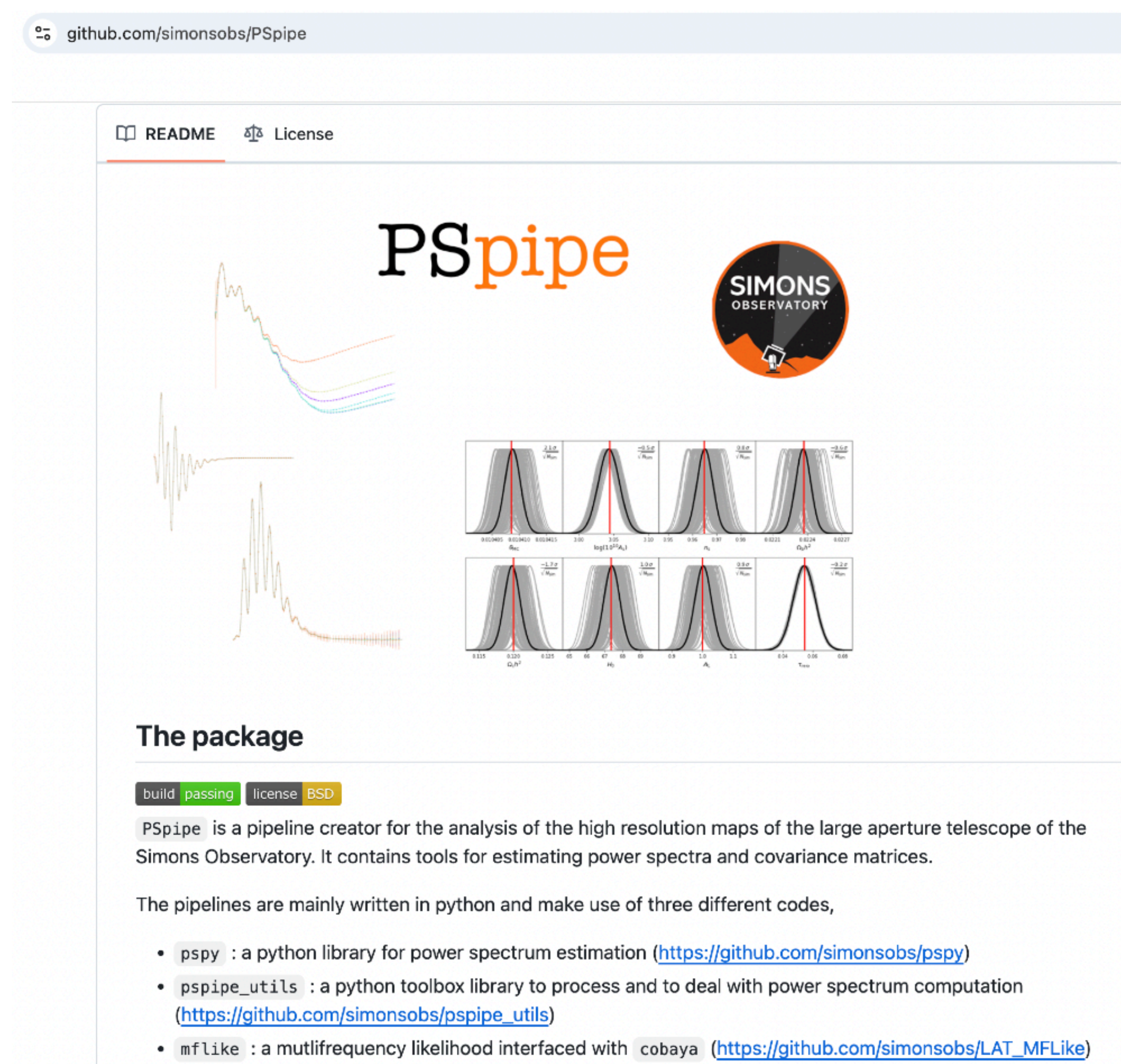
github.com/simonsobs/PSpipe

README License

PSpipe

SIMONS OBSERVATORY

The package

build passing license BSD

`PSpipe` is a pipeline creator for the analysis of the high resolution maps of the large aperture telescope of the Simons Observatory. It contains tools for estimating power spectra and covariance matrices.

The pipelines are mainly written in python and make use of three different codes,

- `pspy` : a python library for power spectrum estimation (https://github.com/simonsobs/pspy)
- `pspipe_utils` : a python toolbox library to process and to deal with power spectrum computation (https://github.com/simonsobs/pspipe_utils)
- `mflike` : a mutlifrequency likelihood interfaced with `cobaya` (https://github.com/simonsobs/LAT_MFLike)

MAPS

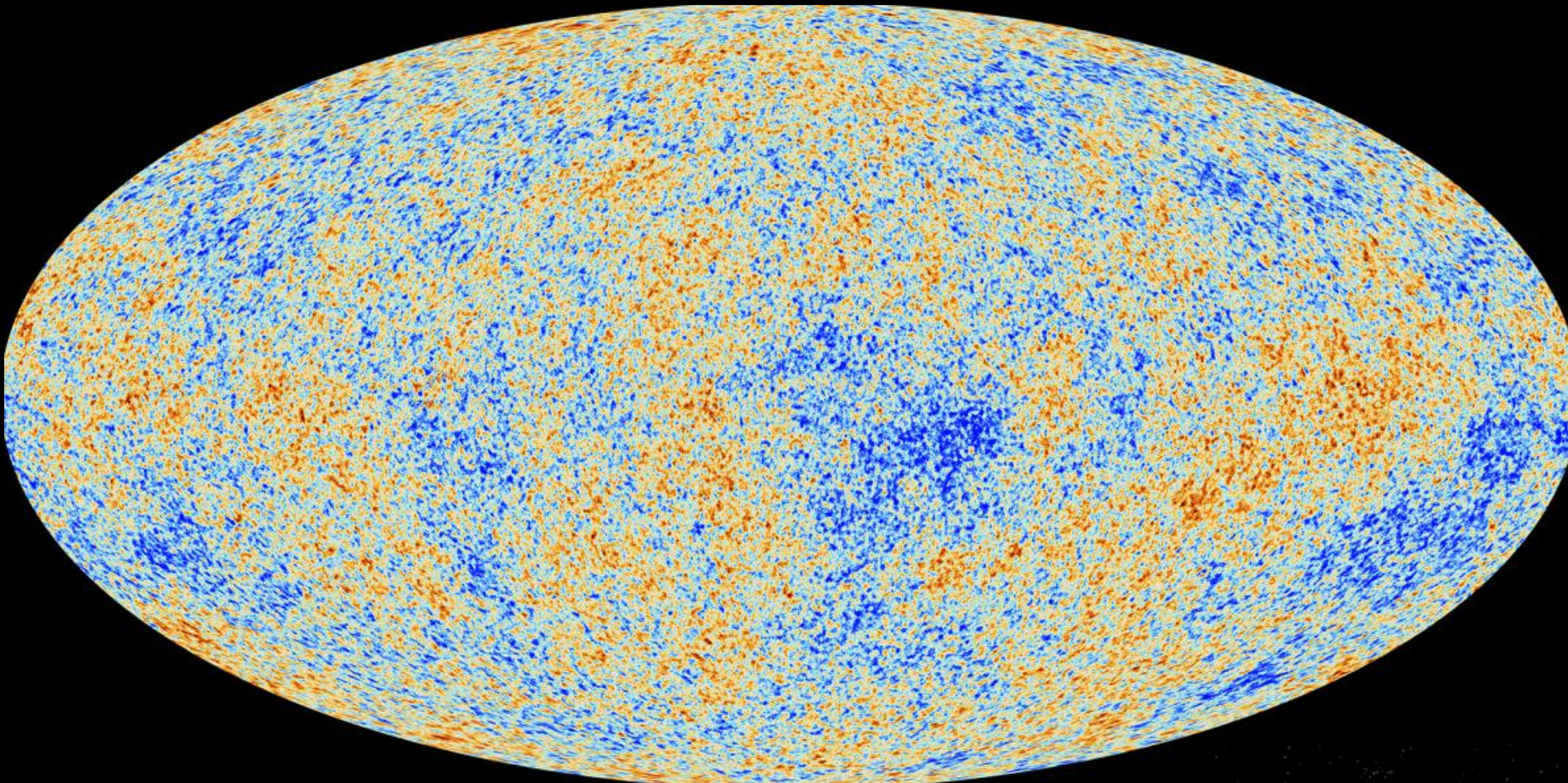

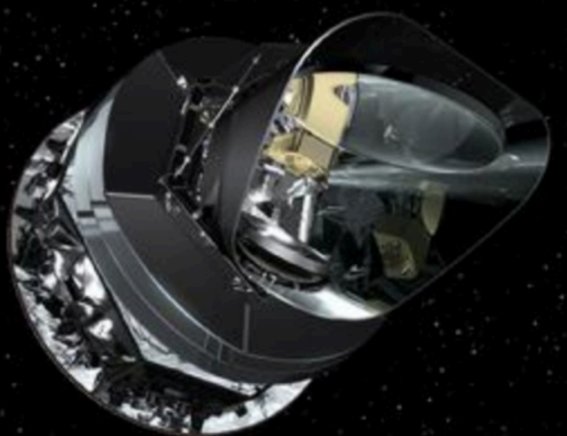

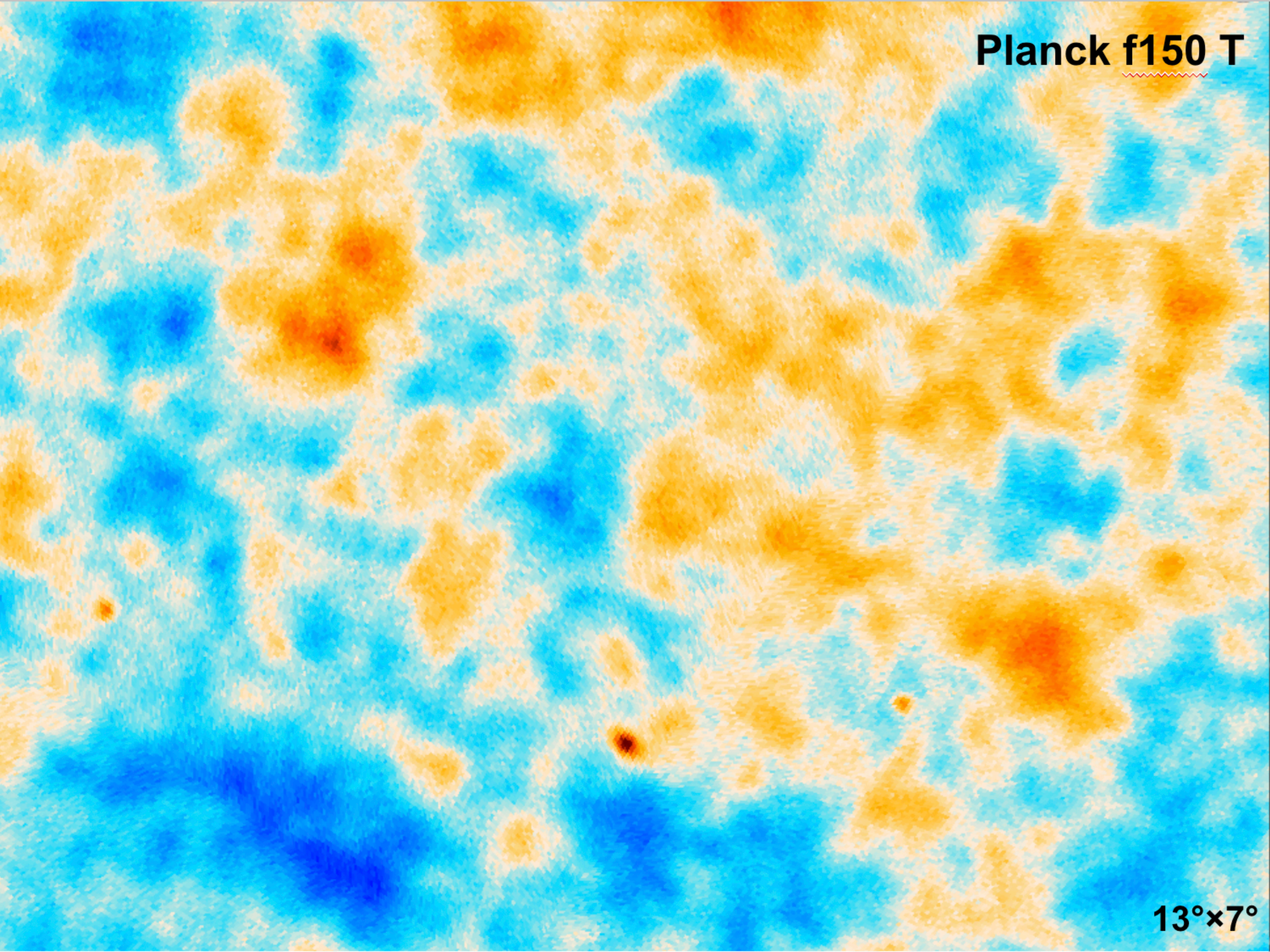
Planck f150 T
13°×7°

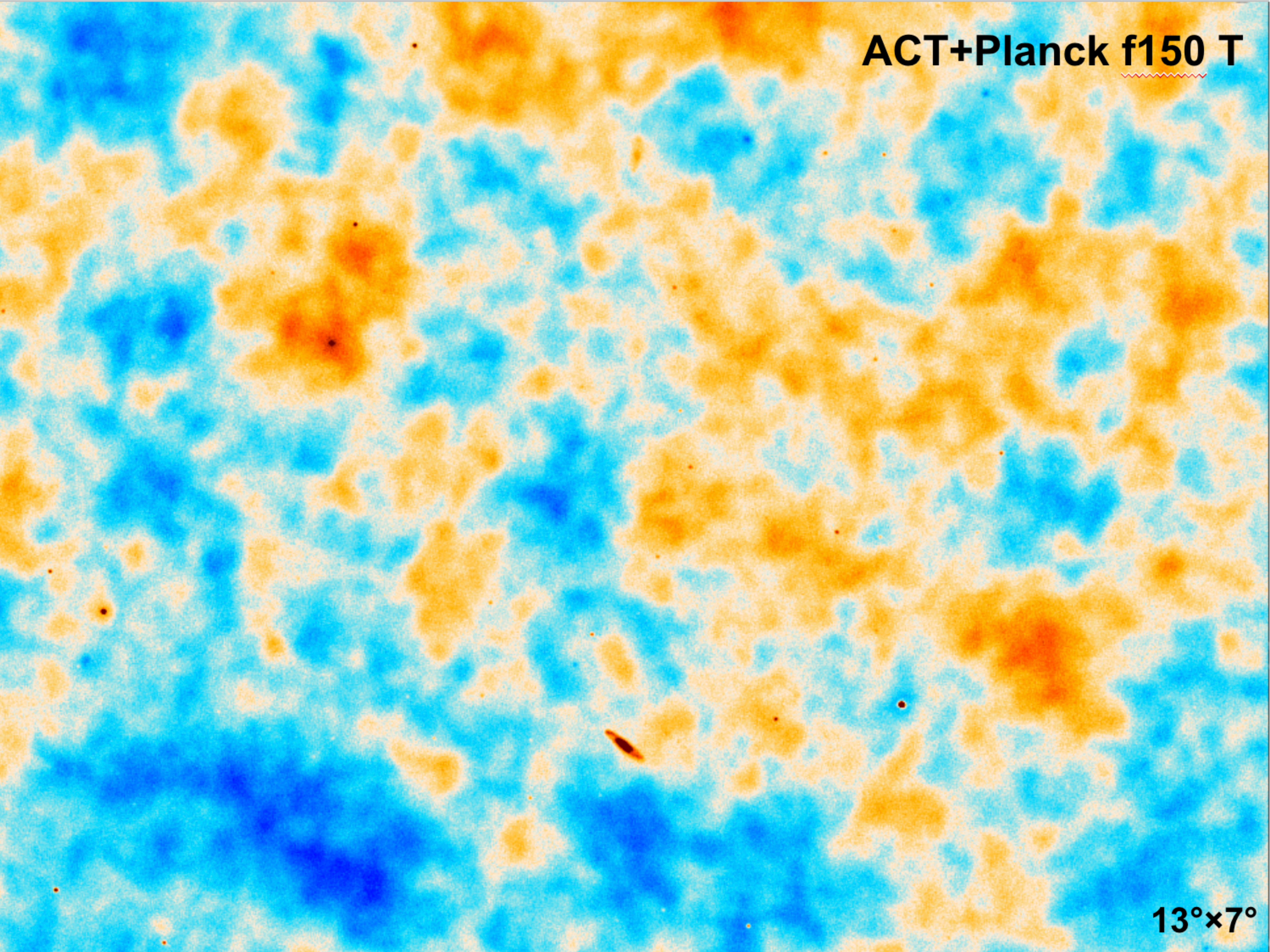
ACT+Planck f150 T
13°×7°

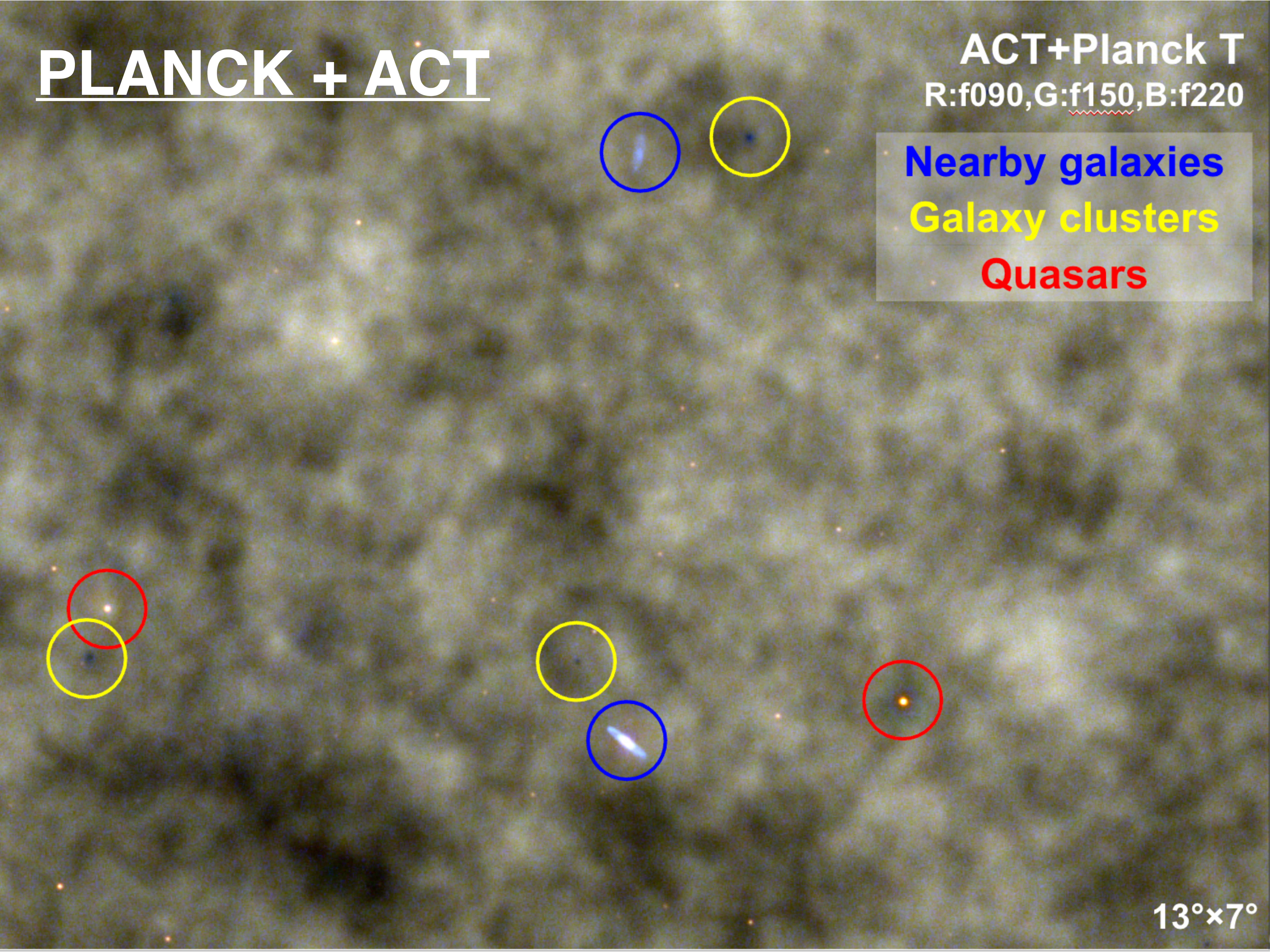
PLANCK + ACT
ACT+Planck T
R:f090,G:f150,B:f220
Nearby galaxies
Galaxy clusters
Quasars
13°×7°

PLANCK E modes

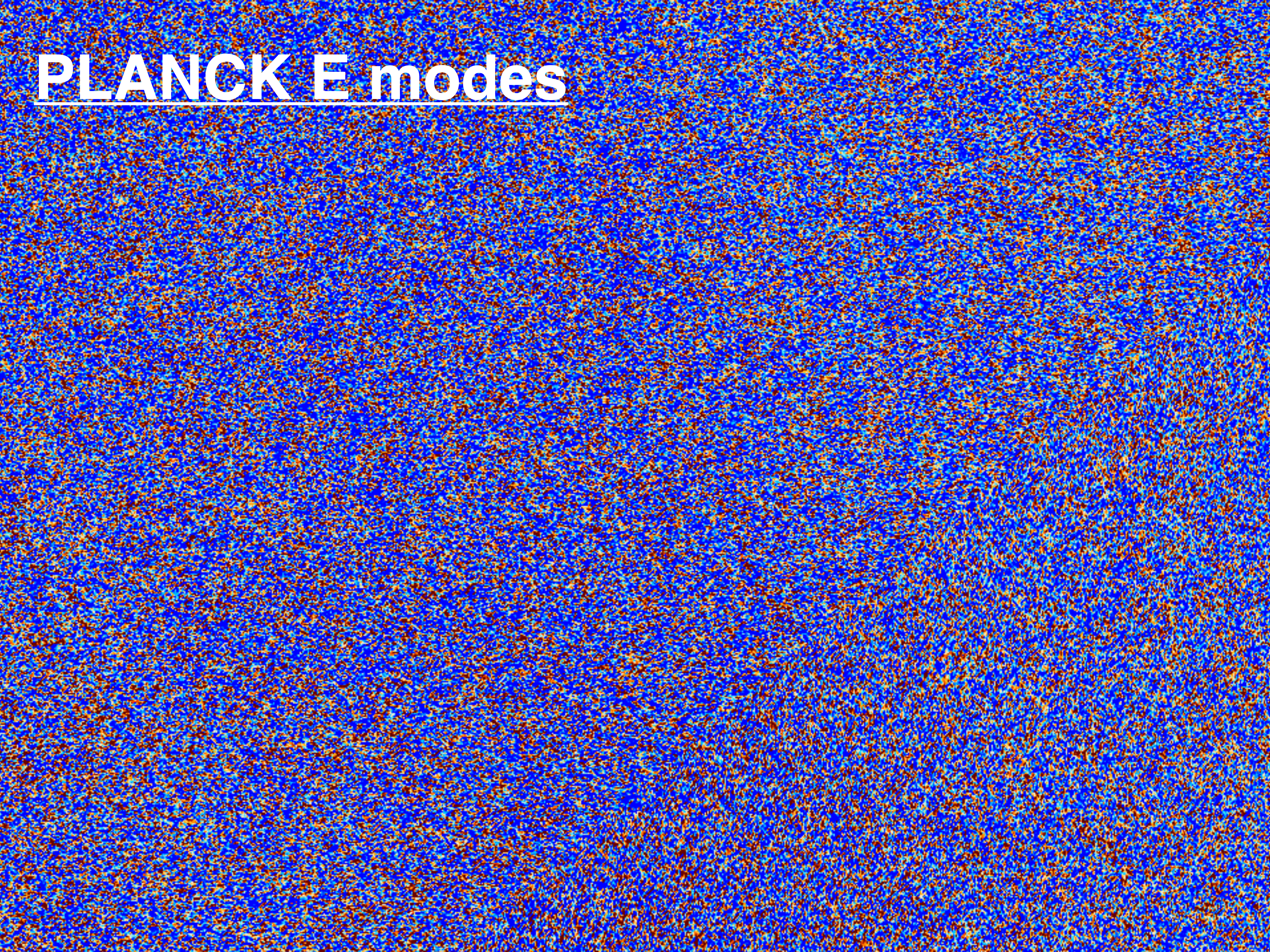

Planck + ACT E modes

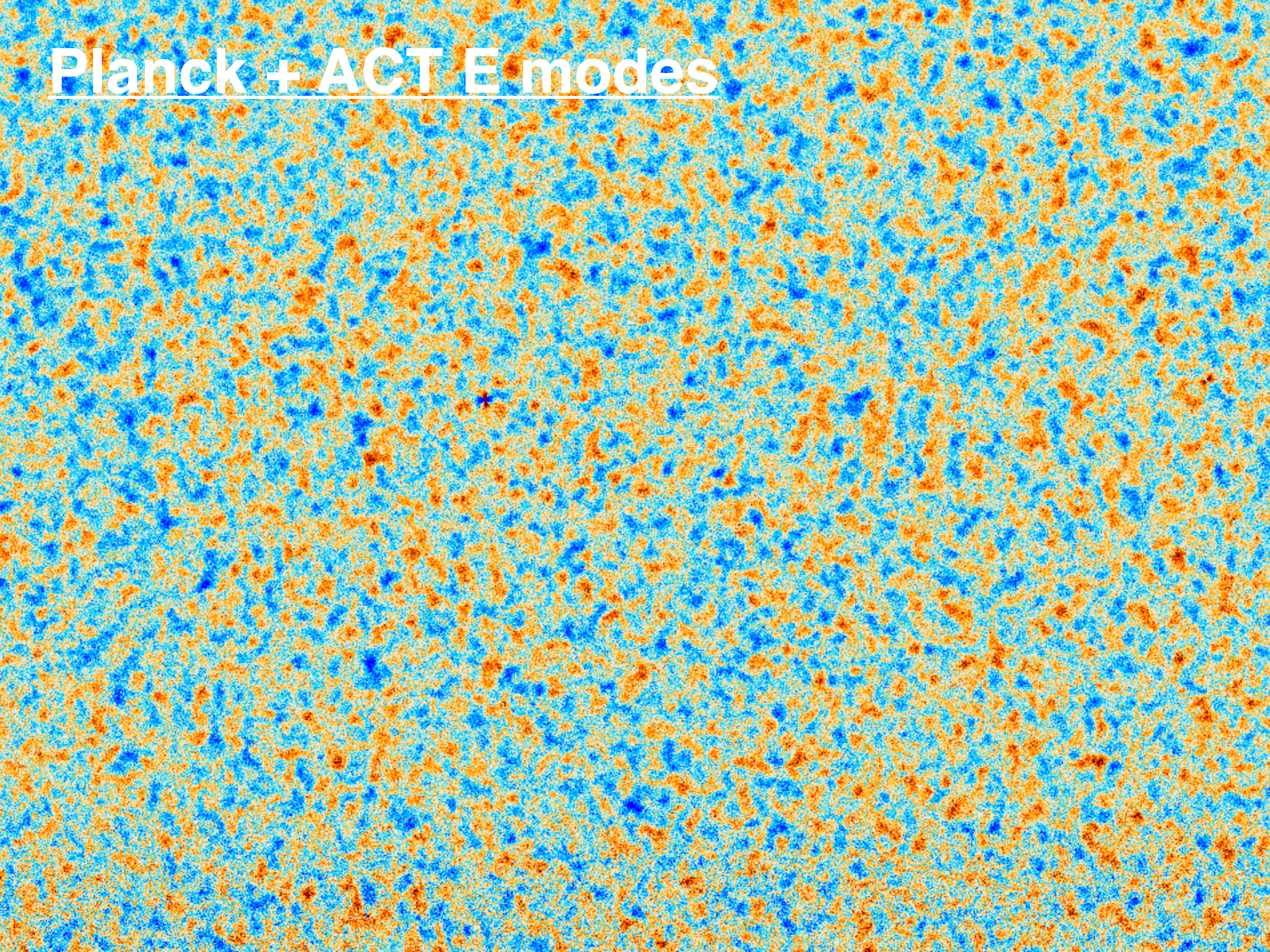

High S/N E-modes over the whole footprint

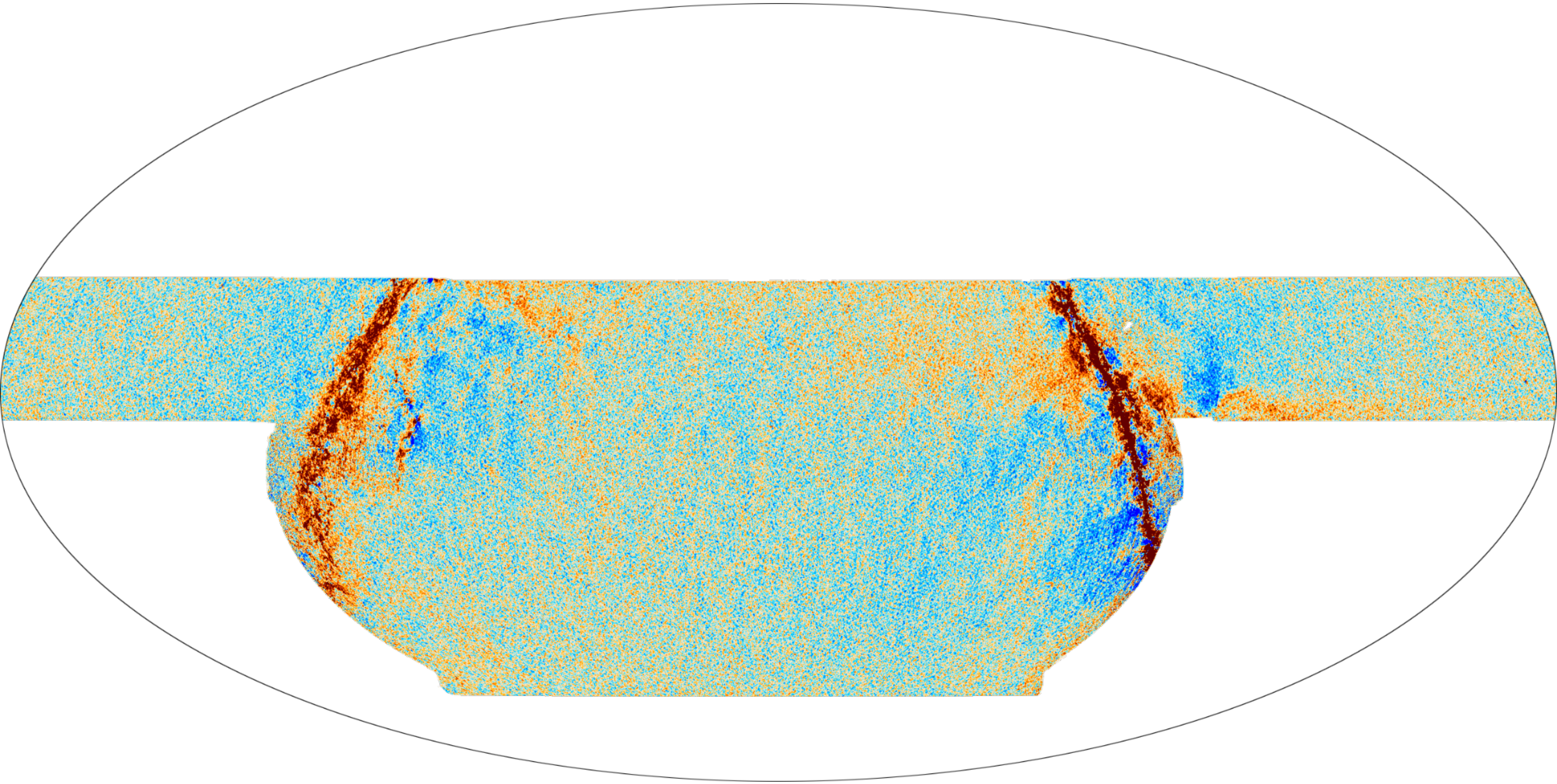

ACT+Planck E

Power spectra

Noise power spectra

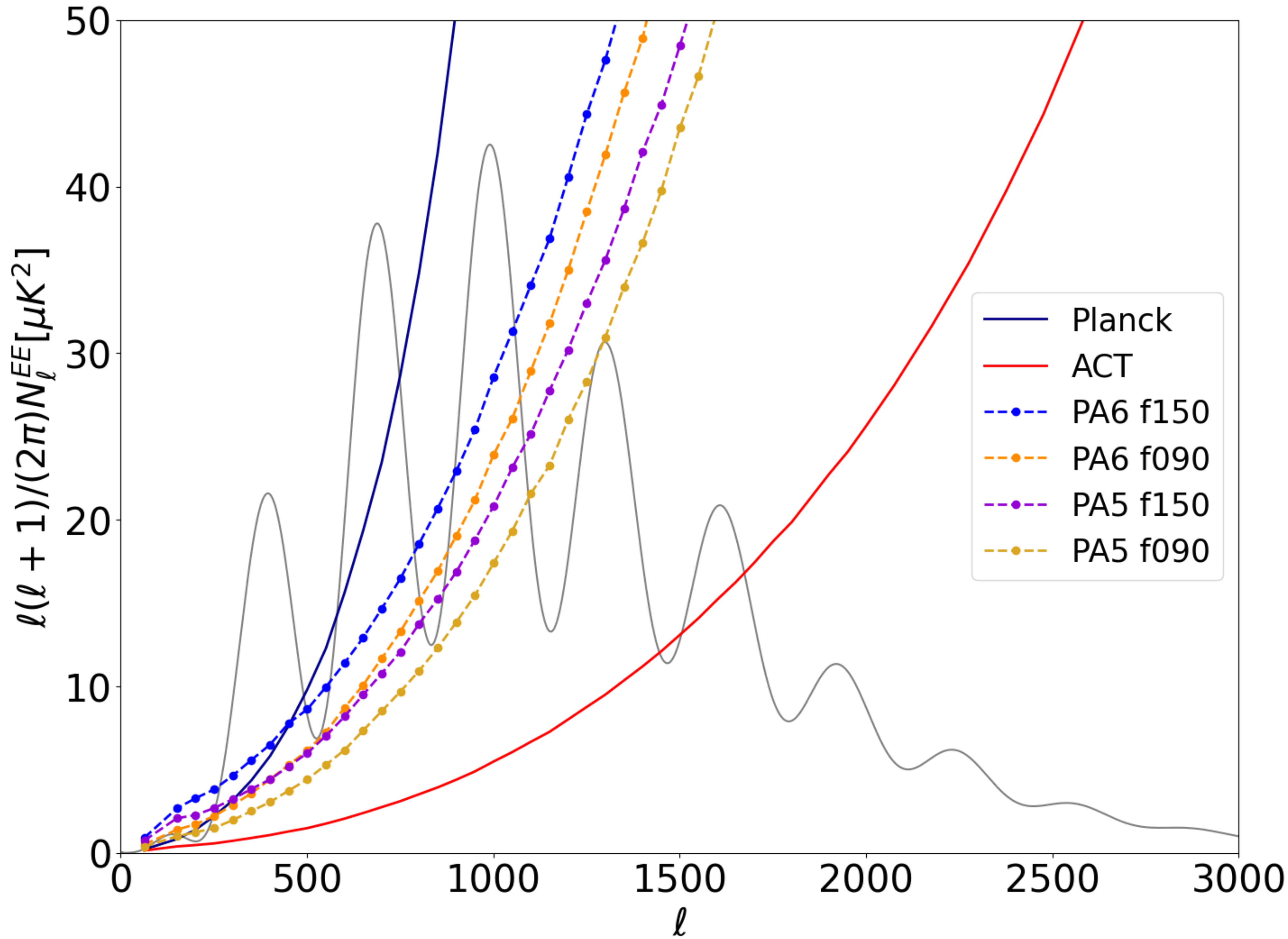

The ACT DR6 polarization data are signal-dominated up to a multipole ℓ=1500, corresponding to an angular scale of ~ 0.1 degrees. The different array-bands have comparable constraining power, providing useful redundancies.

Planck temperature power spectrum

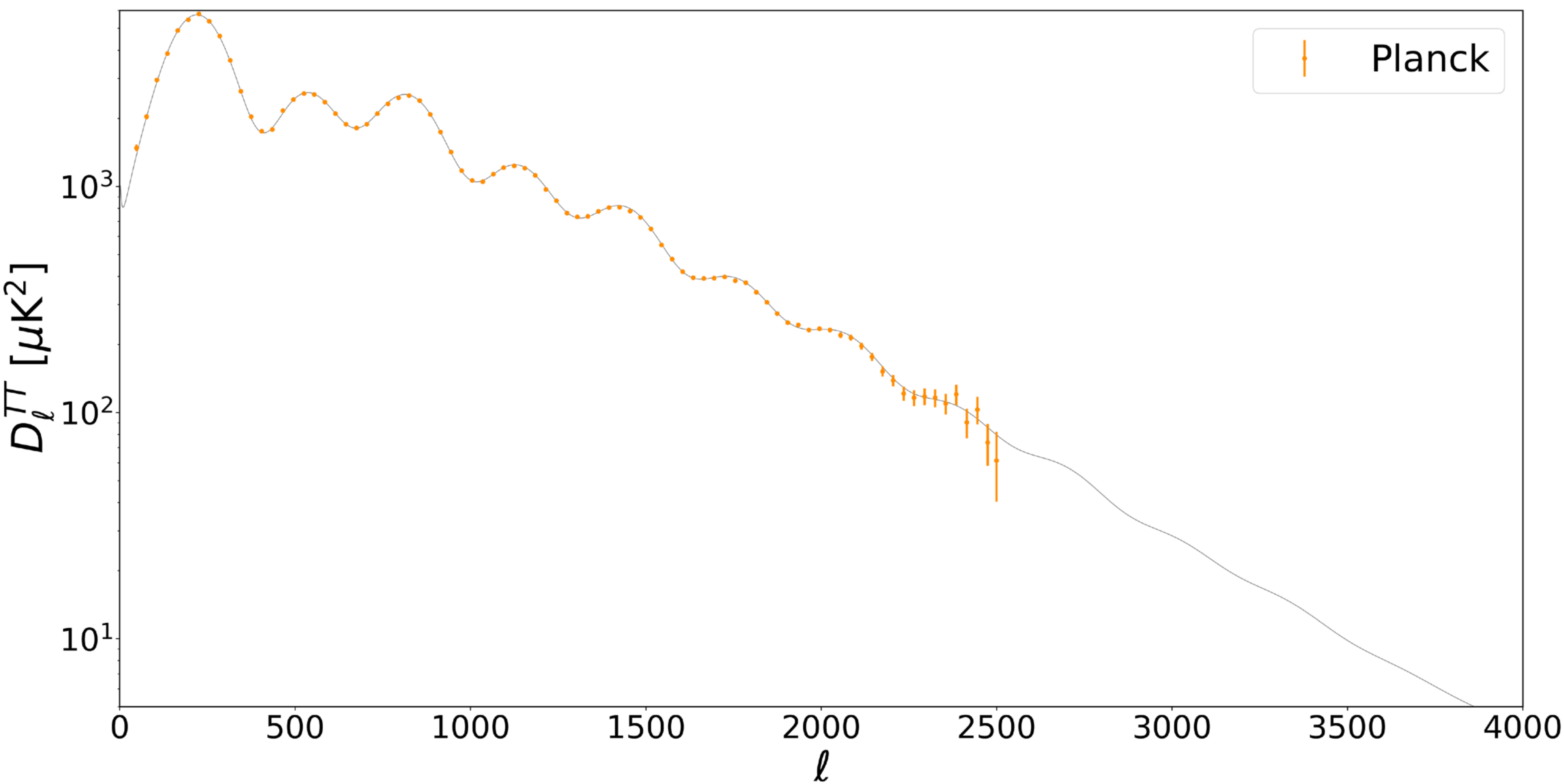

Planck + ACT temperature power spectra

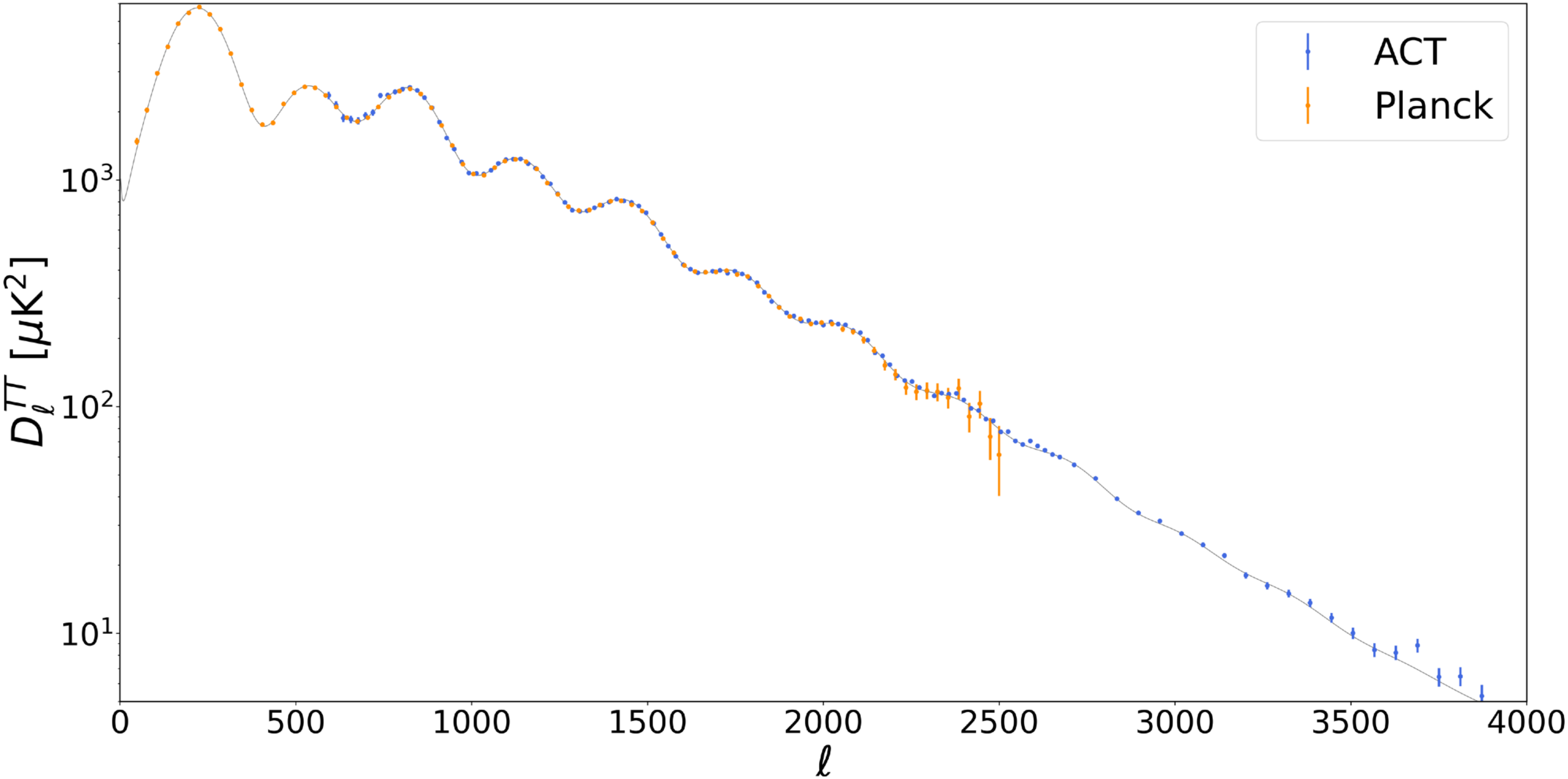

ACT data 1) extend Planck measurement to small angular scales.
2) are very consistent with Planck data on overlapping angular scales.
3) + Planck data are fitted by a common model

Planck E modes power spectra

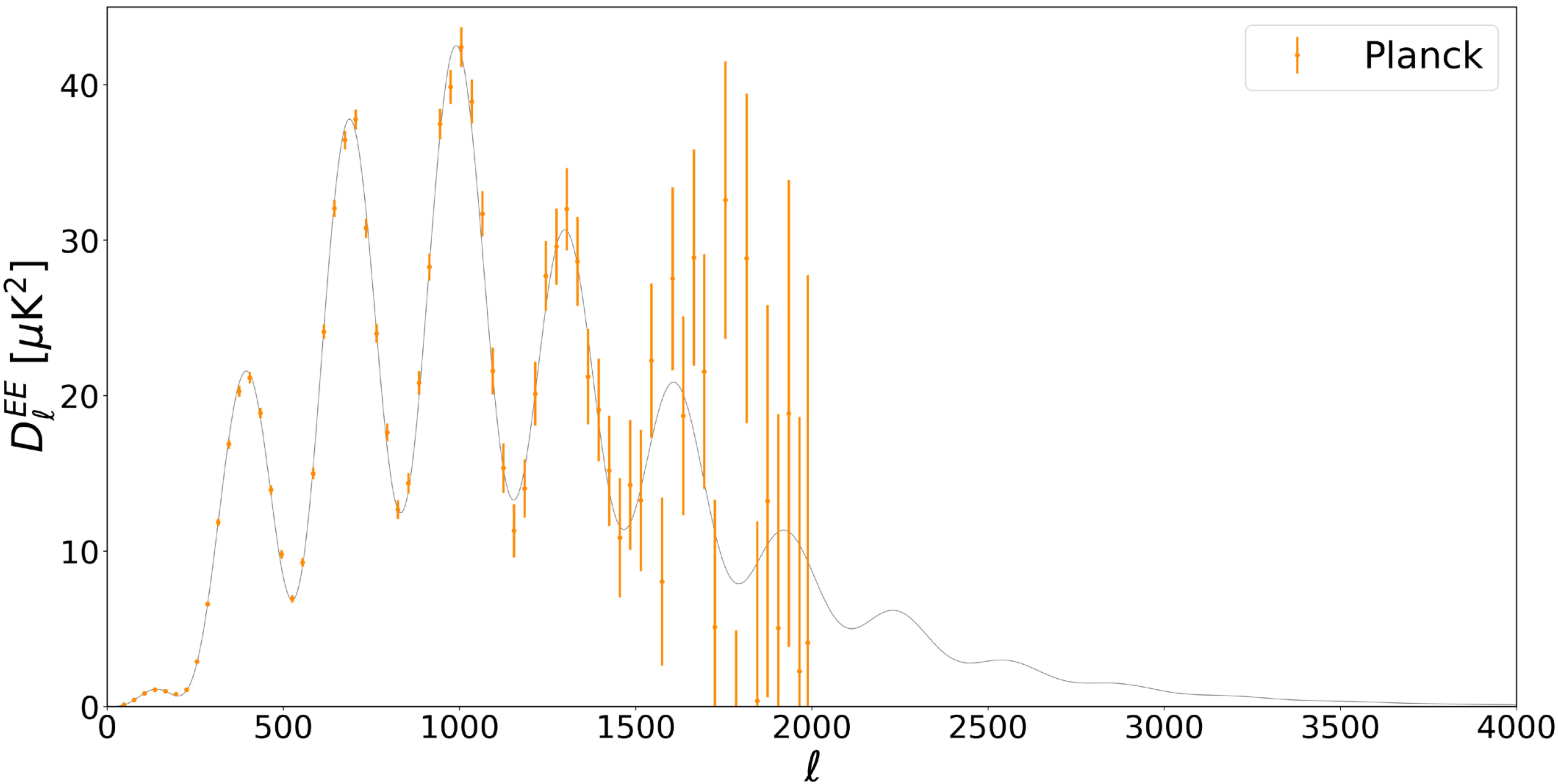

Planck + ACT E modes power spectra

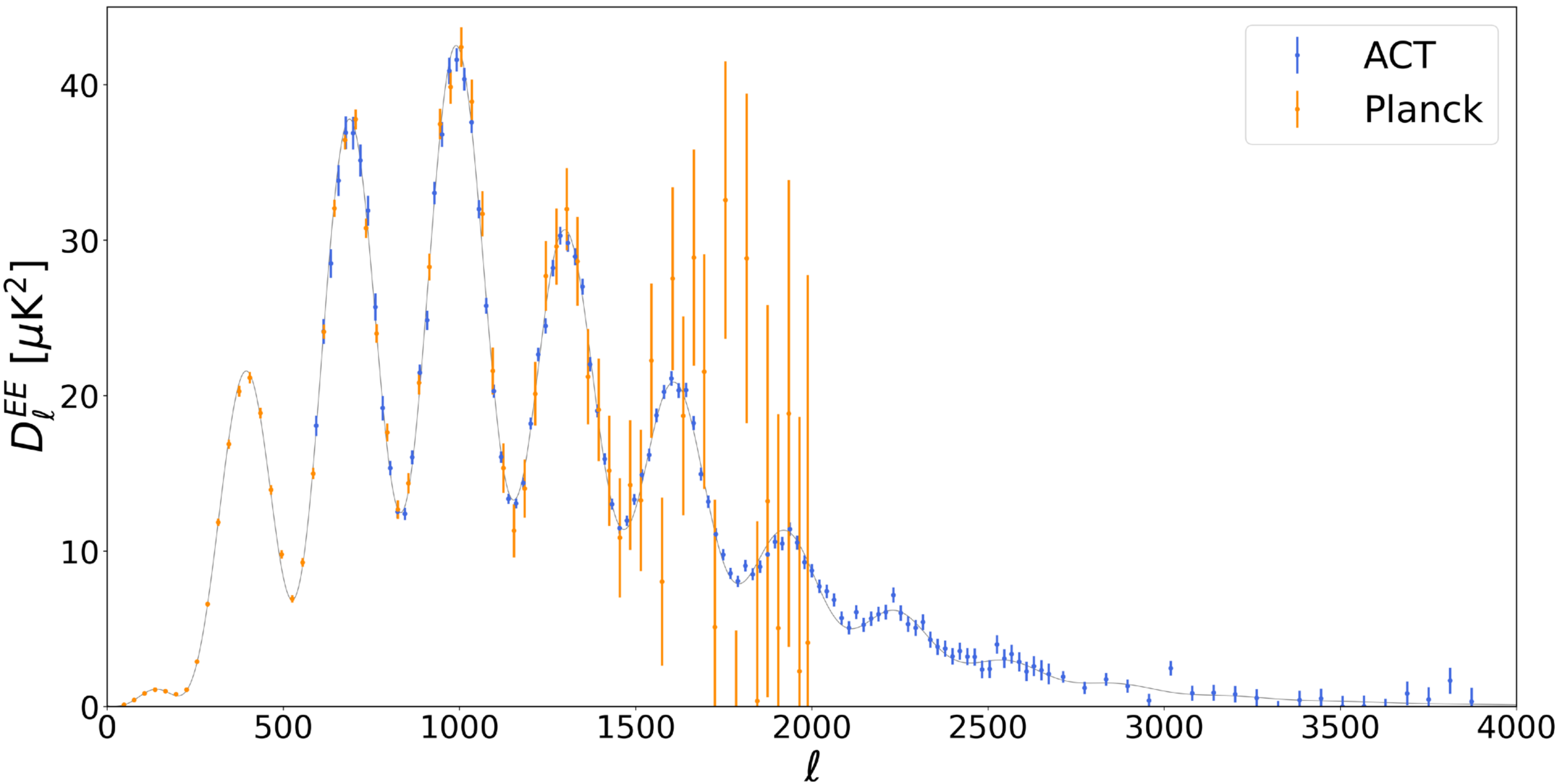

ACT DR6 EE is more sensitive than Planck for multipoles $\ell > 600$

Planck TE power spectrum

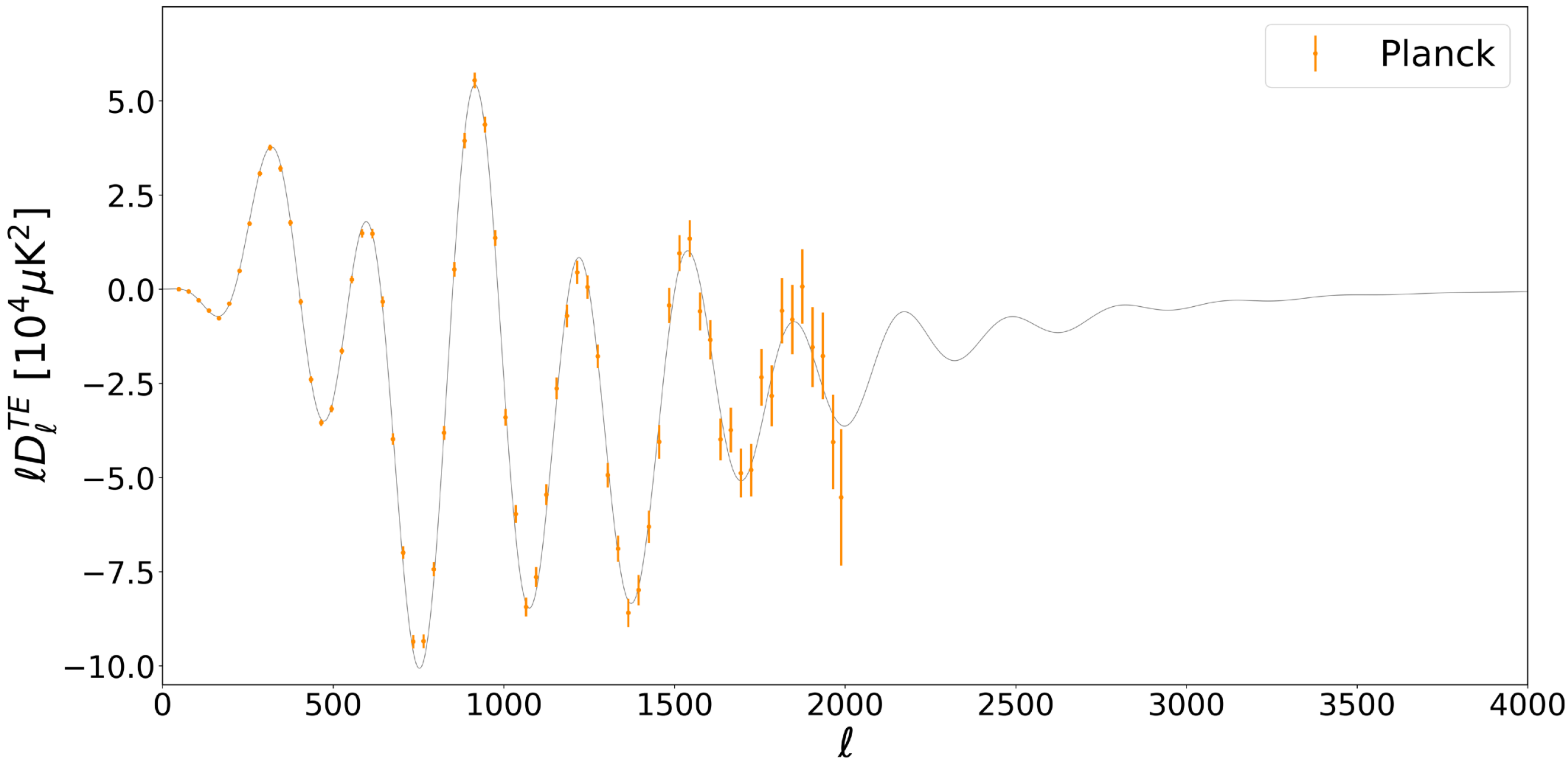

Planck + ACT TE power spectrum

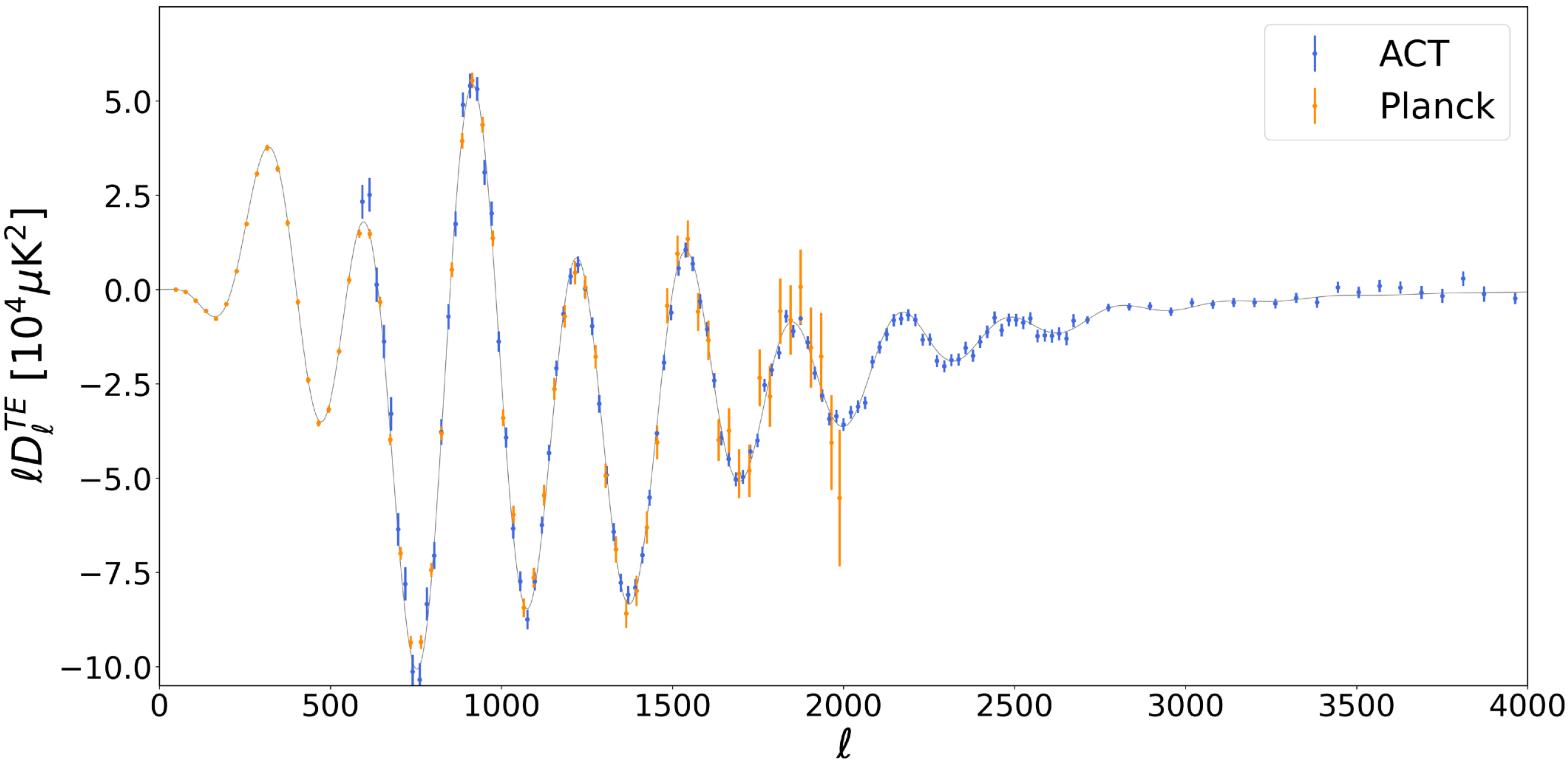

Very clean, foreground free cosmology,
1.1 % constraint on H0 from TE alone

LCDM

Excellent agreement with Planck (PR3) in LCDM

ACT and Planck are consistent at the 1.6 sigma level

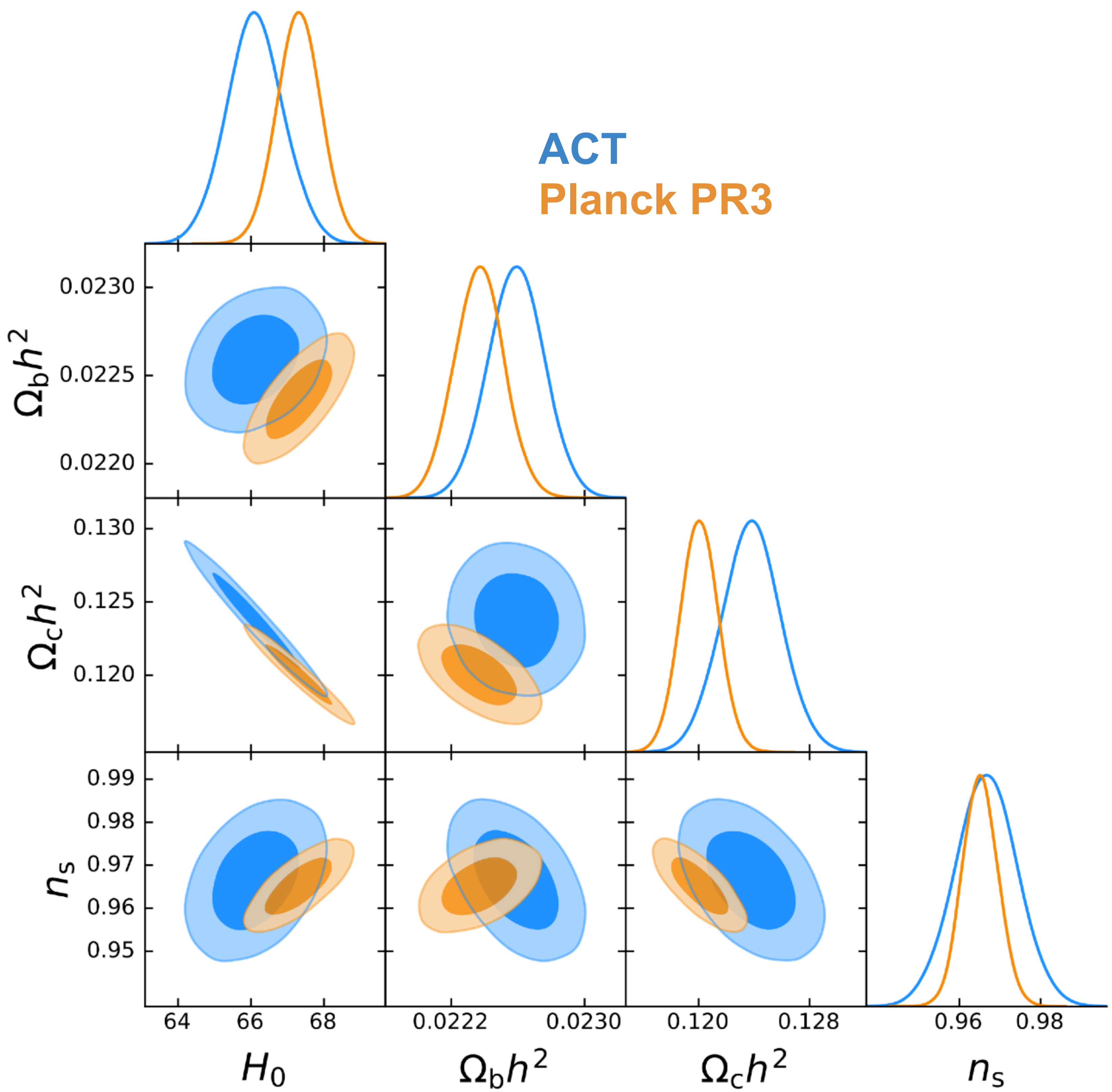

LCDM provides an excellent fit to both Planck and ACT DR6

$\chi^2(\text{ACT}) = 1598/1617$ (63%)

$\chi^2(\text{P-ACT}) = 1842/1897$ (81%)

This motivated the creation of a combined data set:

P-ACT = Planck + ACT

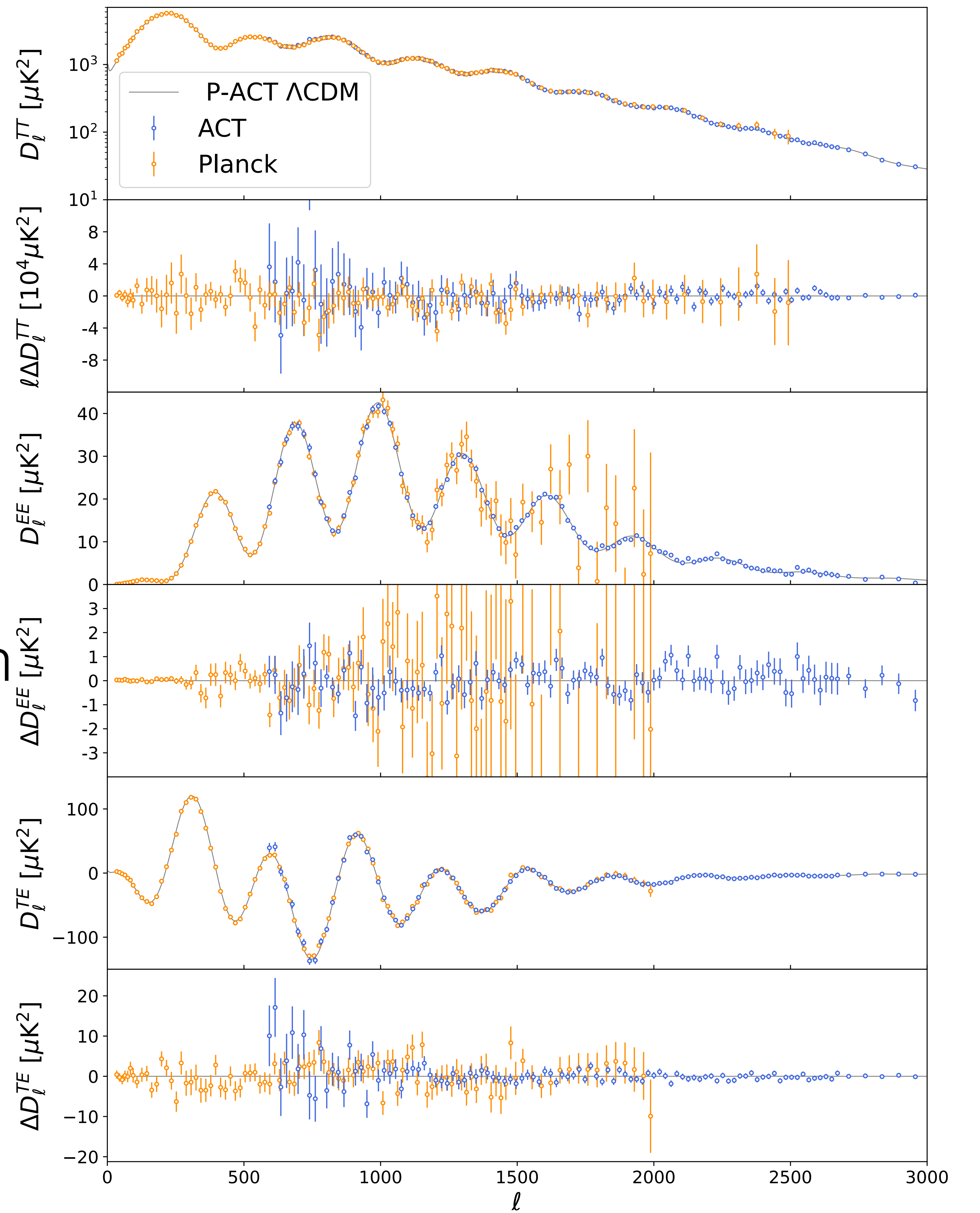

ΛCDM remains a robust model that can be extrapolated over 10 billion years and accurately predict observable at low redshift

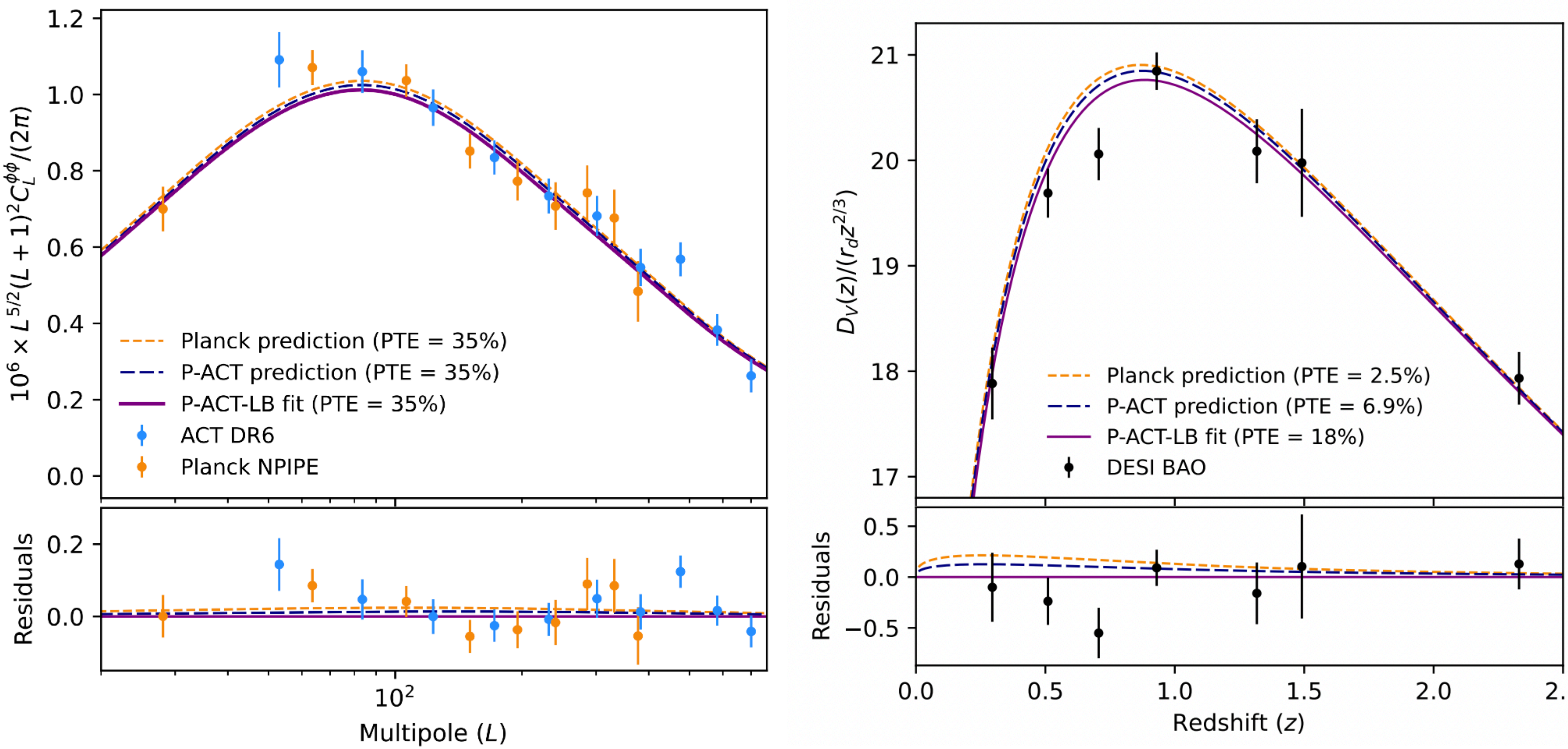

P-ACT-LB = Planck + ACT + Lensing (ACT + Planck)
+ BAO from DESI Y1

Beyond LCDM

Unlike in Planck legacy result, we don't see evidence for curvature or higher than predicted lensing amplitude from CMB power spectra

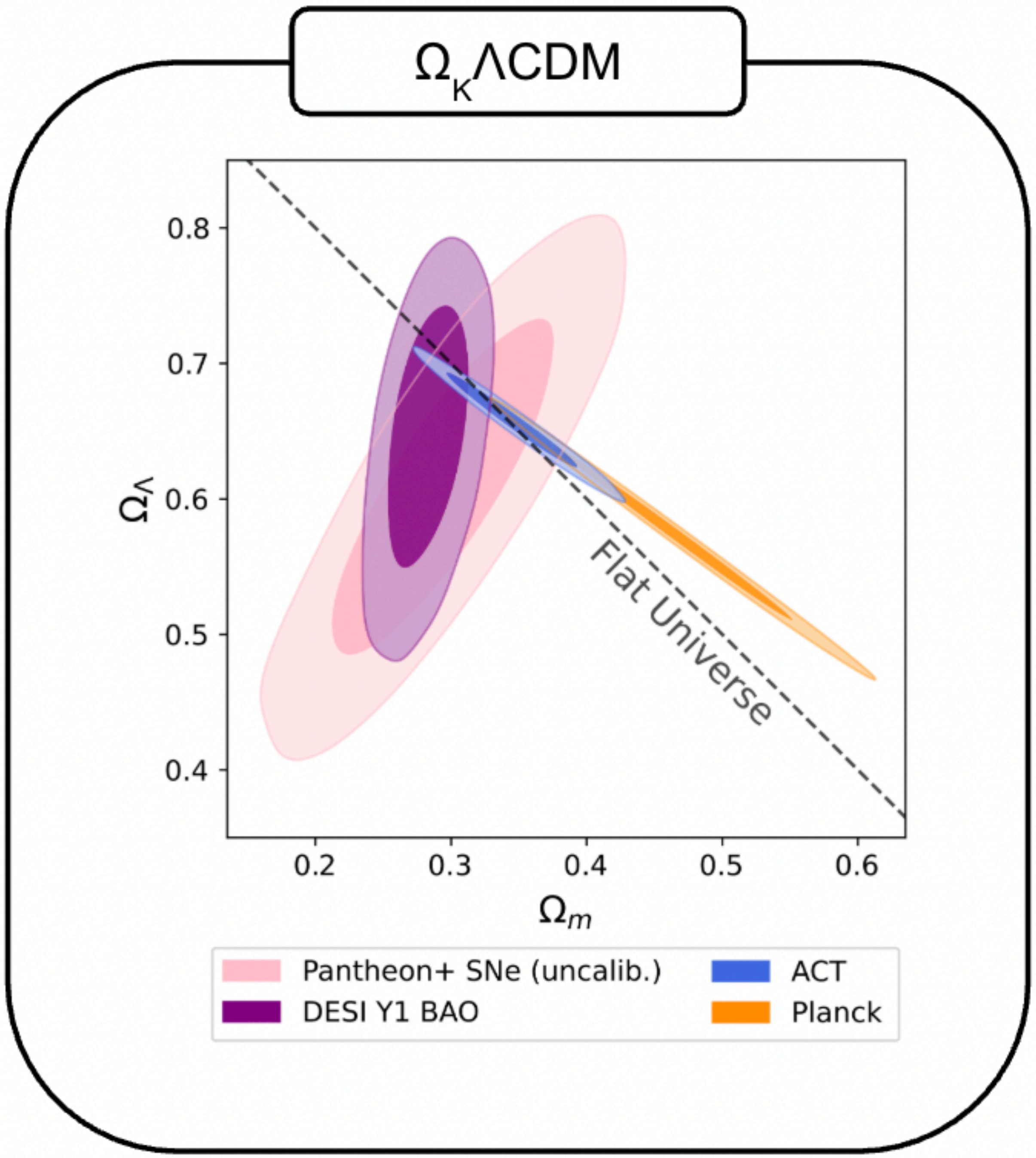

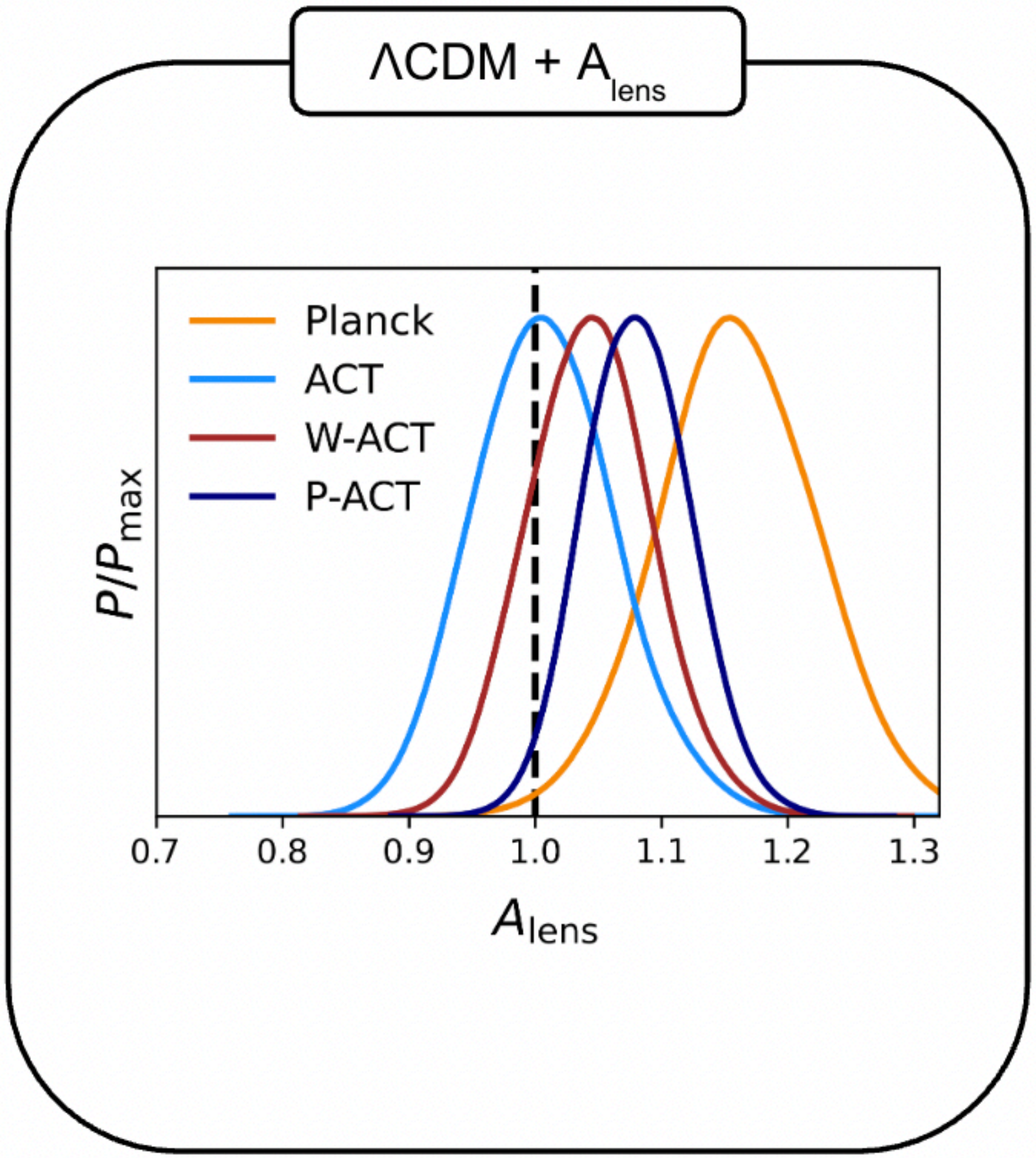

The three possible solutions to the H0 problem

1) SH0ES constraint is affected by un-modelled systematics (leading to artificial high H0)

2) Planck measurement is affected by un-modelled systematics (leading to artificial low H0)

3) Need new physics beyond LCDM ?

An Hubble constant measurement nowhere near the SH0ES value

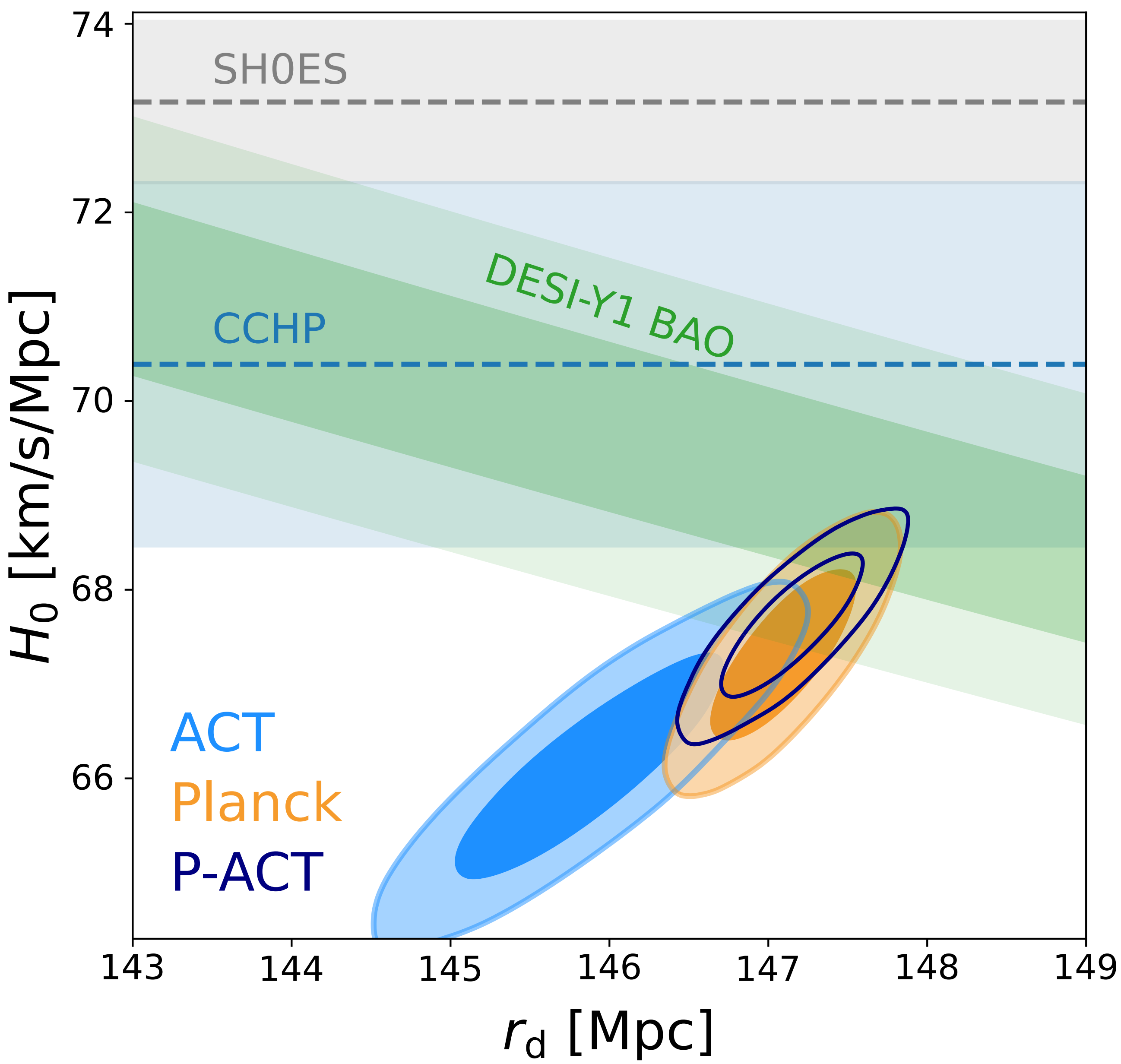

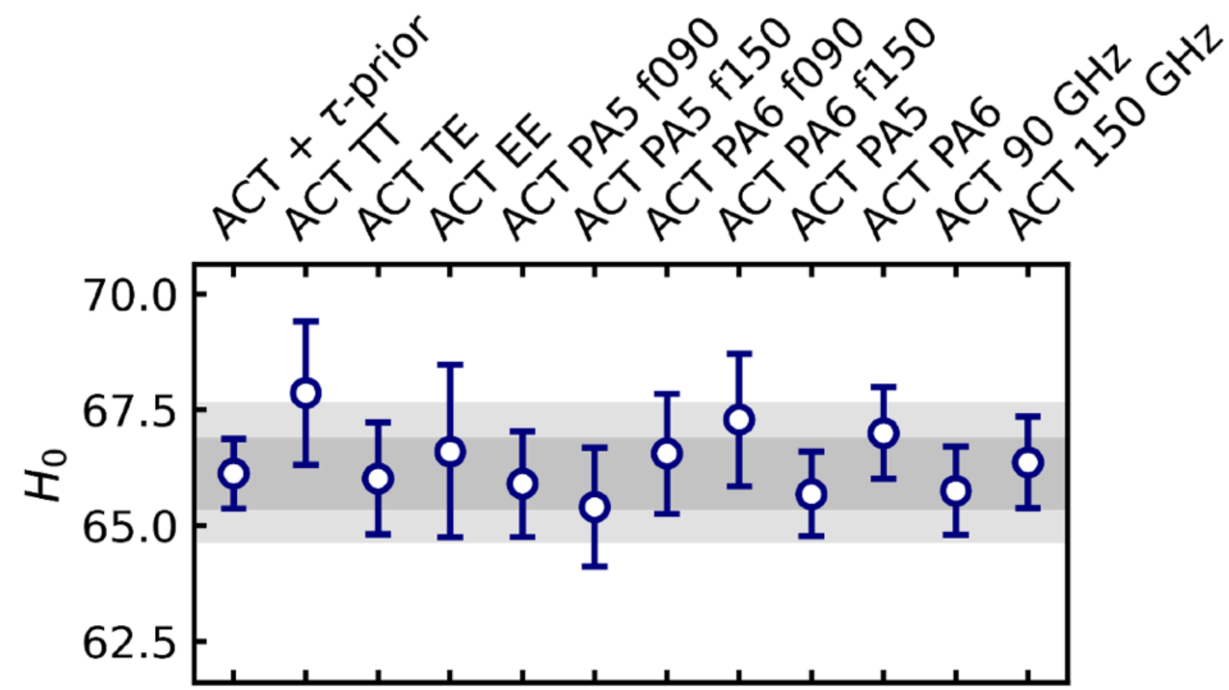

None of ACT probes exceed H0=68 km/s/Mpc

SH0ES: *Breuval et al.* 2024, *Riess et al.* 2022
CCHP: *Freedman et al.* 2024

The three possible solutions to the H0 problem

1) SH0ES constraint is affected by un-modelled systematics (leading to artificial high H0)

2) ~~Planck measurement is affected by un-modelled systematics (leading to artificial low H0)~~

3) Need new physics beyond LCDM ?

We tested a large class of extensions, None of them are preferred over ΛCDM.

$$66.1 < H_0 < 71.0 \text{ km/s/Mpc}$$

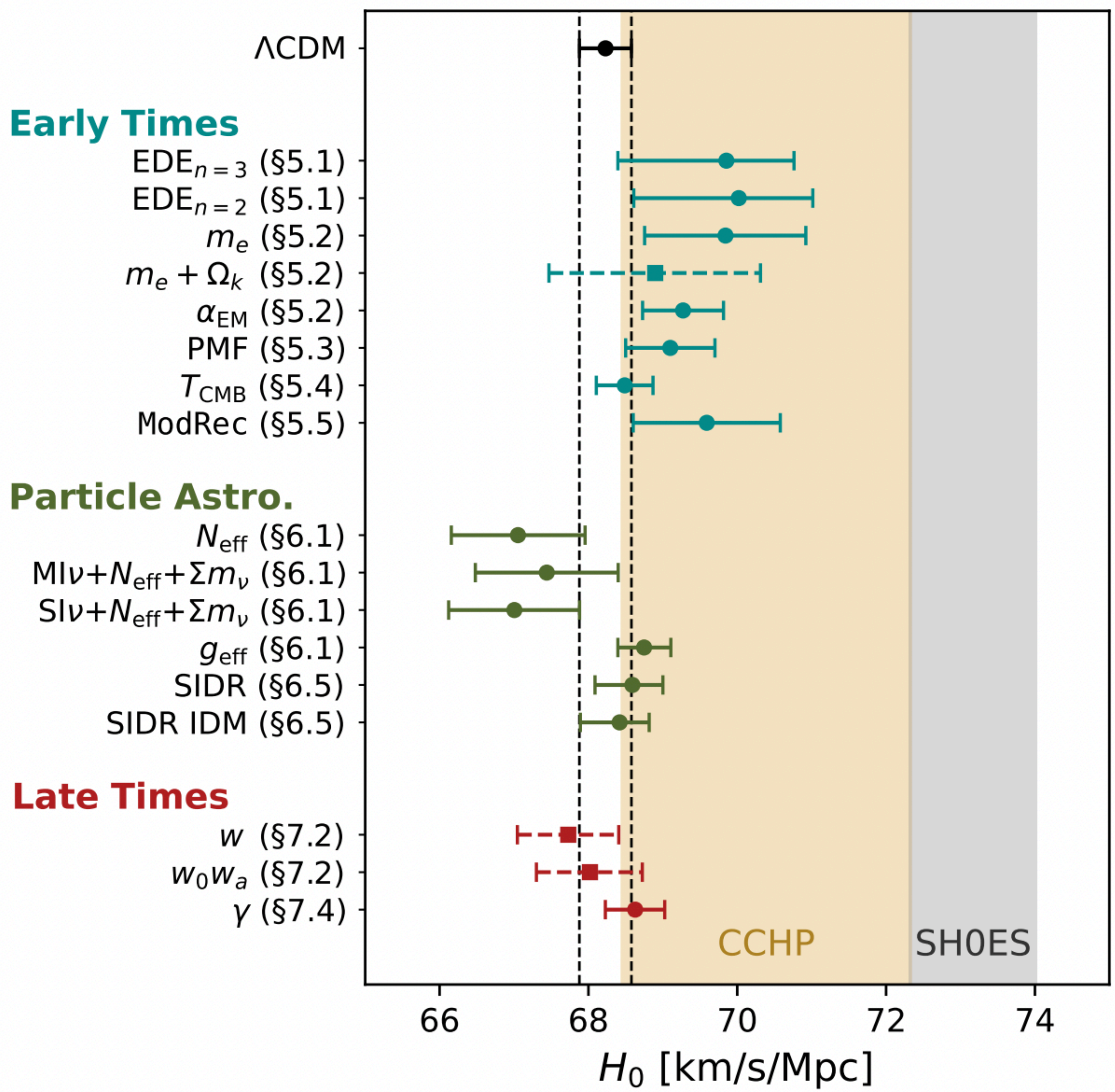

$$X_{\rm e}(z) \equiv n_{\rm e}(z)/n_{\rm H}(z)$$

We can reconstruct the recombination history using a non-parametric reconstruction. This restricts the ability of such scenarios to increase the CMB-inferred Hubble constant.

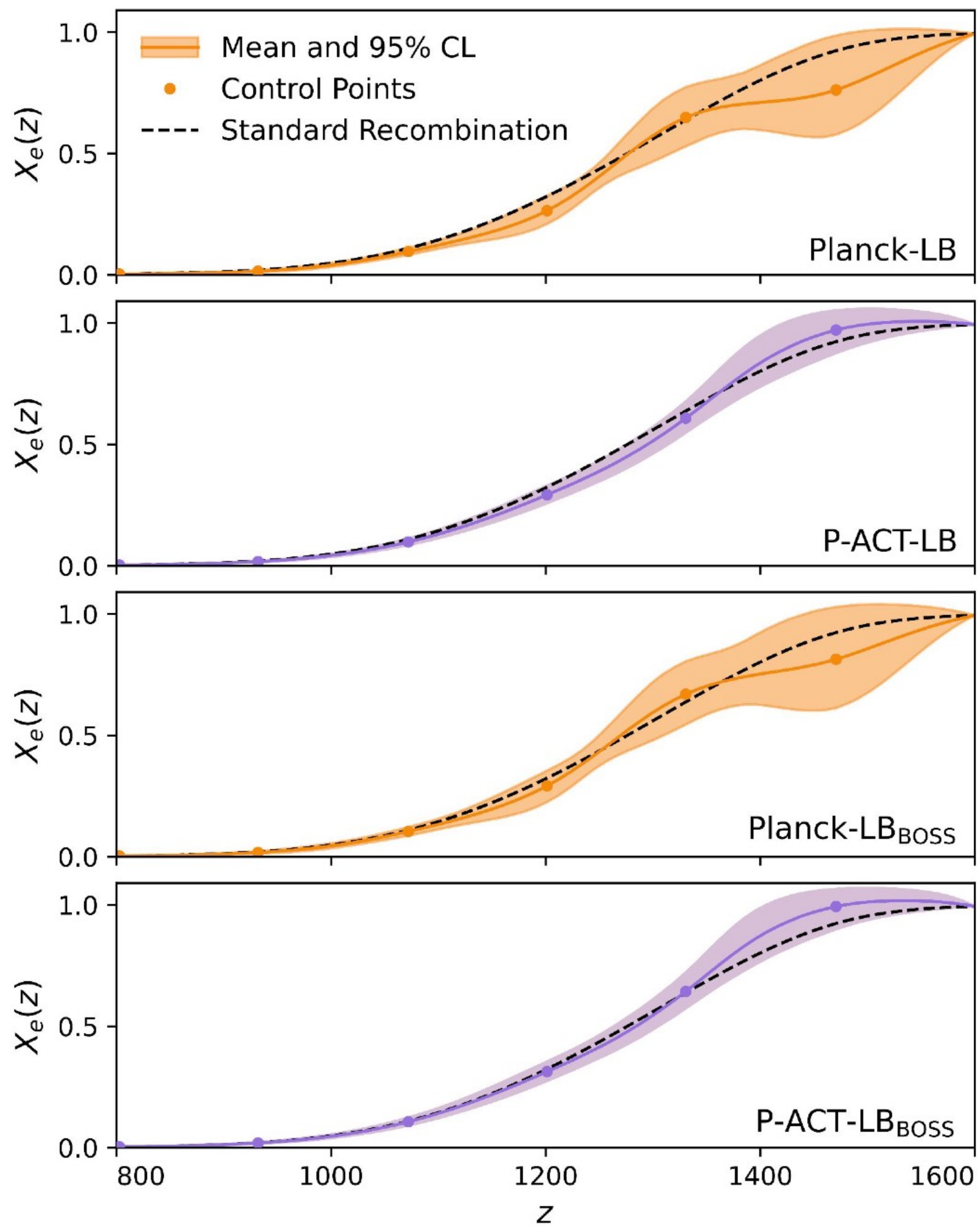

The three possible solutions to the H0 problem

1) SH0ES constraint is affected by un-modelled systematics (leading to artificial high H0)

2) ~~Planck measurement is affected by un-modelled systematics (leading to artificial low H0)~~

3) Need new physics beyond LCDM ?

Hard to cross definitely, but P-ACT poses a challenge to the proposed models

What about B modes ?

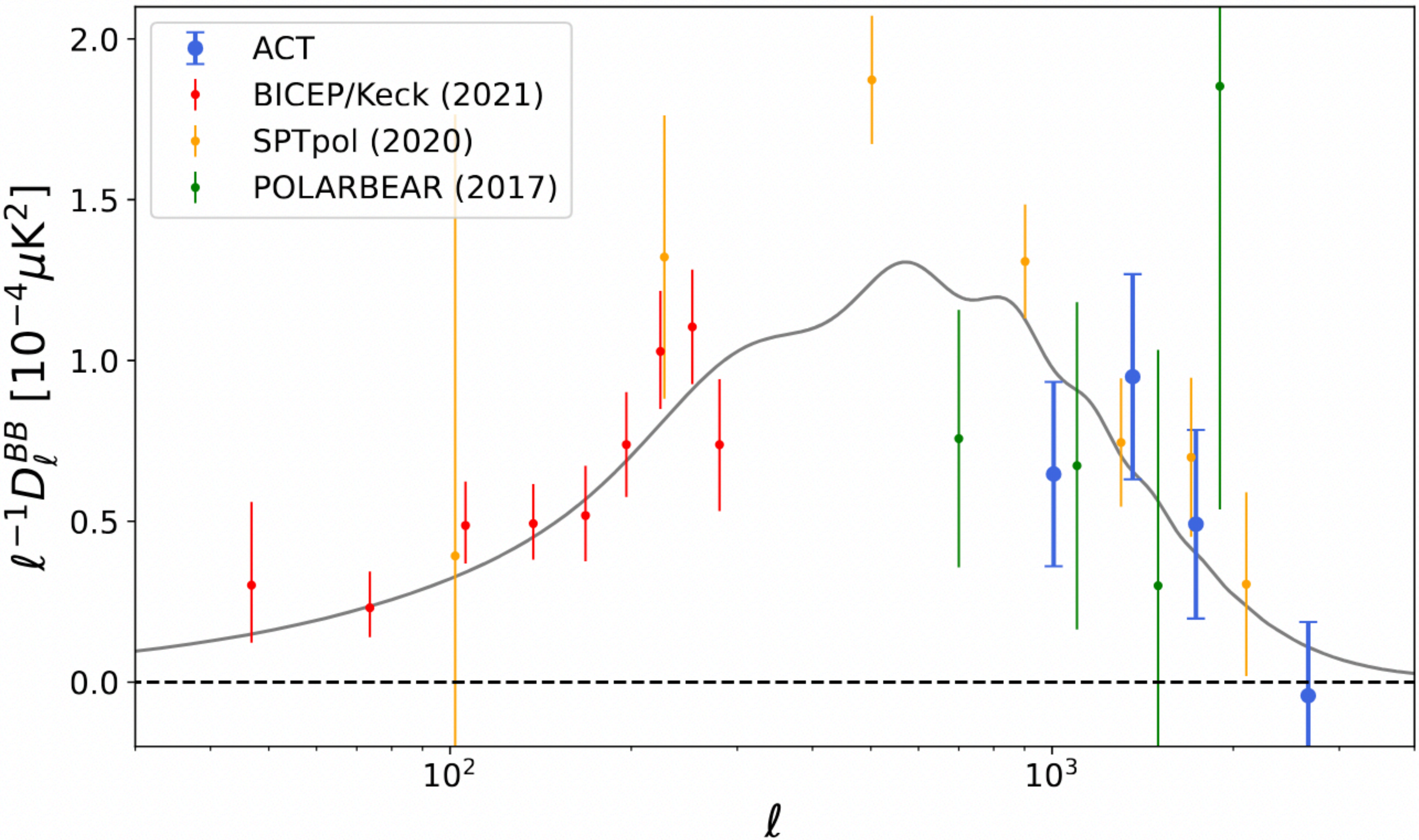

A cloudless sky in CMB anisotropies measurement ?

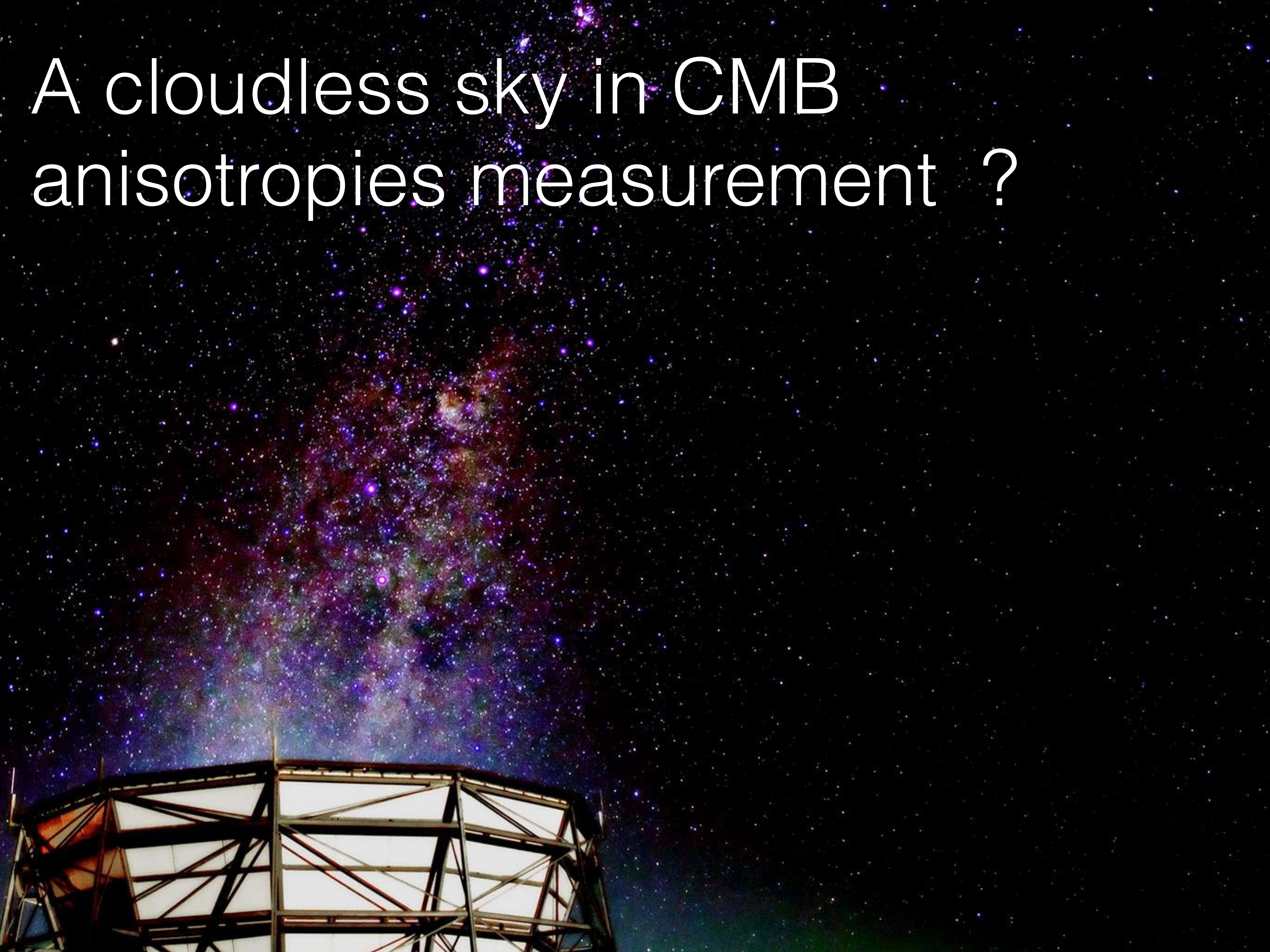

An interesting shape in EE ?

If we compare ACT EE measurement with the expectation from Planck cosmological model, we find a hint of a slope. This slope in ACT is not significative once we propagate Planck uncertainties (our EE cosmology agree with Planck at 2.3 sigma).

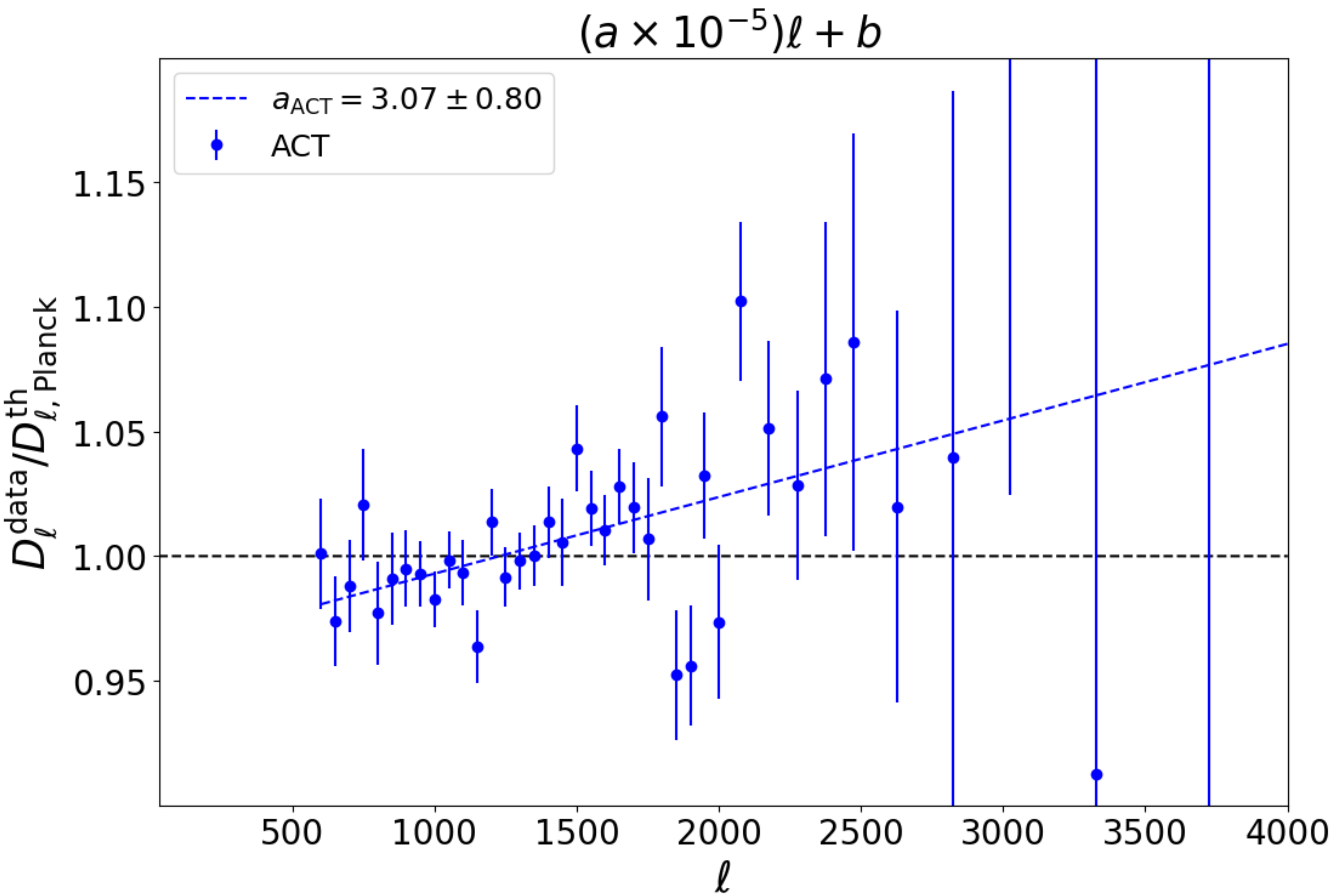

Very interestingly, SPT was finding a very similar slope in their initial unblinding data. If we were to combine both data set, the slope surely would become significative !

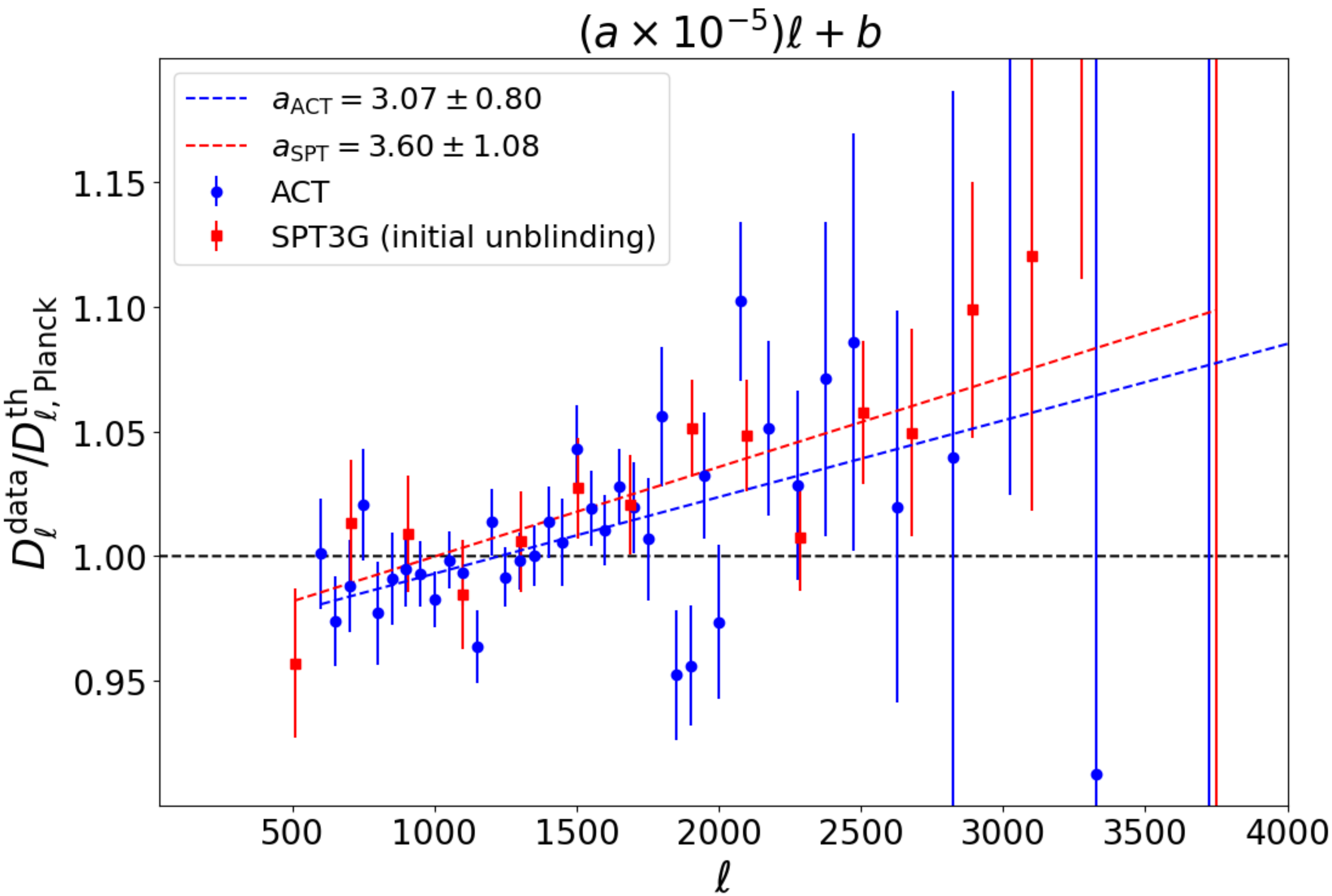

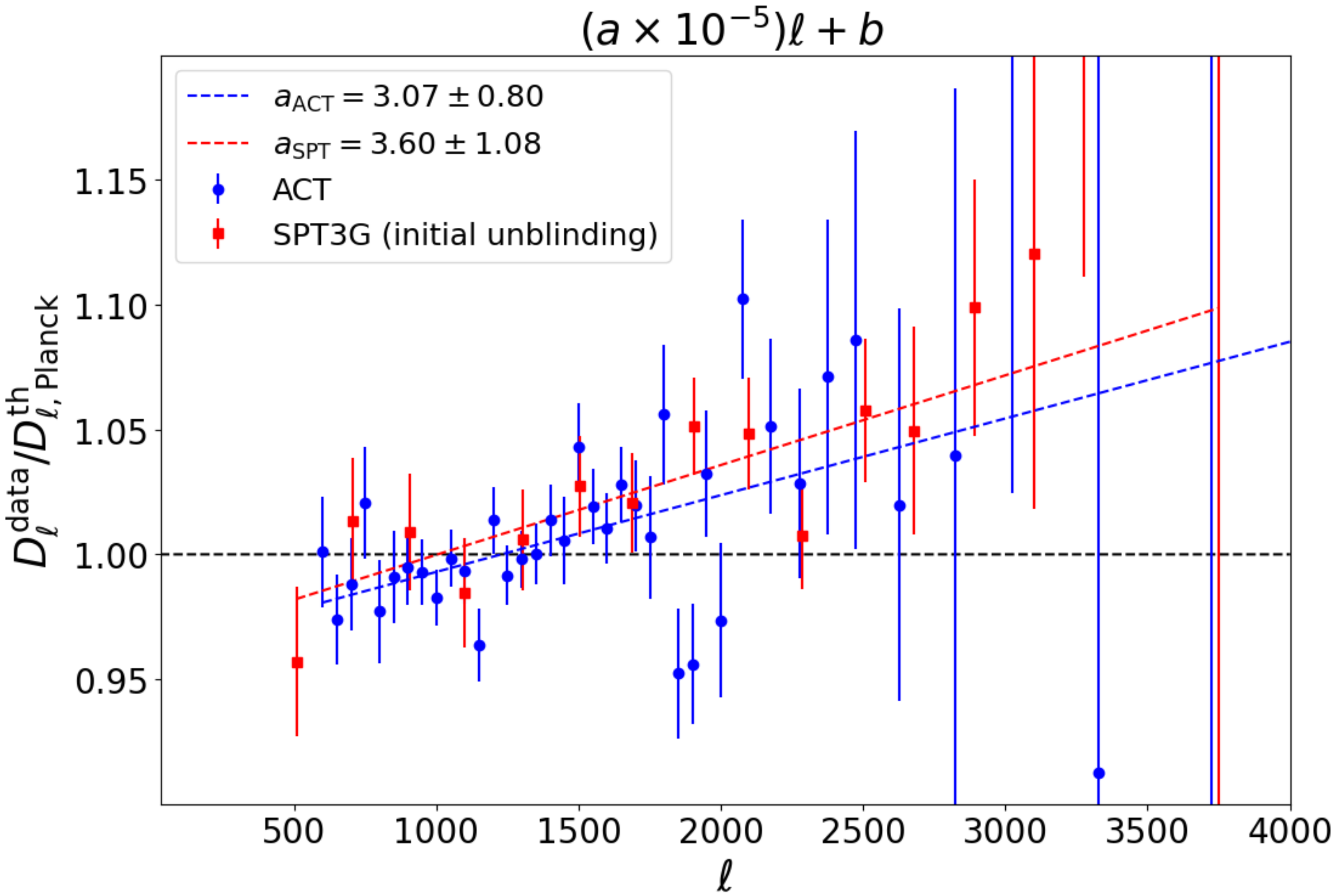

However, SPT, after unblinding their data, and motivated by the mismatch with Planck preferred cosmology attributed this slope to a mismatch between their beam in temperature and polarisation and included extra parameters to correct for it.

To my current knowledge and based on public material,

SPT do not have strong **model-independent** evidence supporting

The claim that their polarisation and temperature beam disagree.

The mismatch between temperature and polarisation beam is attributed to depolarization of their beam side-lobes, **as far as I know** no physical model for this phenomenon is discussed.

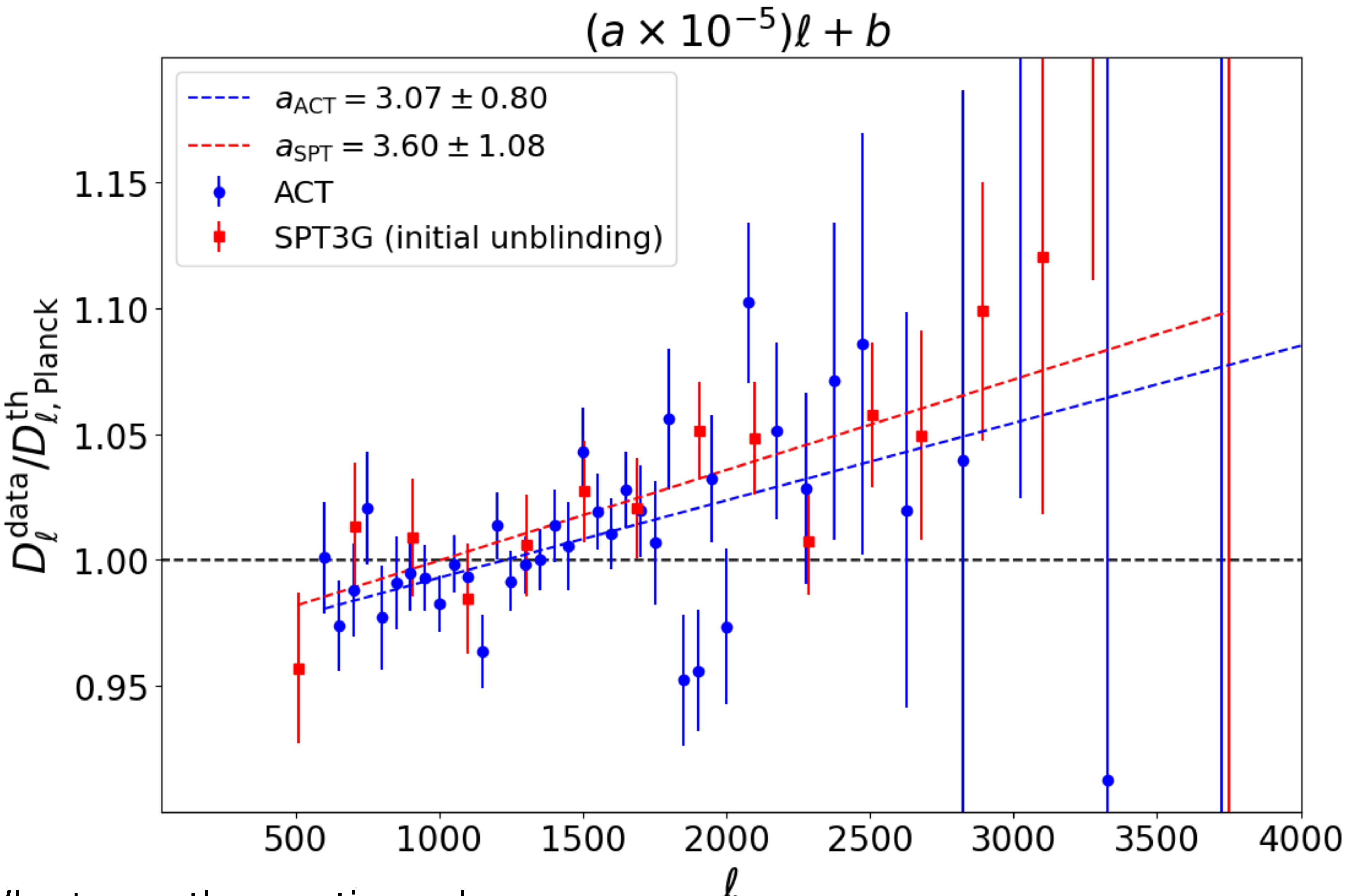

What are the options here:

1) ACT and SPT are affected by a similar systematic, despite being two very different telescopes with different optics. The systematic is not statistically significant enough in ACT to drive cosmological constraints.
2) ACT and SPT are seeing a small departure from Planck TT/TE/EE preferred cosmology in their high ell EE power spectra (that Planck couldn't measure !).

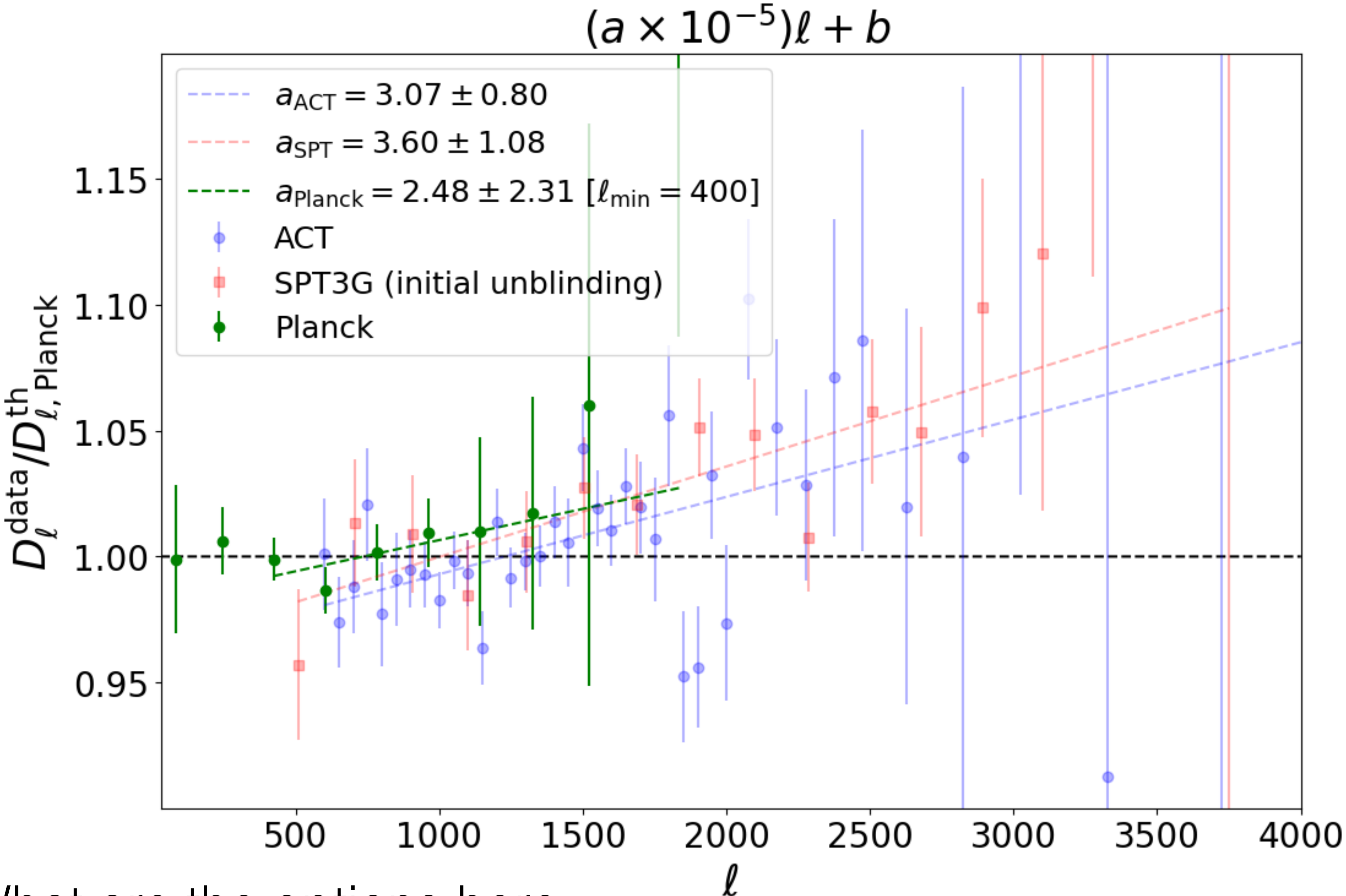

What are the options here:

1) ACT and SPT are affected by a similar systematic, despite being two very different telescopes with different optics. The systematic is not statistically significant enough in ACT to drive cosmological constraints.
2) ACT and SPT are seeing a small departure from Planck TT/TE/EE preferred cosmology in their high ell EE power spectra (that Planck couldn't measure !).


A bright future for CMB observation
from the Atacama desert

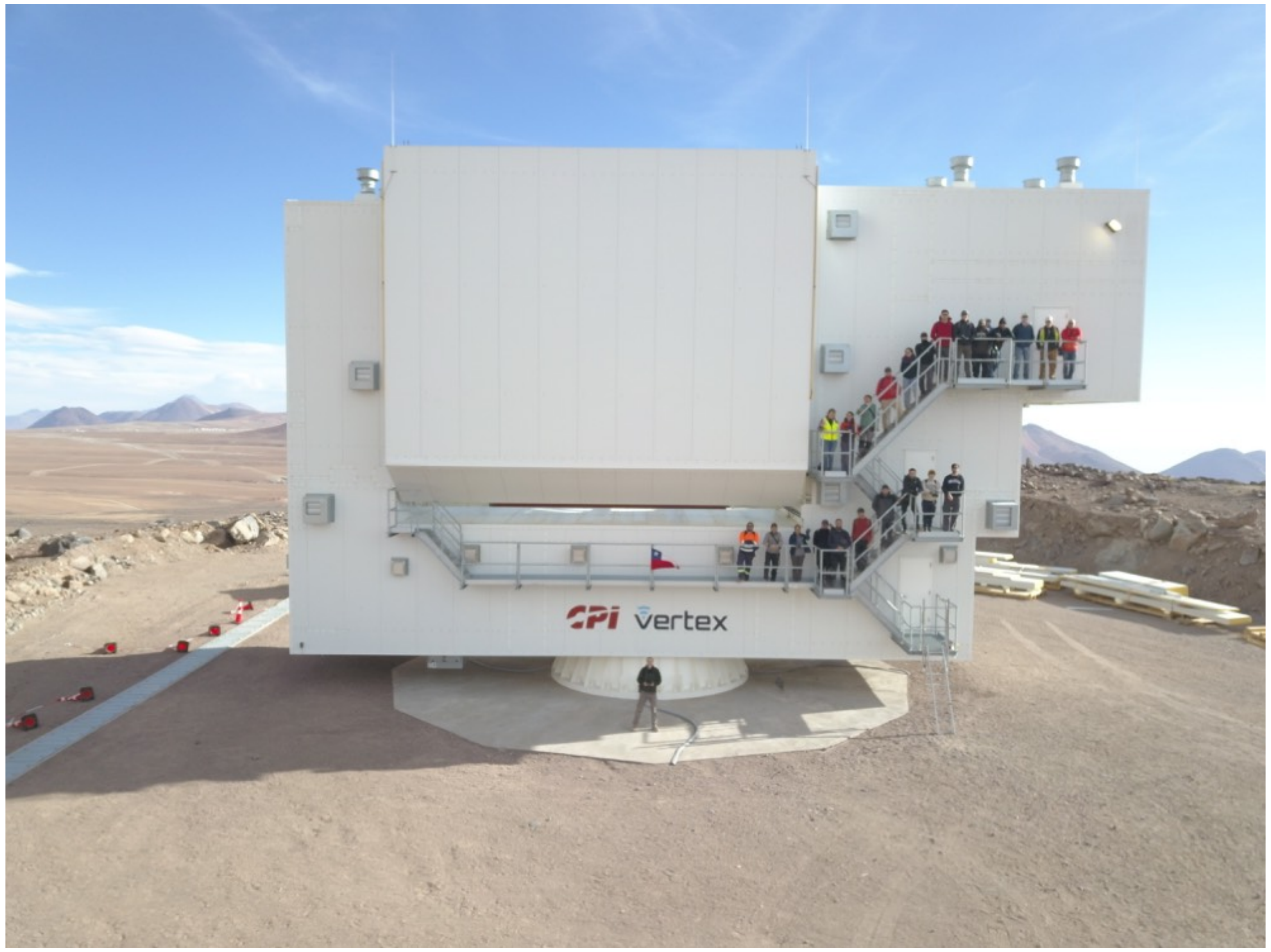

Each tube in the cryostat of the LAT is roughly equivalent to ACT

Large Aperture Telescope – First Light February 2025!

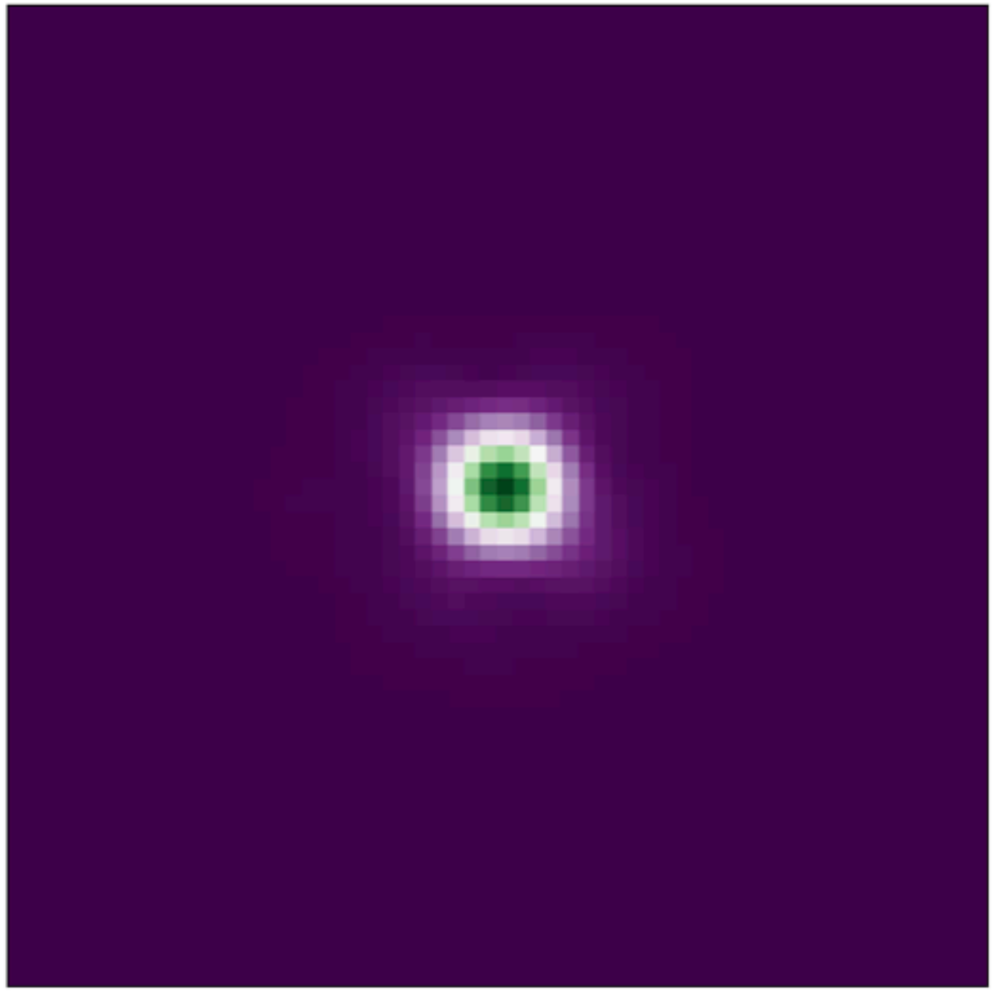

24,000 + Detectors on the Sky.

- Mirrors not yet aligned/focused.
- Signal to Noise of 4000+ per detector.
- 640 detectors used the Mars map.
- CMB maps are already being made.

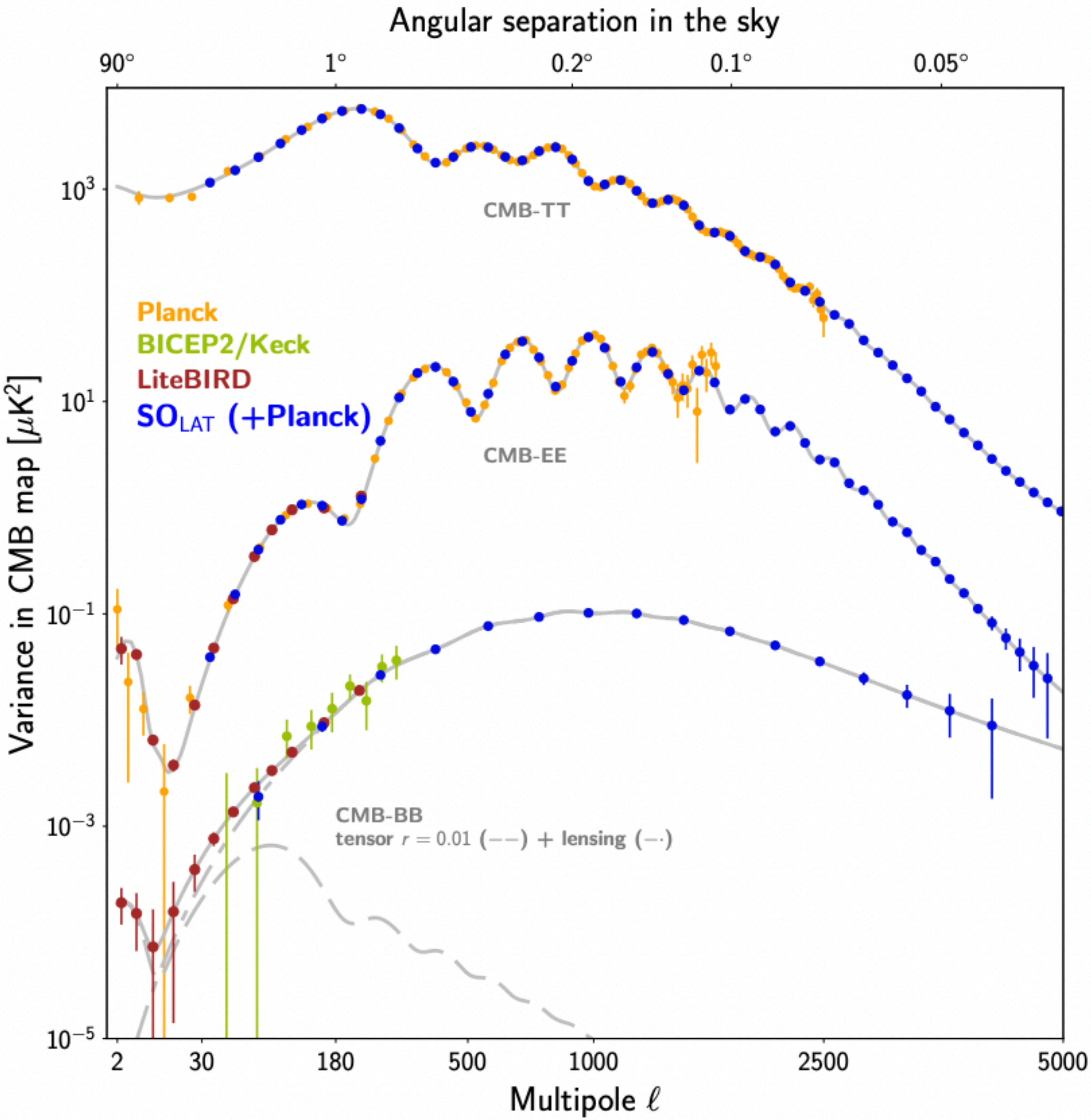

Angular separation in the sky
90°
1°
0.2°
0.1°
0.05°
10^3
10^1
10^{-1}
10^{-3}
10^{-5}
Variance in CMB map [μK^2]
CMB-TT
CMB-EE
CMB-BB
tensor $r = 0.01$ (−−) + lensing (−·)
Planck
BICEP2/Keck
LiteBIRD
SO_{LAT} (+Planck)
2
30
180
500
1000
2500
5000
Multipole ℓ

- ACT has released an unprecedented data set measuring the polarisation of the CMB over 40 % of the sky.

- ***We have released data and code, making our results entirely reproductible (and falsifiable).***

- ***We are consistent with Planck in LCDM, but we do not find anomalous lensing amplitude or curvature.***

- ***Plank + ACT: P-ACT, a constraining data set exploiting the strengths of each survey***

- Simons observatory: a bright an exciting future in CMB cosmology ahead of us !

BACK UP

Data Combinations

We make use of several external datasets and combinations.

Planck	$Planck^{\mathrm{TT/TE/EE}}$ + Sroll2
ACT	$\mathrm{ACT}^{\mathrm{TT/TE/EE}}$ + Sroll2
P-ACT	$\mathrm{ACT}^{\mathrm{TT/TE/EE}}$ + $Planck_{\mathrm{cut}}^{\mathrm{TT/TE/EE}}$ + Sroll2
W-ACT	$\mathrm{ACT}^{\mathrm{TT/TE/EE}}$ + $\mathrm{WMAP}^{\mathrm{TT/TE/EE}}$ + Sroll2
followed by	
-LB	when adding CMB lensing and BAO
-LS	when adding CMB lensing and SNIa
-LBS	when adding CMB lensing, BAO, and SNIa

- Sroll2 uses low-E data from Planck
- P-ACT uses Planck cut at 1000/600/600, with full ACT and Sroll2
- CMB Lensing is from ACT DR6 and Planck PR4
- BAO measurements from DESI Y1 as baseline, BOSS/eBOSS BAO data are used as cross-check in some cases
- Type Ia Supernovae from Pantheon+

BEYOND LCDM models

Exploration of extended cosmological models

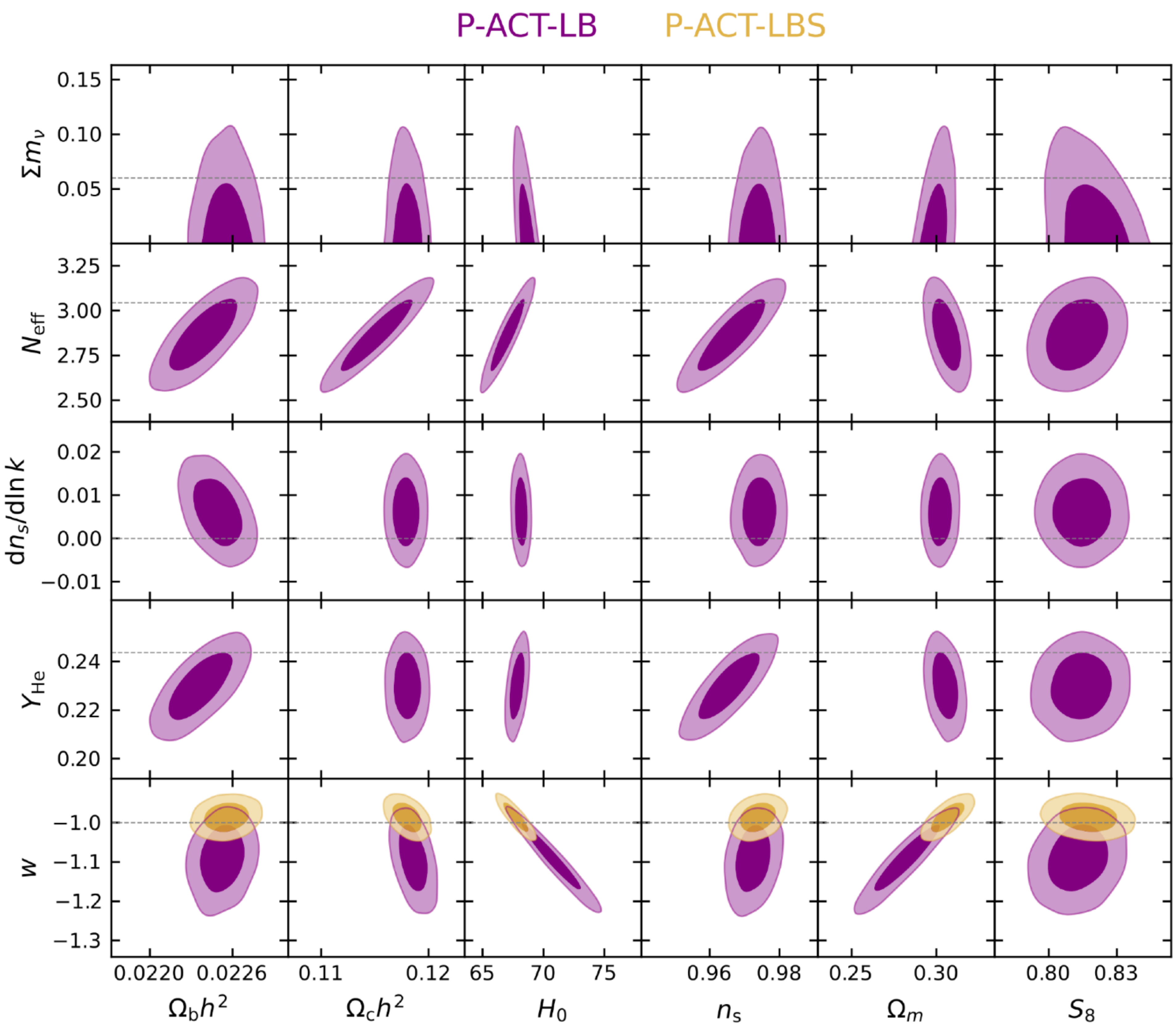

Exploration of extended cosmological models

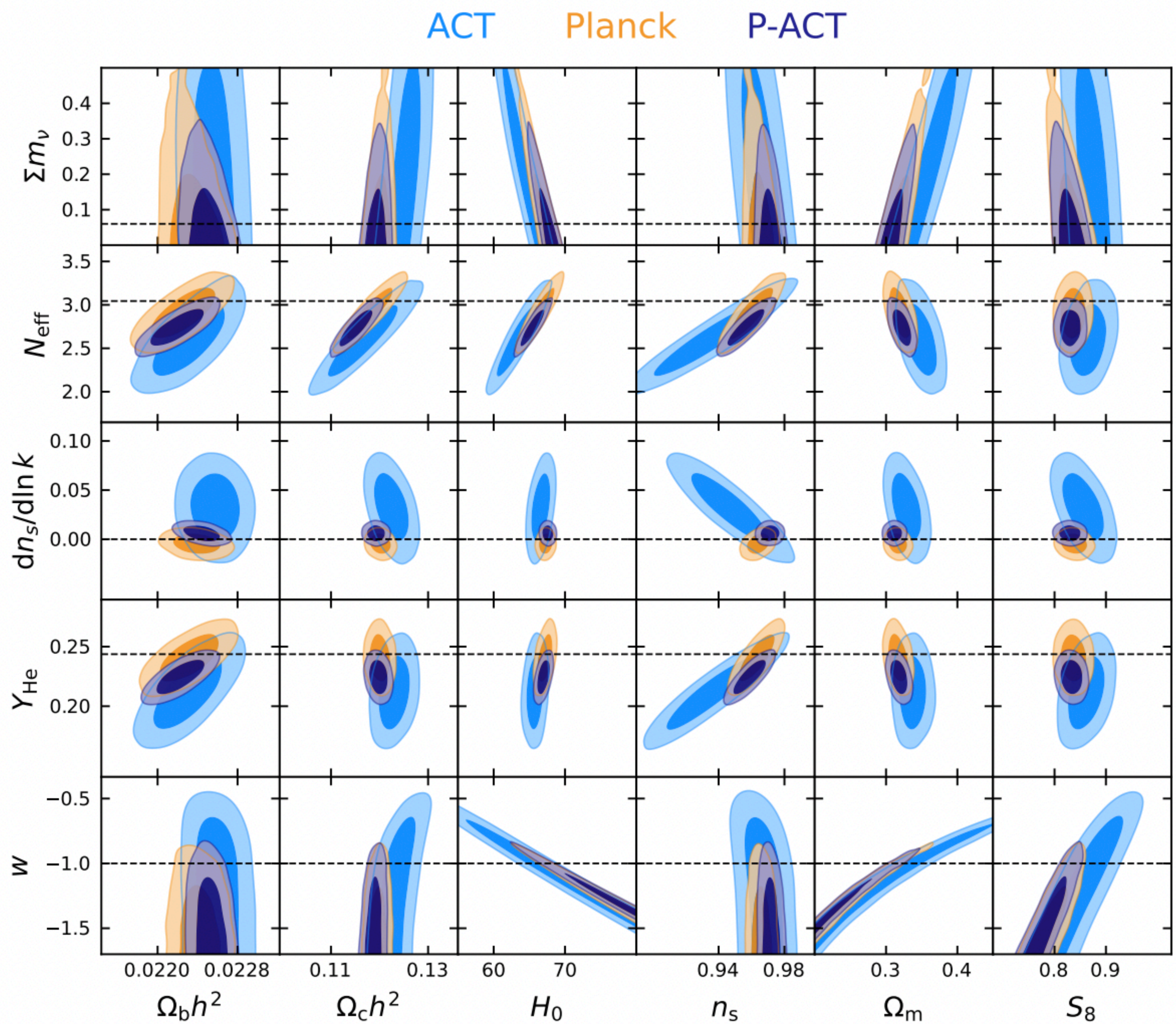

Primordial perturbations and inflation

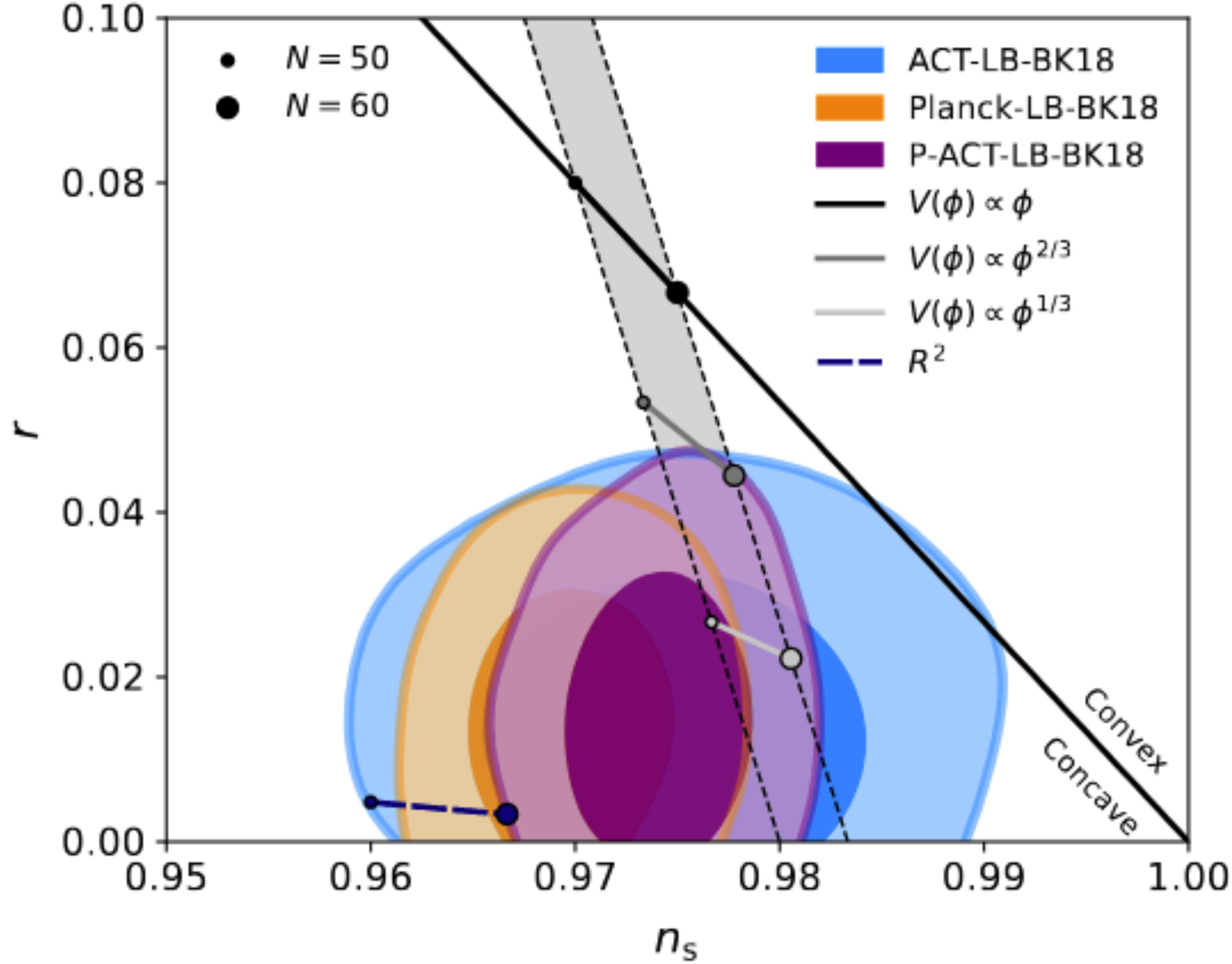

Information on inflation models from scalar spectral index

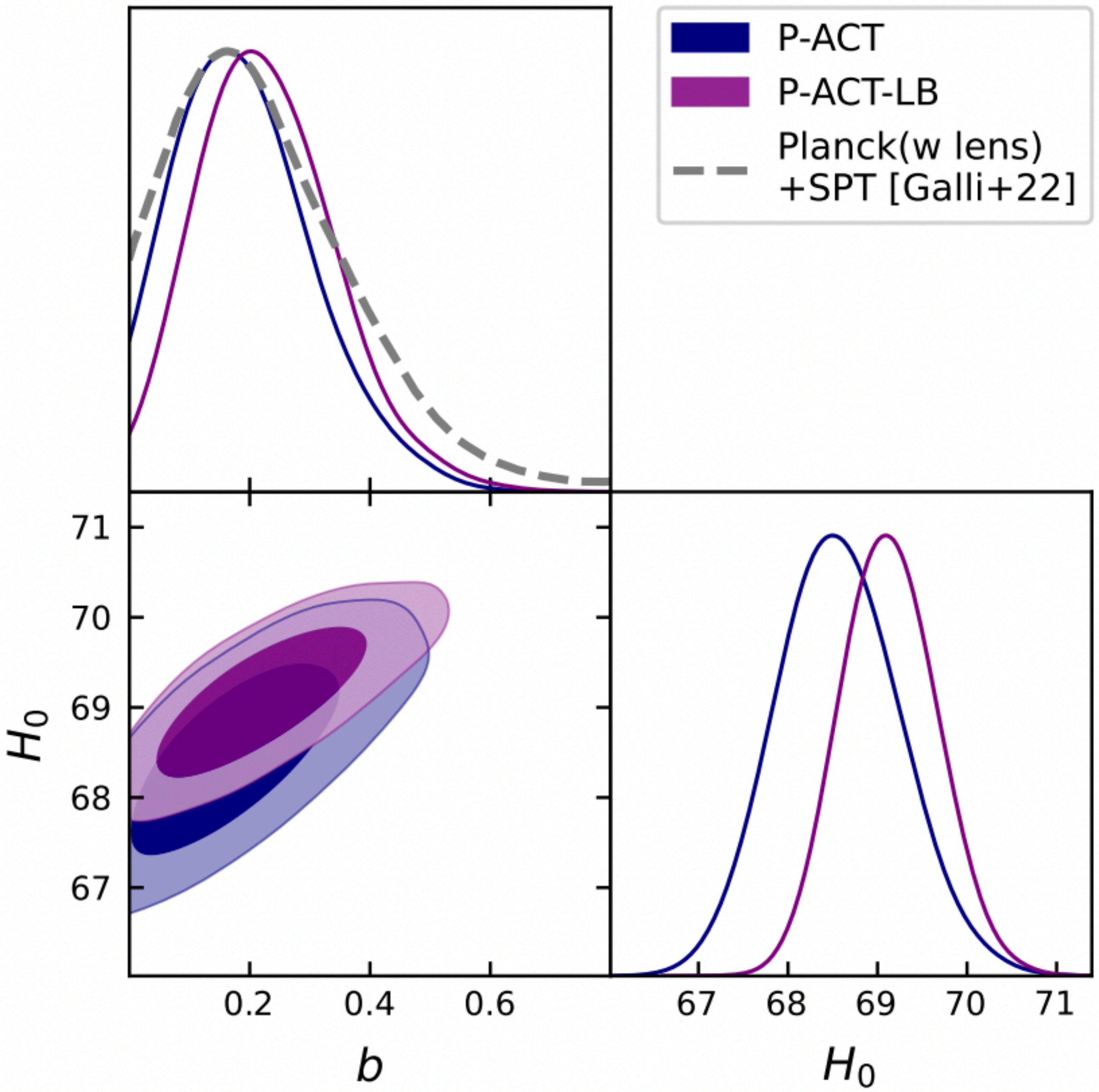

Figure 15. Constraints on the variance b of the small-scale baryon density distribution at recombination from P-ACT (navy) and P-ACT-LB (purple), compared with the latest results from *Planck* (including CMB lensing) combined with SPT small-scale polarization (gray dashed line). Primordial magnetic fields would induce baryon clumping on small scales, and hence $b > 0$. No evidence of clumping is seen in our analysis.

Varying m_e + curvature

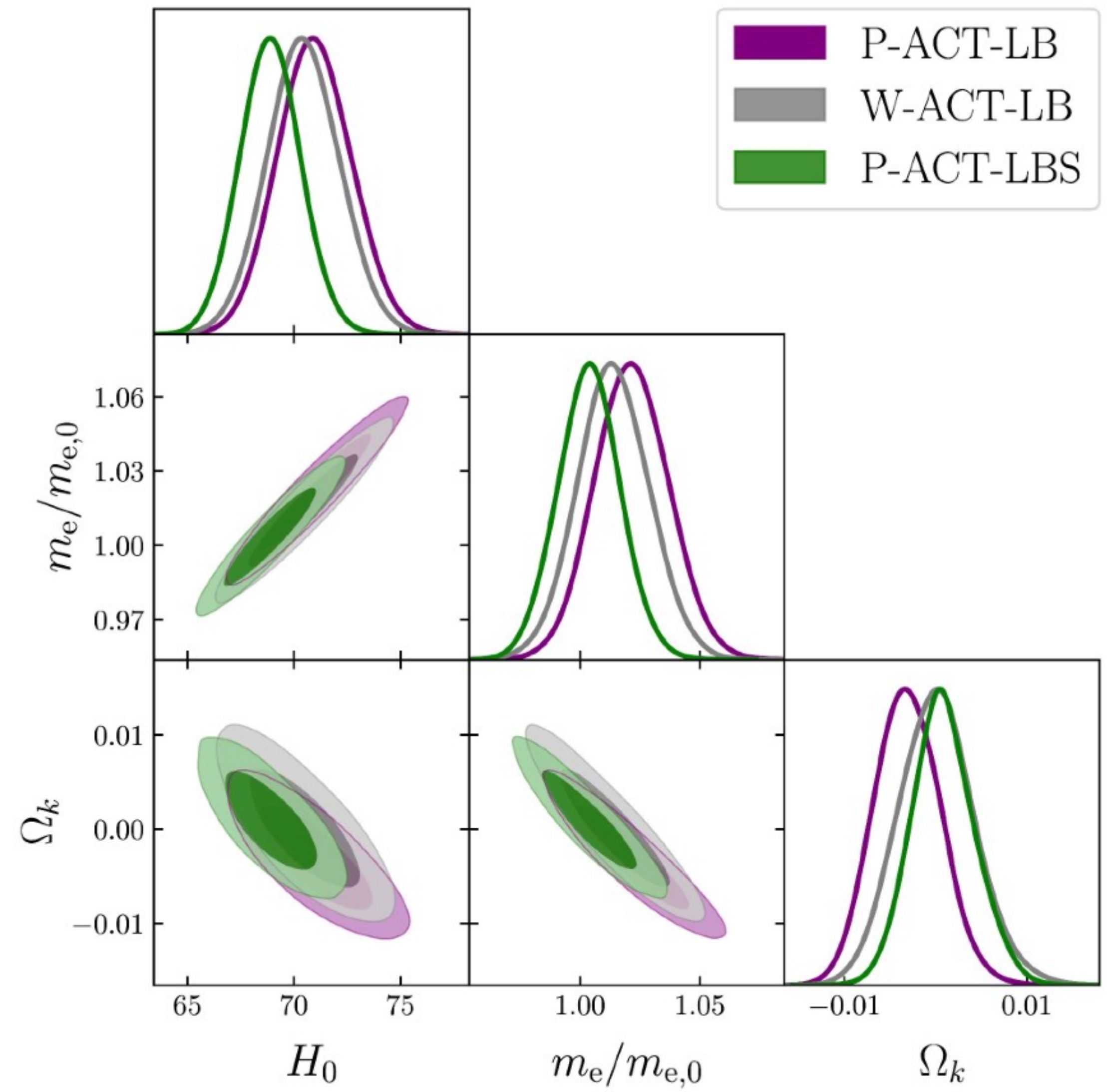

Particle cosmology

No evidence for new light, relativistic species

Free-streaming:

N_{eff} = 2.86 ± 0.13 (68%, P-ACT-LB)
N_{eff} = 2.89 ± 0.11 (68%, P-ACT-LB-BBN)

in the acoustic peaks (Bashinsky & Seljak 2004). Combining the *Planck* legacy CMB with *Planck* CMB lensing and BOSS BAO, the neutrino number is measured to be $N_{\rm eff} = 2.99 \pm 0.17$ at 68% CL (Planck Collaboration 2020c), or $N_{\rm eff} = 3.06 \pm 0.17$ at 68% CL when we evaluate this estimate using Planck-LB.

With the new ACT DR6 spectra we find $N_{\rm eff} = 2.60^{+0.21}_{-0.29}$ at 68% CL, combining into

$$\begin{aligned} N_{\rm eff} &= 2.73 \pm 0.14 \quad (68\%, \text{P-ACT}), \\ &= 2.86 \pm 0.13 \quad (68\%, \text{P-ACT-LB}), \qquad (30) \end{aligned}$$

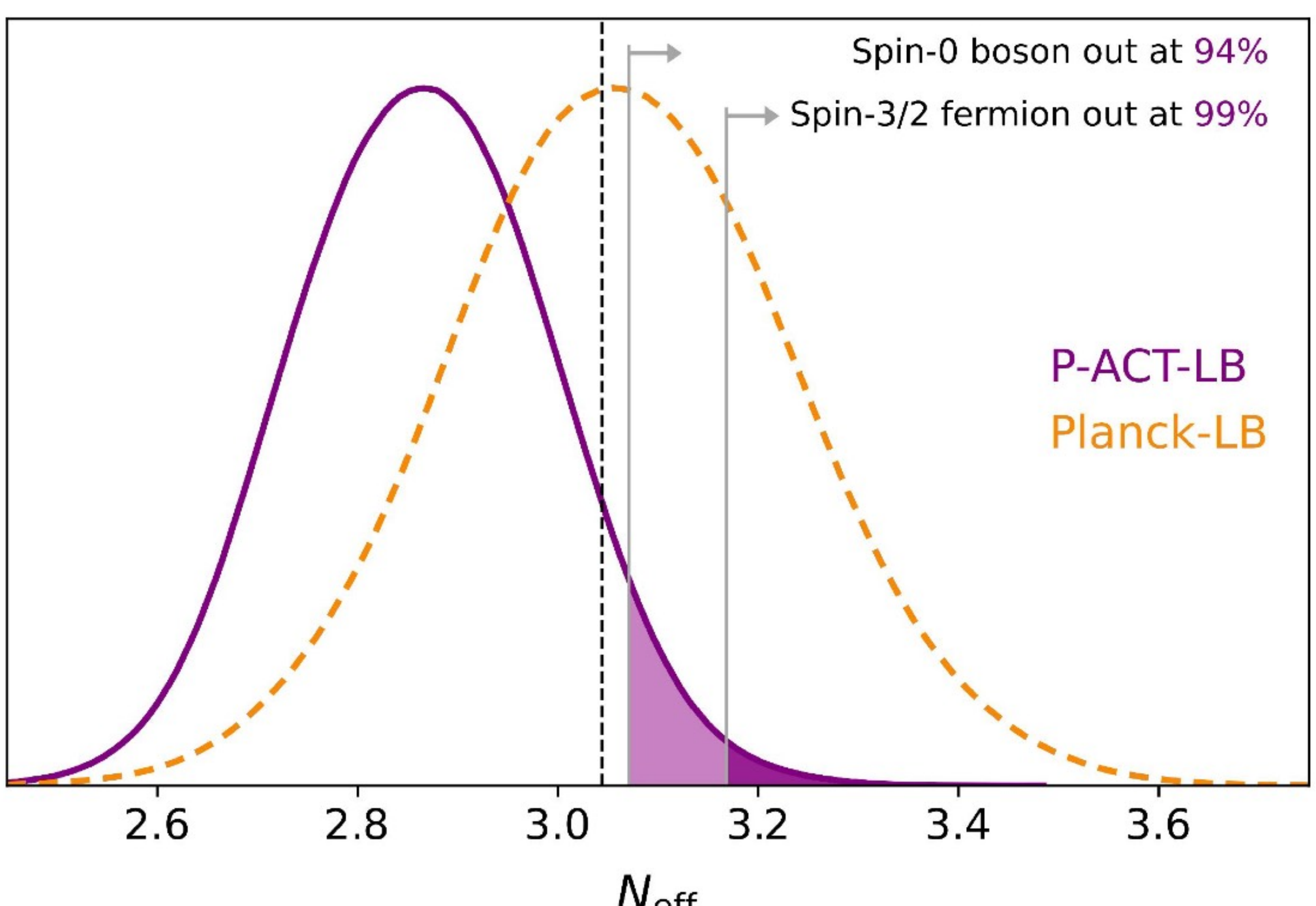

Particle cosmology

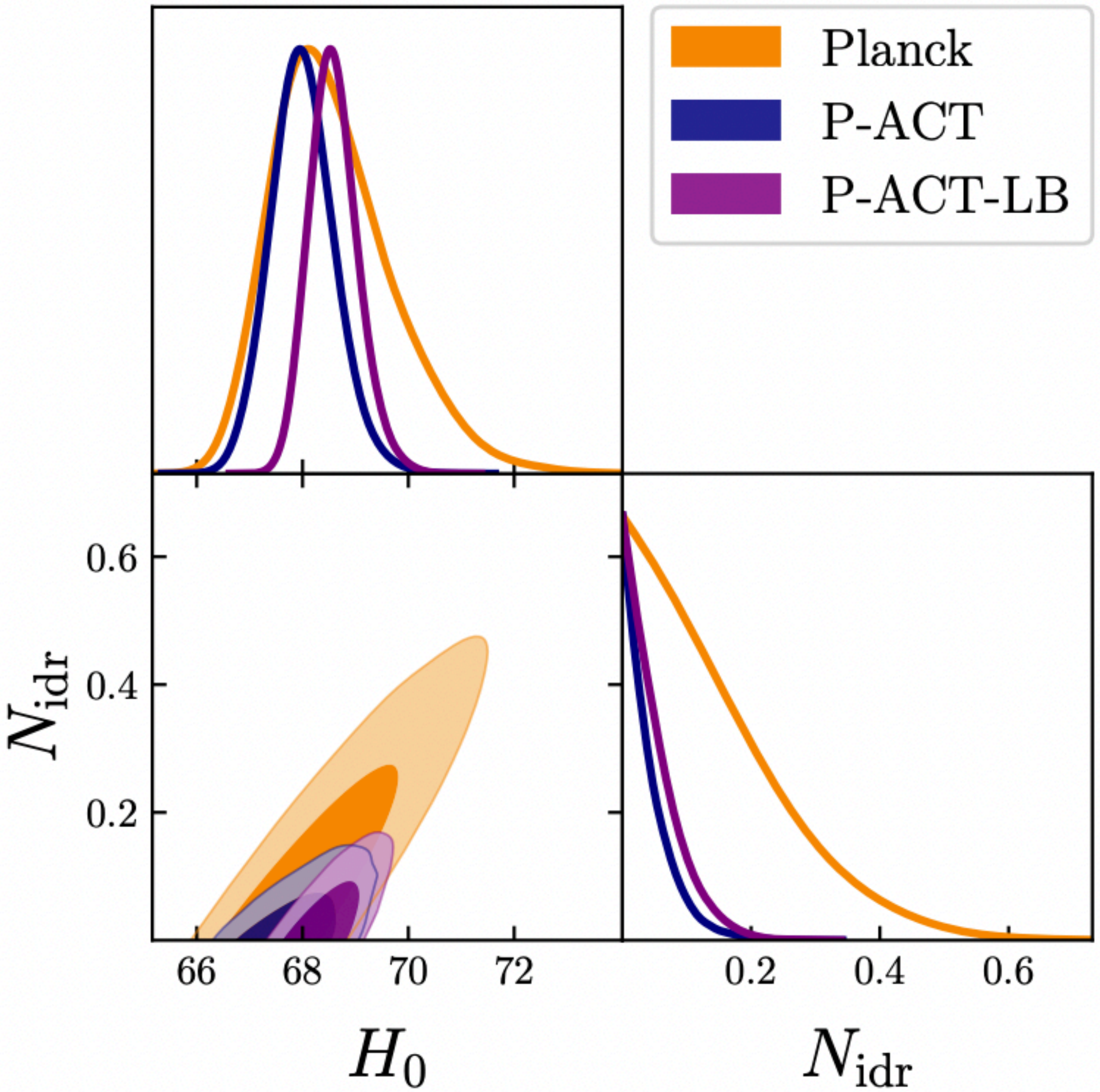

Figure 34. Constraints on the number of strongly self-interacting dark relativistic species, $N_{\rm idr}$. The addition of ACT DR6 spectra improves the constraint from *Planck* by more than a factor of three (navy versus orange) and notably disfavors values of H_0 above 70 km/s/Mpc that are allowed by *Planck* alone. Inclusion of CMB lensing and DESI BAO data (purple) slightly weakens the SIDR upper limit due to small shifts in the best-fit model parameters, but nevertheless further tightens the H_0 posterior. These are the tightest bounds on SIDR obtained to date.

Pre- and modified recombination physics

No evidence for an early dark energy (EDE) component:

A mild hint (2-3σ) of EDE was seen in ACT DR4 (Hill+2022); the new ACT DR6 spectra show that this was a statistical fluctuation.

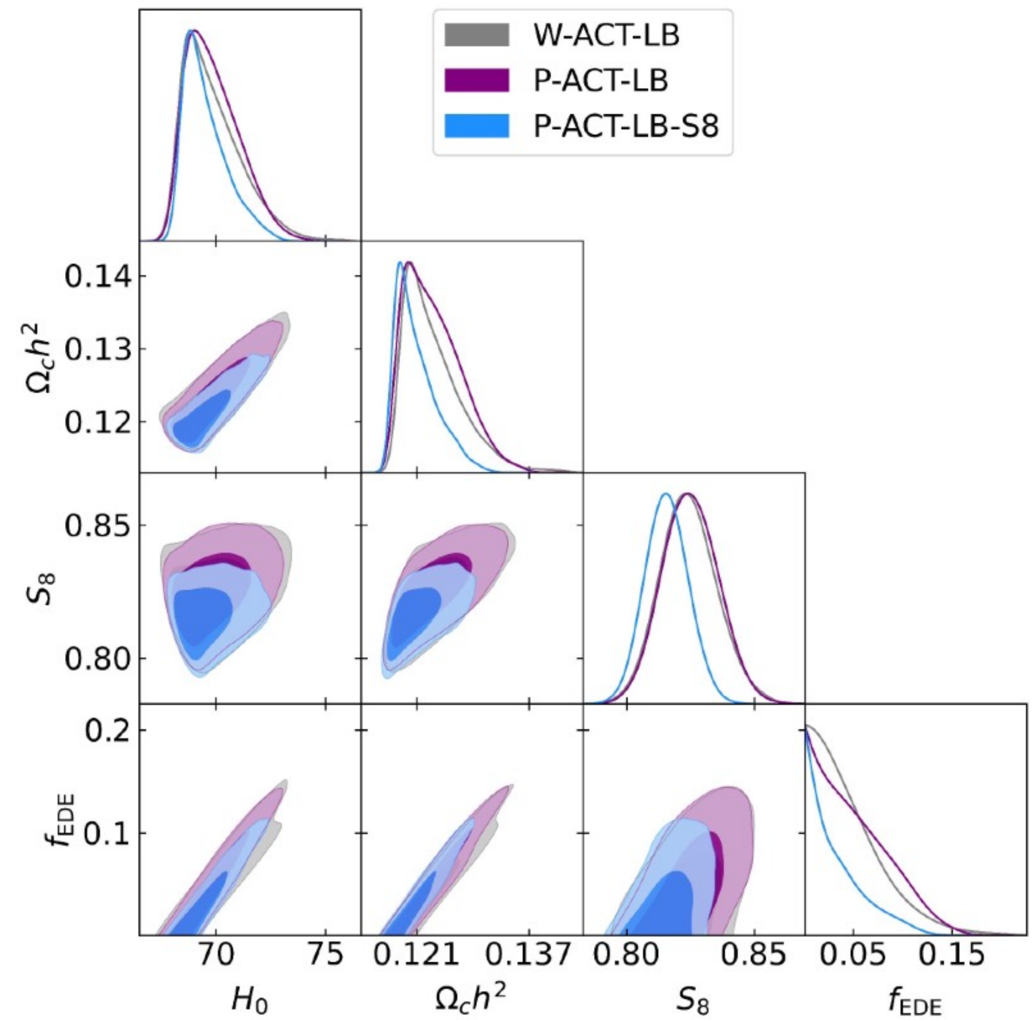

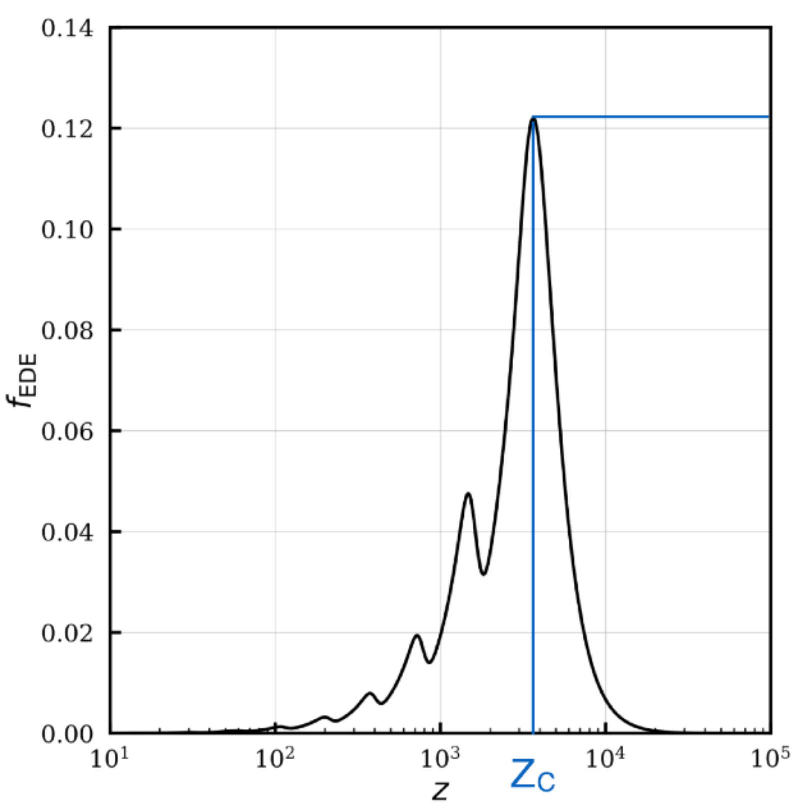

Maximal contribution:

$$f_{\rm EDE}(z_c) \equiv (\rho_{\rm EDE}/3M_{pl}^2 H^2)|_{z_c}$$

which occurs at redshift z_c

Final parameter: $\theta_i = \phi_i/f$ (initial field displacement)

→ $\{f_{EDE}, z_c, \theta_i\}$

	$\Delta\chi^2$	Pref. in σ	$H_0^{(\rm EDE)}$	$f_{\rm EDE}$	$\log_{10} z_c$
ACT	≈ 0.0	0.0	66.5	0.012	3.00
W-ACT	1.9	0.5	69.9	0.089	3.55
P-ACT	4.3	1.2	70.4	0.091	3.56
W-ACT-LB	2.9	0.8	70.2	0.070	3.52
P-ACT-LB	6.6	1.7	71.2	0.093	3.56

Table 2. The $\Delta\chi^2 = \chi^2_{\Lambda\rm CDM} - \chi^2_{\rm EDE}$ from the **MFLike** likelihood MAP points for the $n = 3$ EDE model compared to ΛCDM for each dataset combination, and preference (in units of σ) for EDE over ΛCDM using the likelihood-ratio test statistic. The values for H_0, $f_{\rm EDE}$, and $\log_{10} z_c$ in the MAP EDE model are also reported. The data show no significant preference for non-zero EDE. For ACT alone, the MAP χ^2 for EDE is indistinguishable from that for ΛCDM within our numerical precision, indicating that adding EDE parameters does not improve the fit at all in this case.

Neutrinos

We find no evidence for non-zero neutrino masses:

$\Sigma m_\nu < 0.082$ eV (95%, P-ACT-LB)

$\Sigma m_\nu < 0.083$ eV (95%, W-ACT-LB)

with significant contribution from DESI BAO

$\Sigma m_\nu < 0.13$ eV (95%, P-ACT-LB$_{BOSS}$)

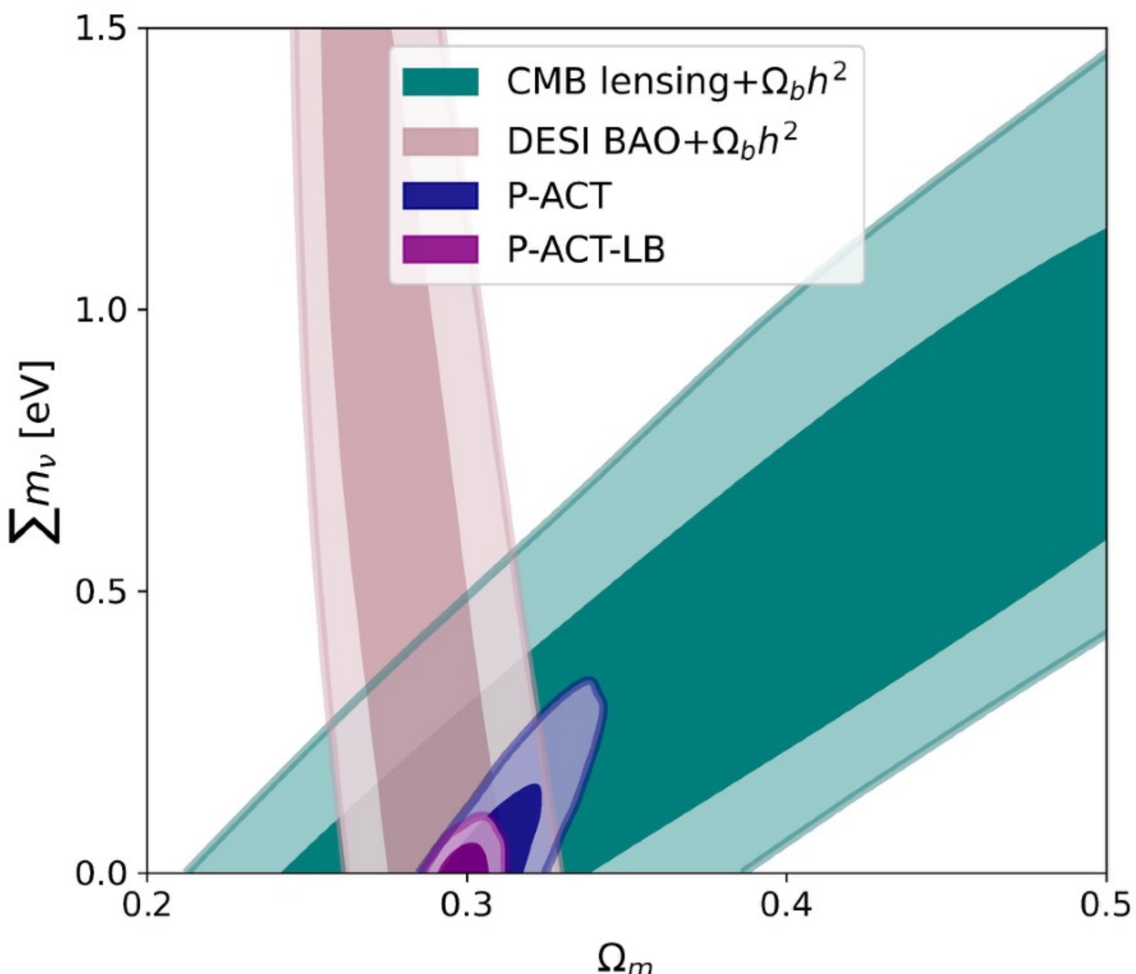

Particle astrophysics

We also find the abundances of primordial elements to be consistent with standard BBN.

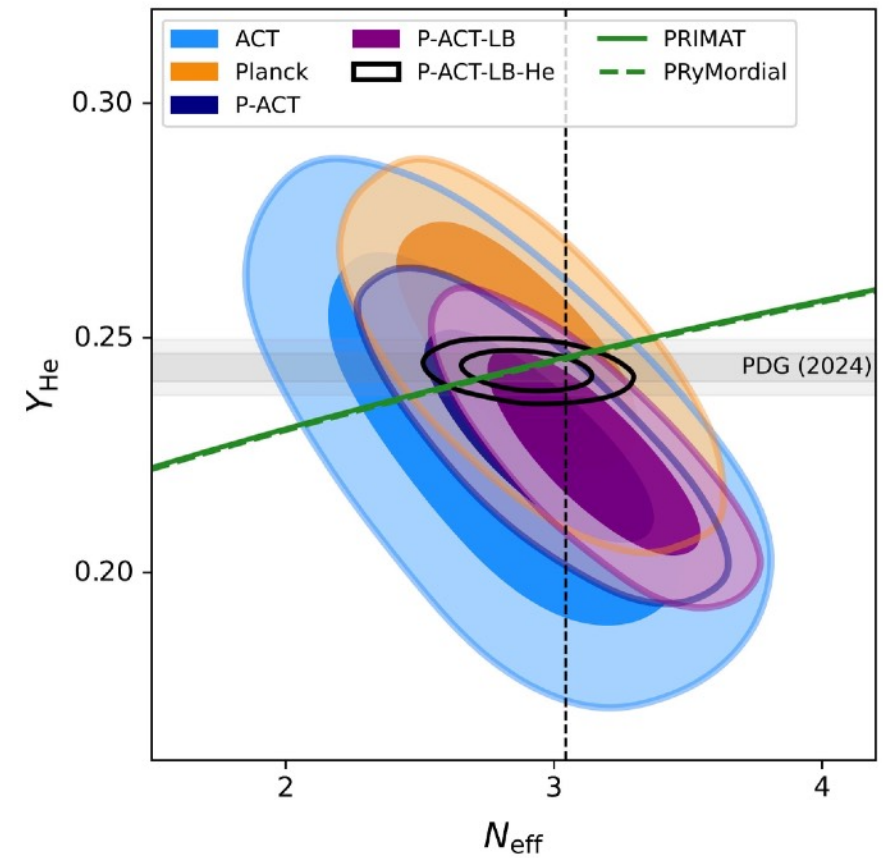

We find dark matter to follow the standard CDM paradigm, with no evidence for scattering with baryons, self-annihilation, contribution from axion-like particles, or scattering off a dark radiation component.

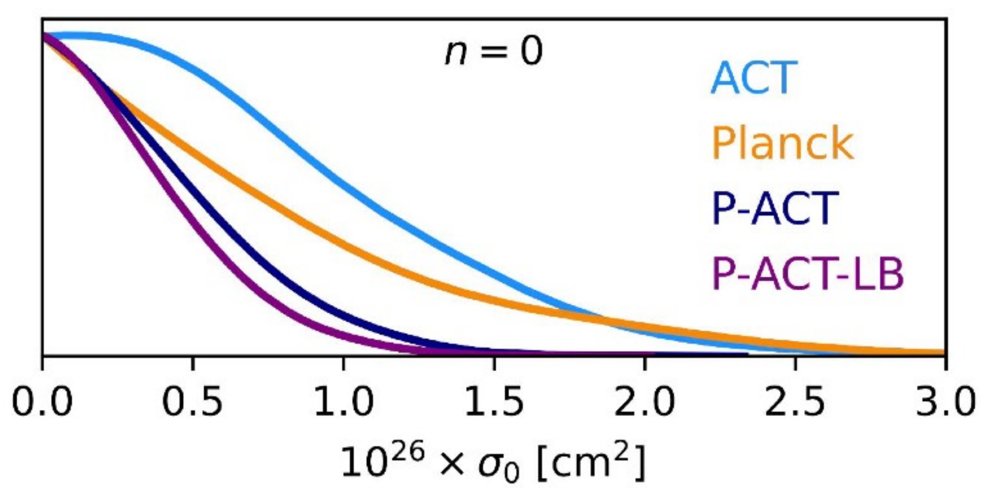

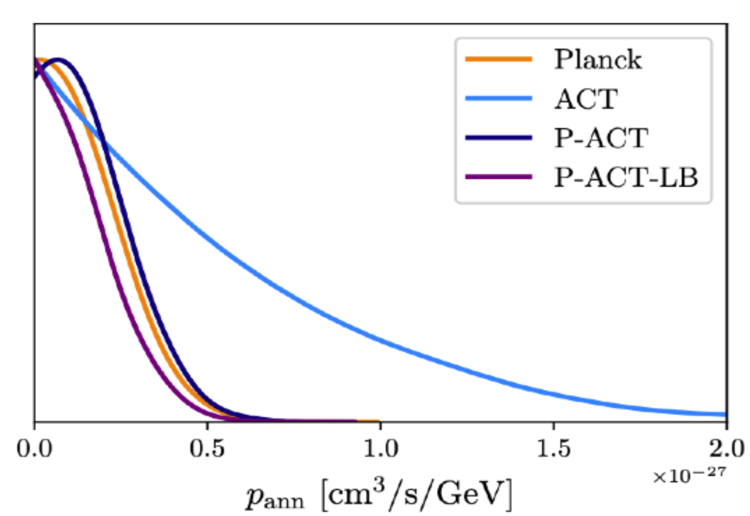

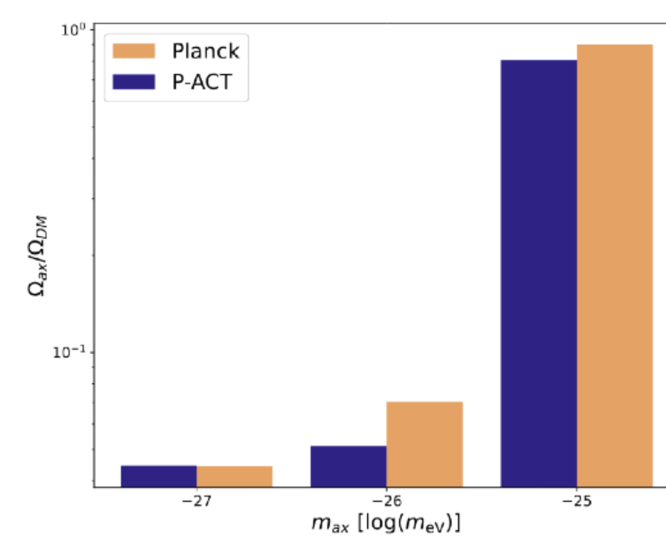

Late-time physics: dark energy

From primary CMB data, we find no evidence for non-standard dark energy; hints of non-standard evolution are driven by low-redshift data and consistent with previous analyses of DESI and SNIa data.

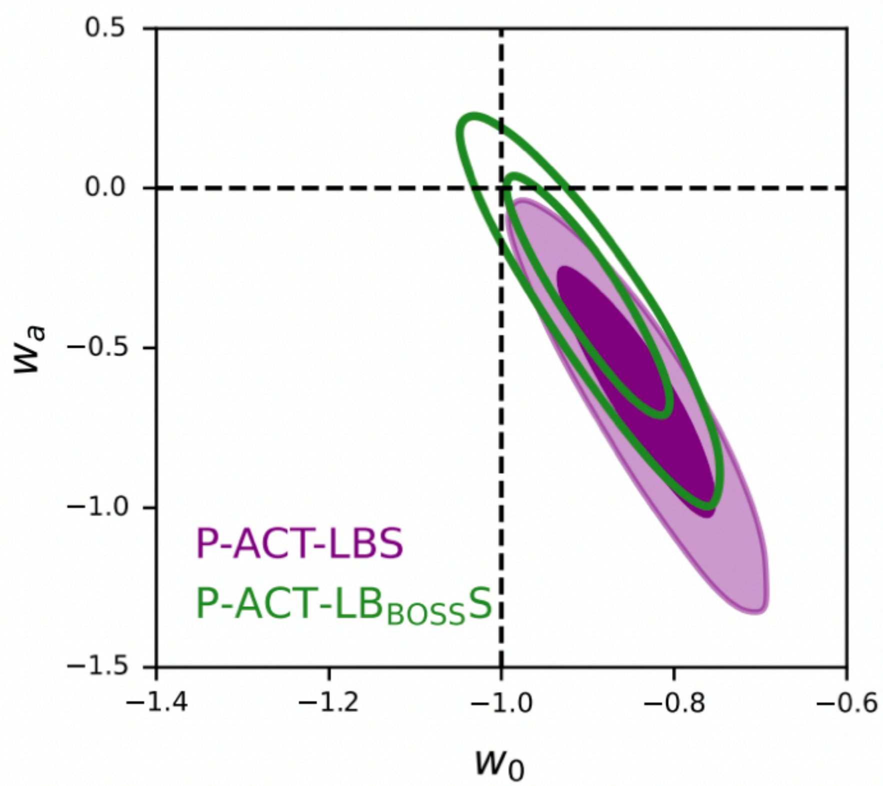

Figure 37. Constraints on the dark energy equation of state parameters, varying both today's value, w_0, and its time variation, w_a. Similar to other studies, we find that DESI drives a preference for time-varying dark energy (compared to the dashed ΛCDM line), which is relaxed when considering BOSS BAO instead (green contours). The CMB contribution to this measurement is sub-dominant, apart from breaking parameter degeneracies, with Planck, W-ACT, and P-ACT giving similar results.

P-ACT-LBS consistent with Λ at 2.2σ [P-LBS (in)consistent with Λ at 2.5σ (DESI+2024)]

$$\left.\begin{aligned} w_0 &= -0.837 \pm 0.061 \\ w_a &= -0.66^{+0.27}_{-0.24} \end{aligned}\right\} \text{(68\%, P-ACT-LBS)}$$

Late-time physics: modified growth

We also see no evidence of modified growth, e.g., due to beyond-GR gravity (modulo two slightly outlying $f\sigma_8$ measurements at very low redshifts).

$$f(a) = \Omega_m^{\gamma}(a)$$

$$\left.\begin{aligned} \gamma &= 0.663 \pm 0.052 \\ S_8 &= 0.799 \pm 0.012 \end{aligned}\right\} \text{(68\%, P-ACT-LB)}$$

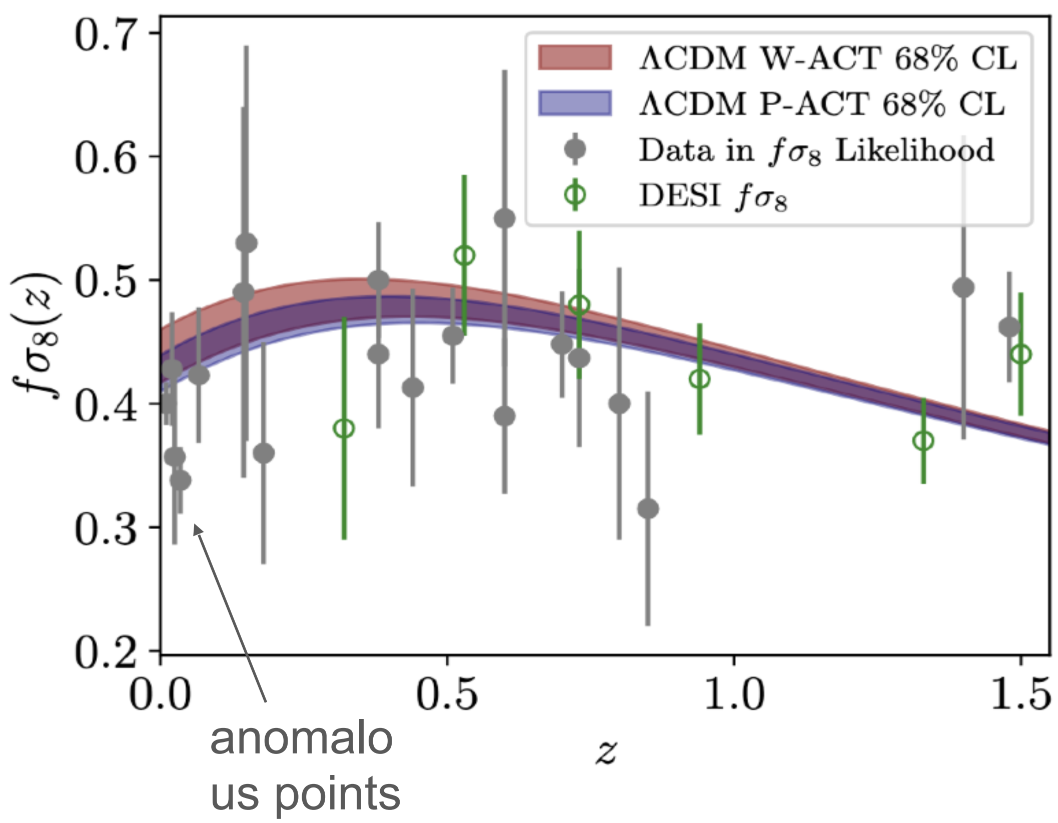

$f\sigma_8$

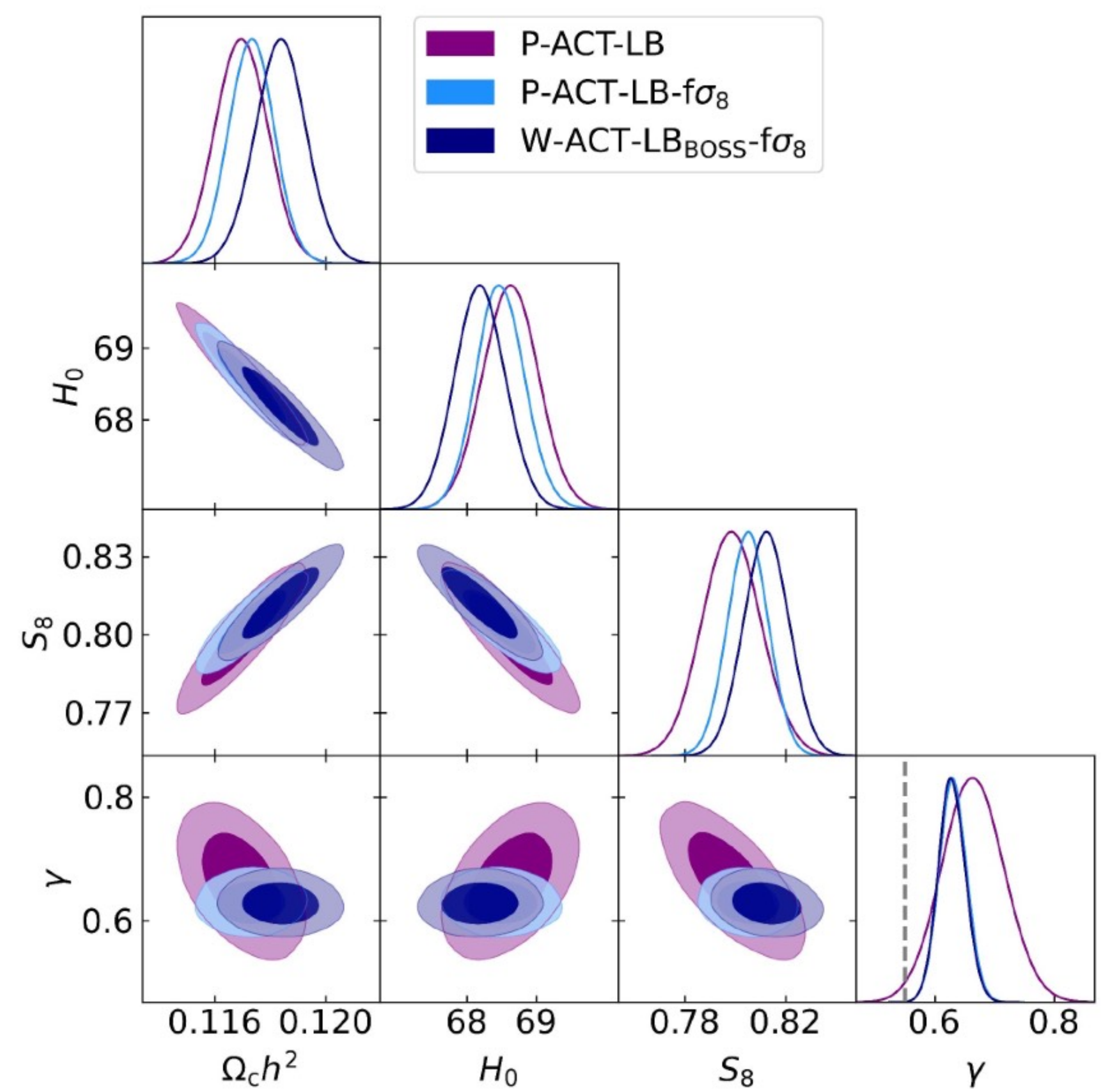

DR6 data set test

We have done around 2000 null tests on the data, we checked that the results do not depends on

- array bands
- weather conditions
- scan elevation
- sky location
- time of observation
- detectors positions

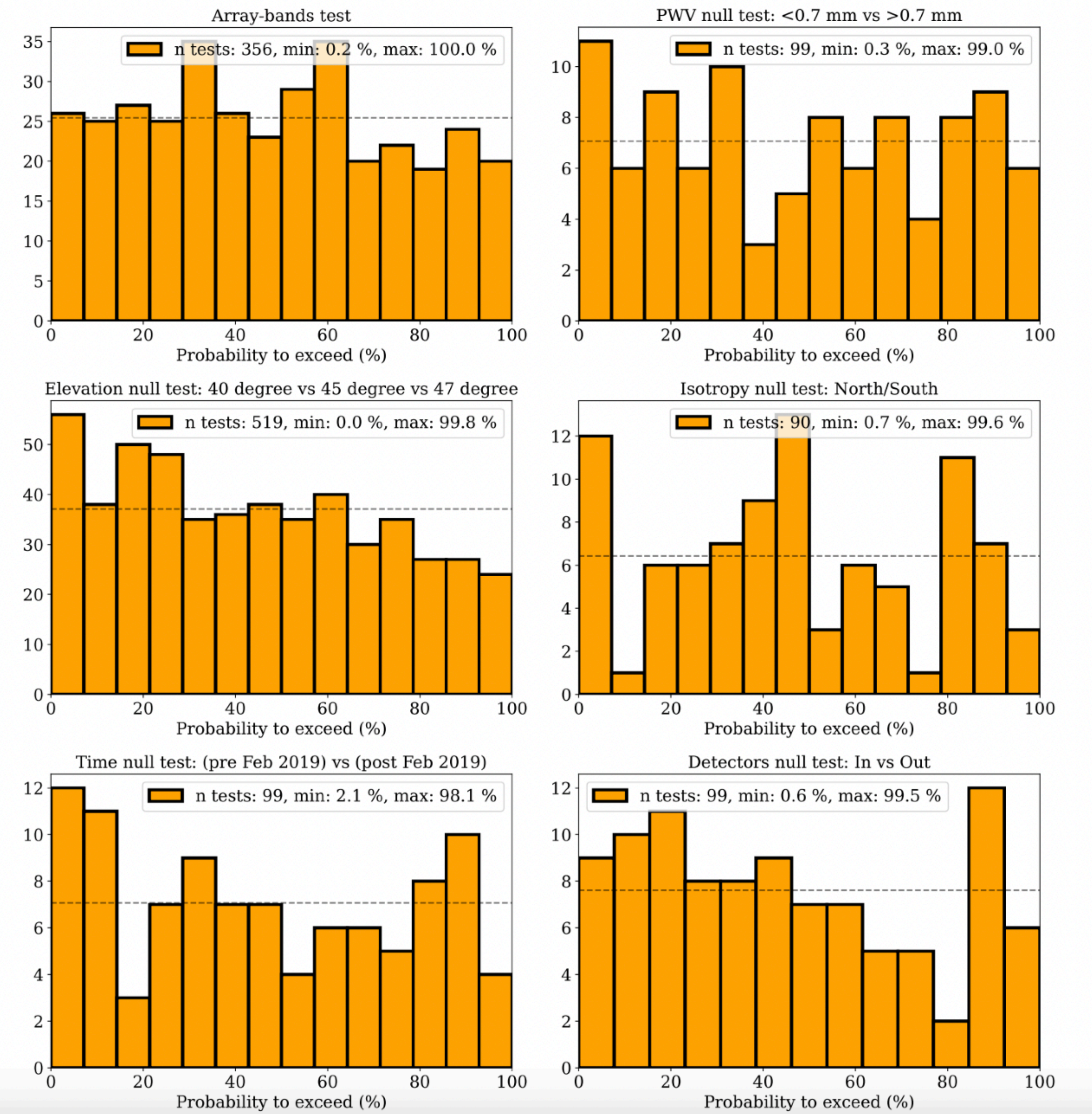

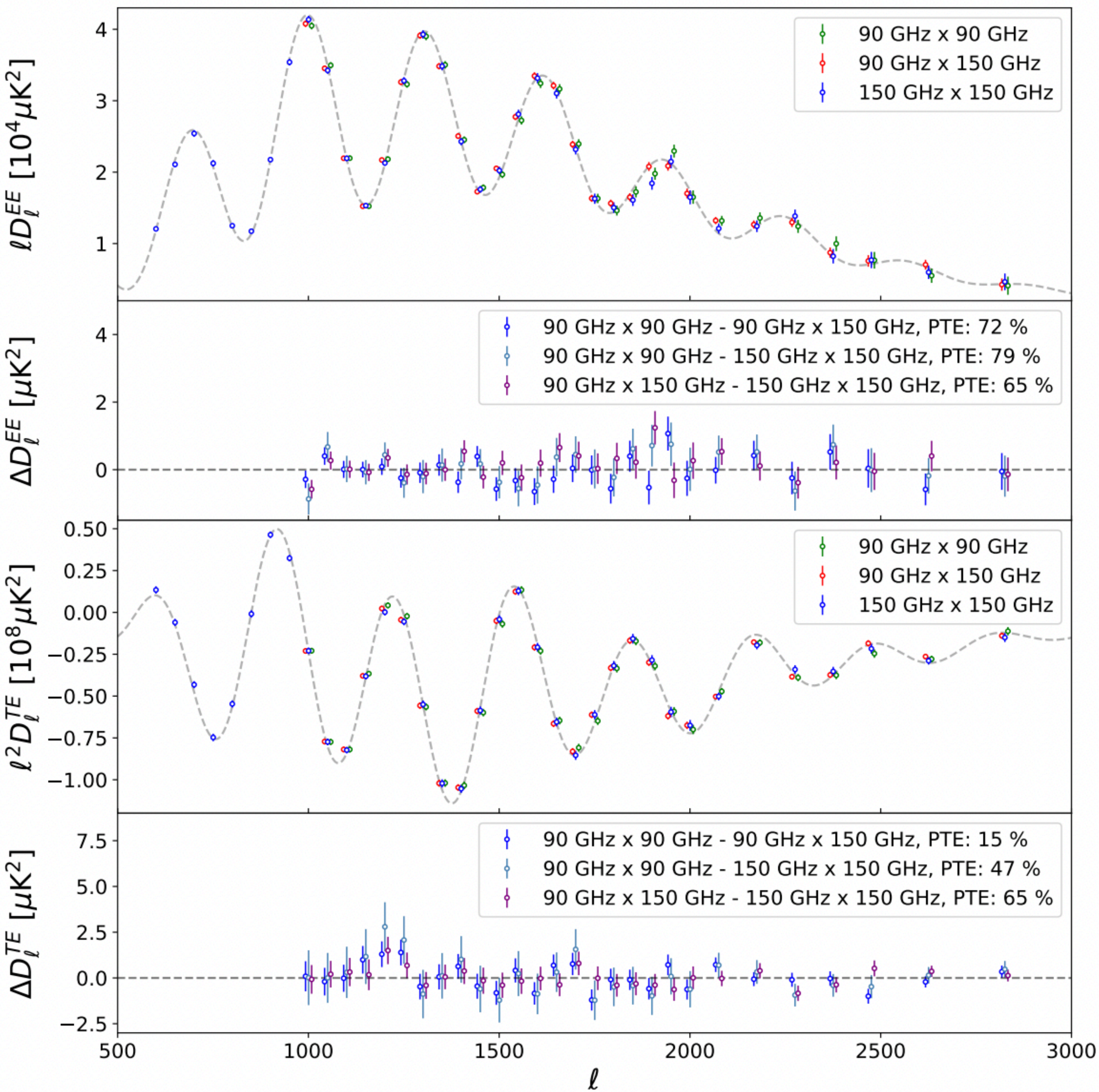

90 GHz x 90 GHz
90 GHz x 150 GHz
150 GHz x 150 GHz
ℓD_ℓ^{EE} [$10^4\mu$K^2]
90 GHz x 90 GHz - 90 GHz x 150 GHz, PTE: 72 %
90 GHz x 90 GHz - 150 GHz x 150 GHz, PTE: 79 %
90 GHz x 150 GHz - 150 GHz x 150 GHz, PTE: 65 %
ΔD_ℓ^{EE} [μK^2]
90 GHz x 90 GHz
90 GHz x 150 GHz
150 GHz x 150 GHz
$\ell^2 D_\ell^{TE}$ [$10^8\mu$K^2]
90 GHz x 90 GHz - 90 GHz x 150 GHz, PTE: 15 %
90 GHz x 90 GHz - 150 GHz x 150 GHz, PTE: 47 %
90 GHz x 150 GHz - 150 GHz x 150 GHz, PTE: 65 %
ΔD_ℓ^{TE} [μK^2]
ℓ

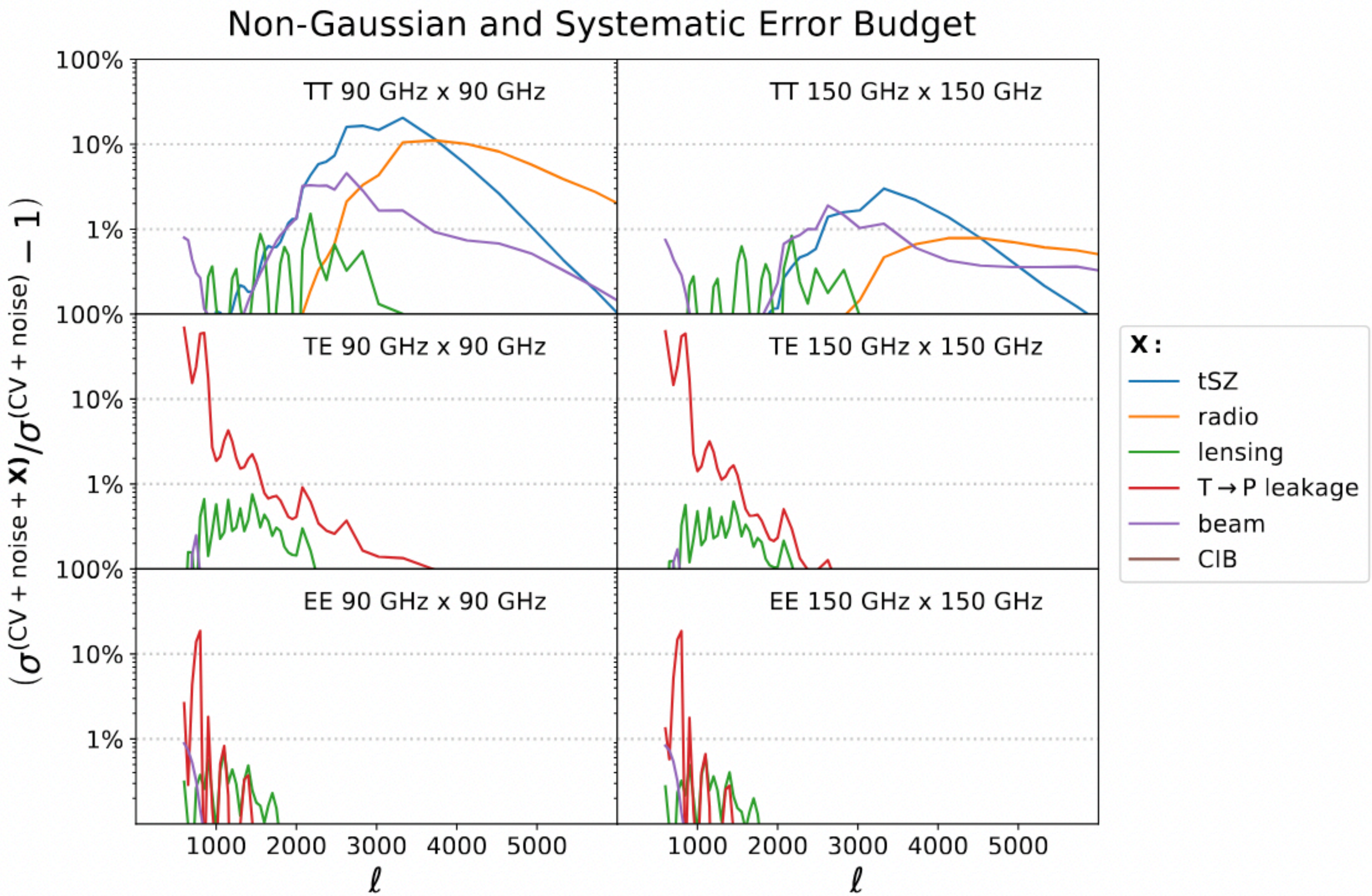

Figure 4. Relative contributions of additional error terms compared to cosmic variance and noise. The contributions to σ_{TT} are shown in the top panel for 90 GHz (left) and 150 GHz (right). For f090, uncertainties from non-Gaussian tSZ and non-Gaussian radio sources are important on small scales. The contribution from unclustered CIB non-Gaussianity is smaller than 0.1% and not visible in the figure. The middle panel shows the contributions to σ_{TE}, where uncertainties in the measurement of the leakage beam are a significant source of uncertainty on large scales. The bottom panel highlights that these uncertainties only mildly affect σ_{EE}, reaching up to 15% at $\ell = 800$. In addition to increasing errors, the additional covariance contributions also result in nonzero off-diagonal correlations.

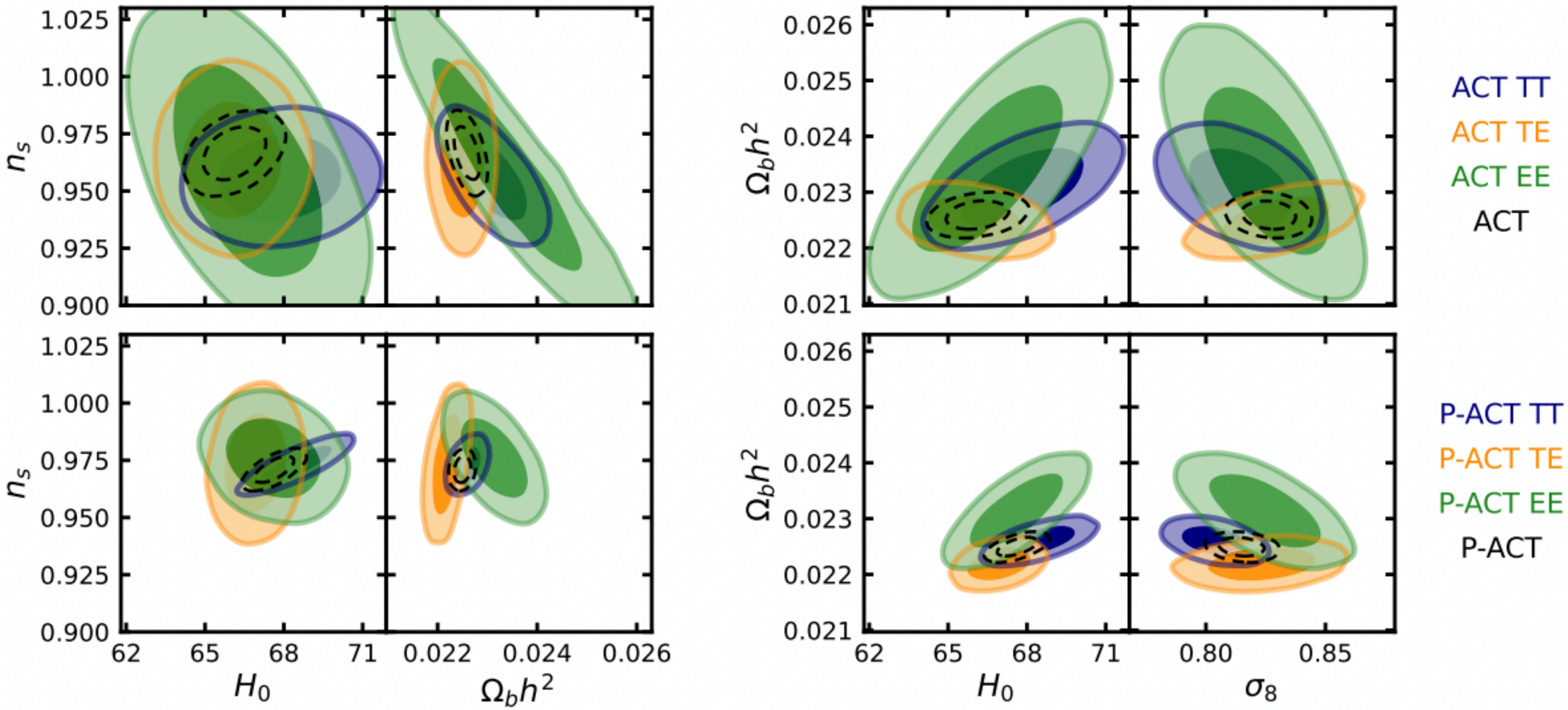

Figure 14. Cosmological parameter distributions estimated from TT, TE or EE from ACT (top) and P-ACT (bottom), including the optical depth prior. Black dashed contours correspond to the distributions estimated from TT, TE, and EE simultaneously, again for ACT (top) and P-ACT (bottom). A prior on the ACT polarization efficiencies, derived from the joint T+E fit, is imposed for the ACT (top) results. For ACT, the TE data provide the tightest constraints on the baryon density, cold dark matter density and the Hubble constant, while the TT data best measure the spectral index. The EE-only constraints are now competitive with those from TT and TE. There is less foreground contamination in the TE and EE spectra than TT; the consistent results add confidence in the model.

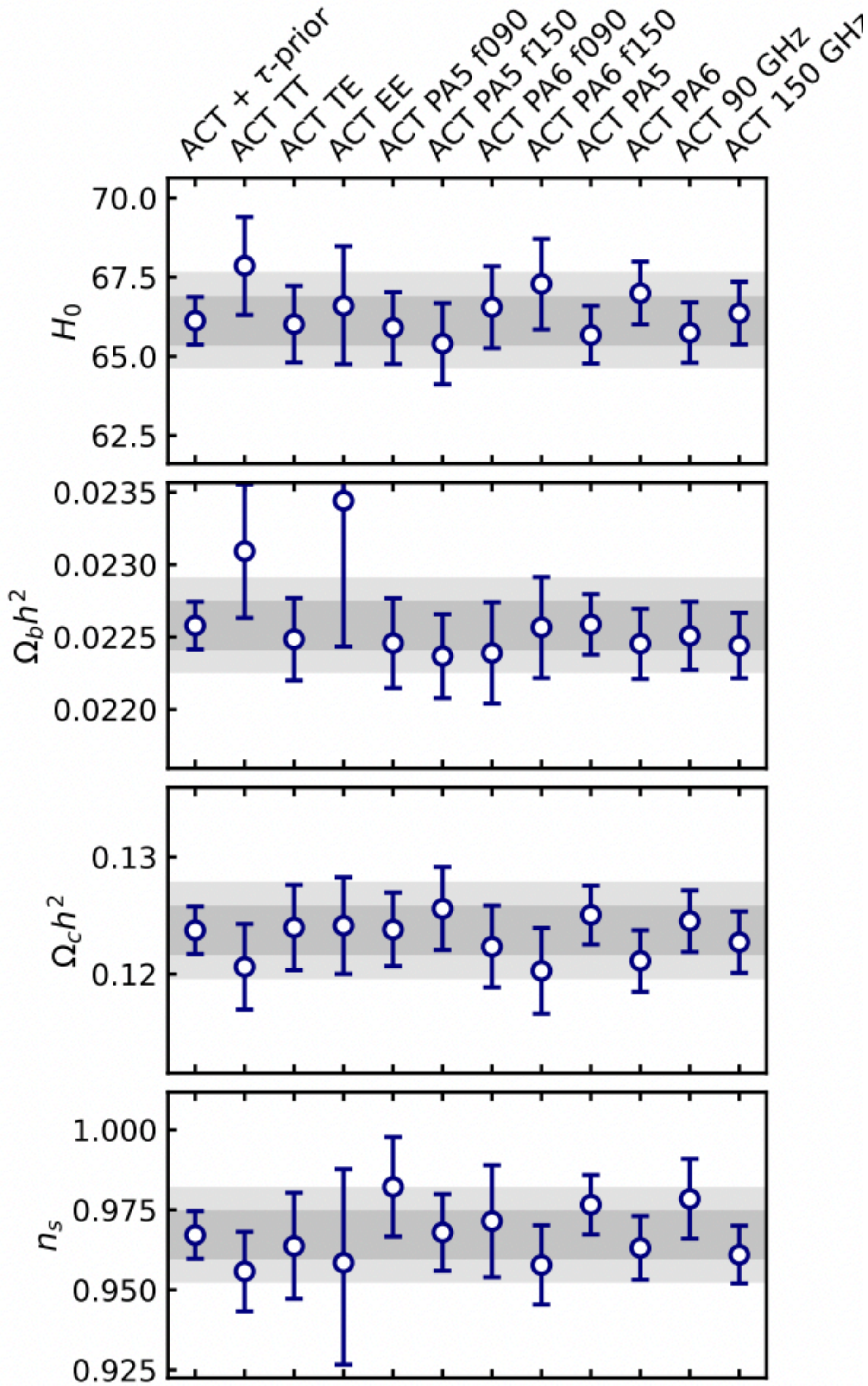

Figure 13. 1D marginalized 68% confidence levels (CL) on cosmological parameters estimated from subsets of the ACT DR6 dataset. The baryon and CDM densities are best measured by the TE spectrum, and the spectral index by the TT spectrum. The different arrays and frequencies give consistent results. All the results shown here use the same optical depth prior. The shaded band shows the 68% and 95% CL on the baseline ACT results.

Breakdown of goodness-of-fit for P-ACT

TT:

- ACT: 566.05/601
- Planck: 89.05/114

TE:

- ACT: 651.77/644
- Planck: 67.82/69

EE:

- ACT: 392.19/406
- Planck: 68.93/69

Measuring H0 from the CMB

Measuring the Hubble constant using the CMB

The angular size of the sound horizon is given as the ratio of the physical size of the sound horizon and the diameter angular distance of the last scattering surface

$$\theta_* = r_s^*/D_A^*$$

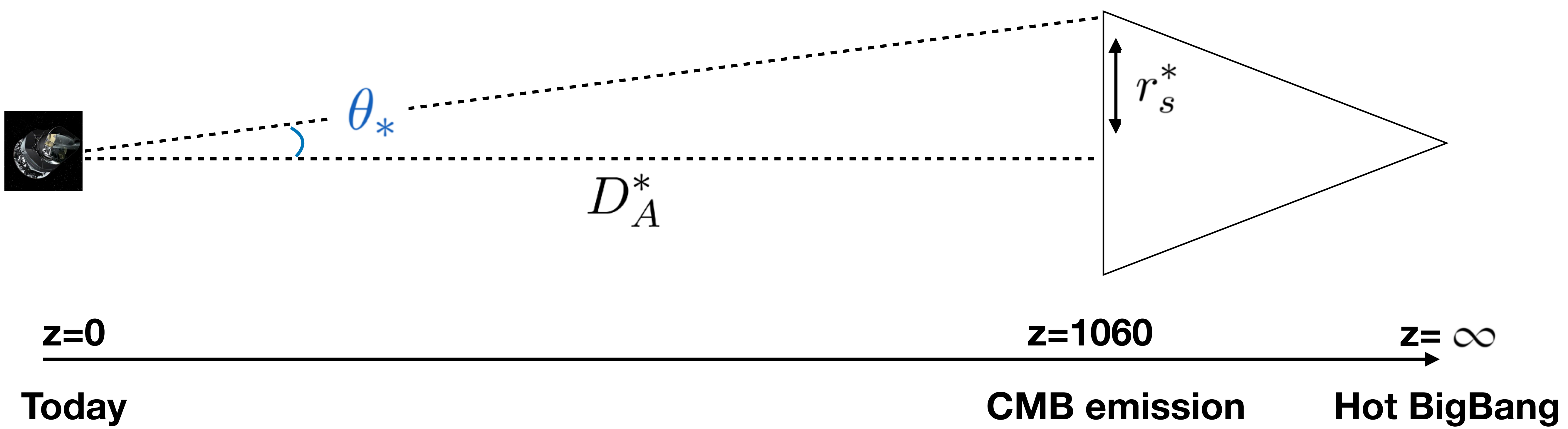

Measuring the Hubble constant using the CMB

The angular size of the sound horizon is given as the ratio of the physical size of the sound horizon and the diameter angular distance of the last scattering surface

$$\theta_* = r_s^*/D_A^*$$

$$r_s^* = \int_0^{t^*} \frac{dt}{a(t)} c_s(t) = \int_{z^*}^{\infty} \frac{dz}{H(z)} c_s(z)$$

r_s^* **is fully determined by the cosmological parameters we have measured**

$$c_s(z) = c\sqrt{\frac{1}{3\left[1 + 3\rho_b^0/4\rho_\gamma^0(1+z)^{-1}\right]}}$$

$$\left.\frac{3H^2(z)}{8\pi G}\right|_{\text{high z}} = \left[\rho_{\text{rad}}^0(1+z)^4 + (\rho_b^0 + \rho_{\text{CDM}}^0)(1+z)^3\right]$$

We know r_s^* **and** θ_* **this gives us** D_A^*

$$D_A^* = c\int_0^{z^*} \frac{dz}{H(z)}$$

$$\left.\frac{3H^2(z)}{8\pi G}\right|_{\text{low z}} = \left[(\rho_b^0 + \rho_{\text{CDM}}^0)(1+z)^3 + \rho_\Lambda\right]$$

Which gives us ρ_Λ

Once ρ_Λ **known, we get** H_0

PR3 and PR4

Comparison with Planck PR4 (NPIPE)

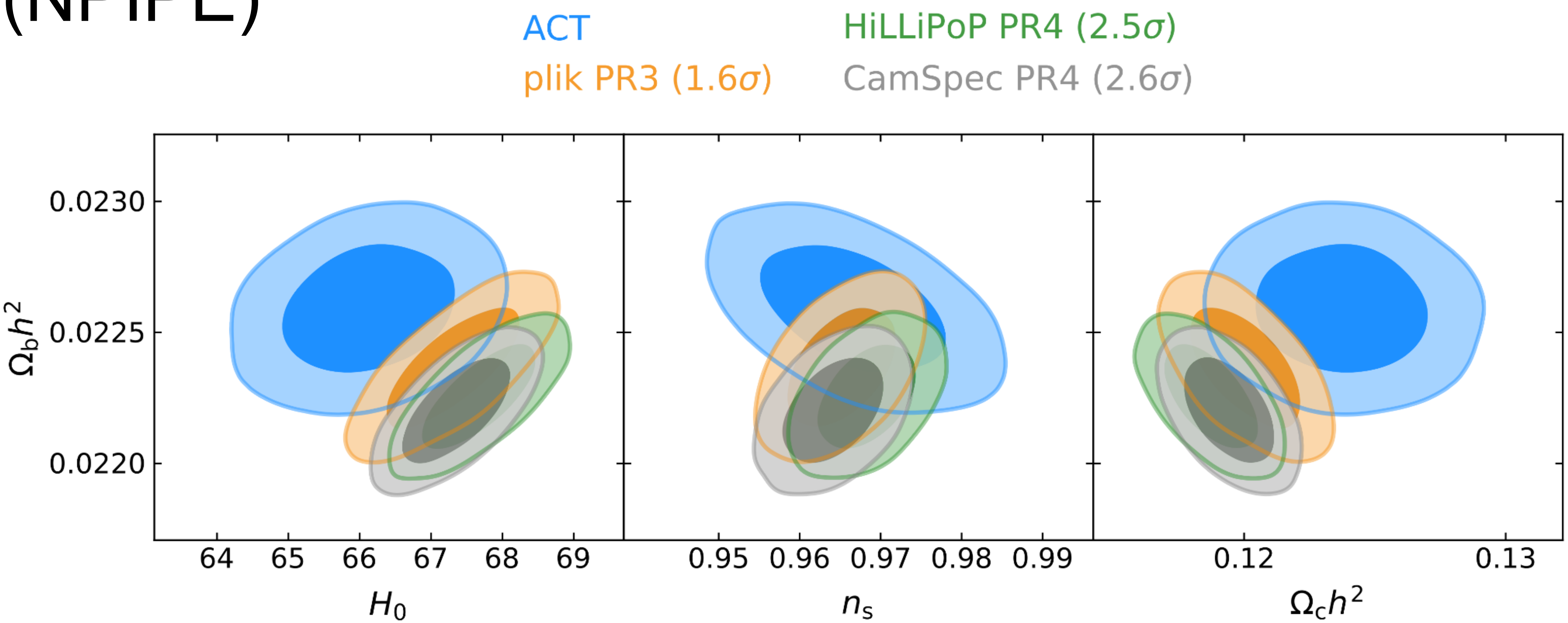

HiLLiPoP/NPIPE, curvature

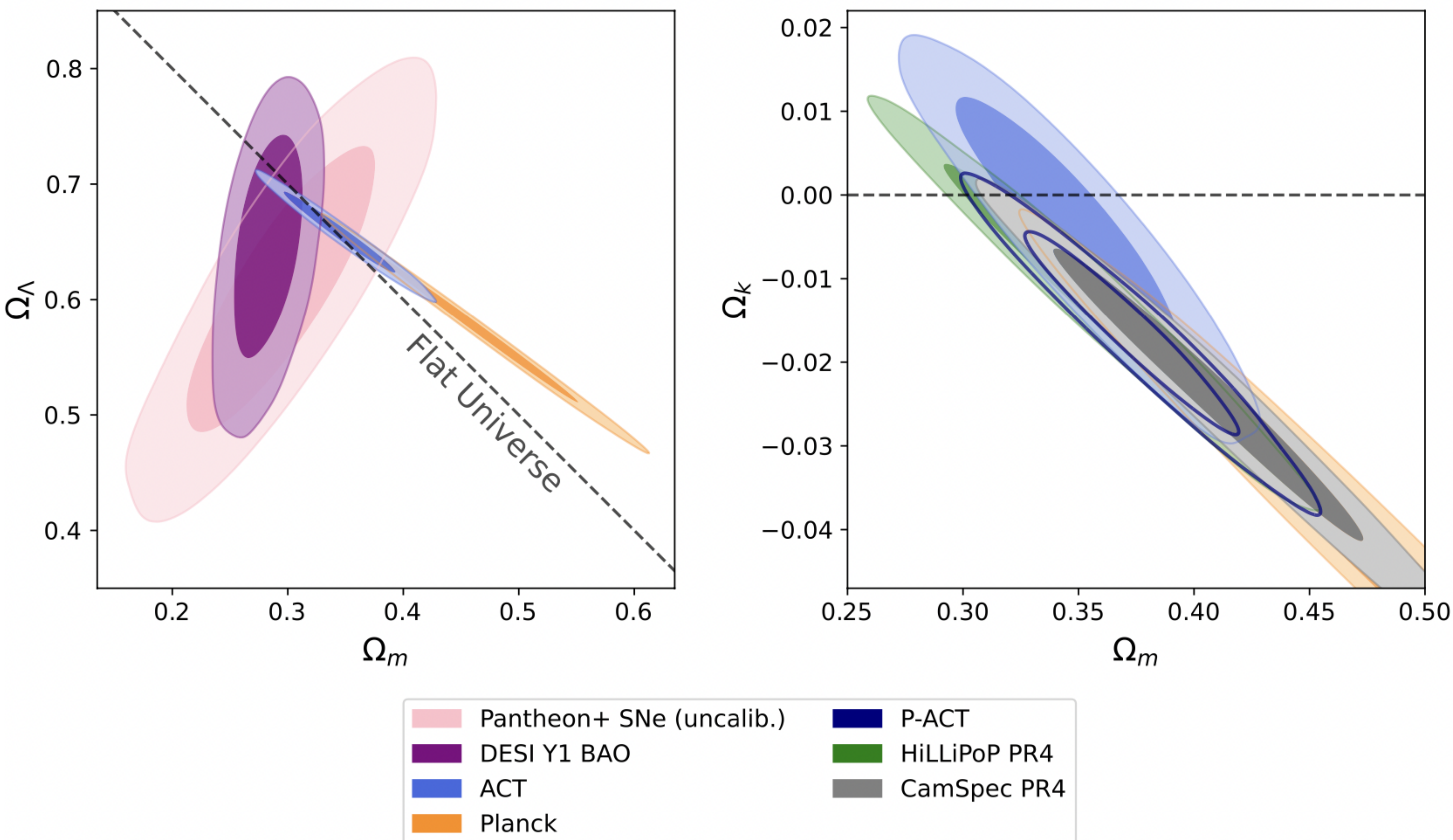

ACT and Planck on the same patch of the sky

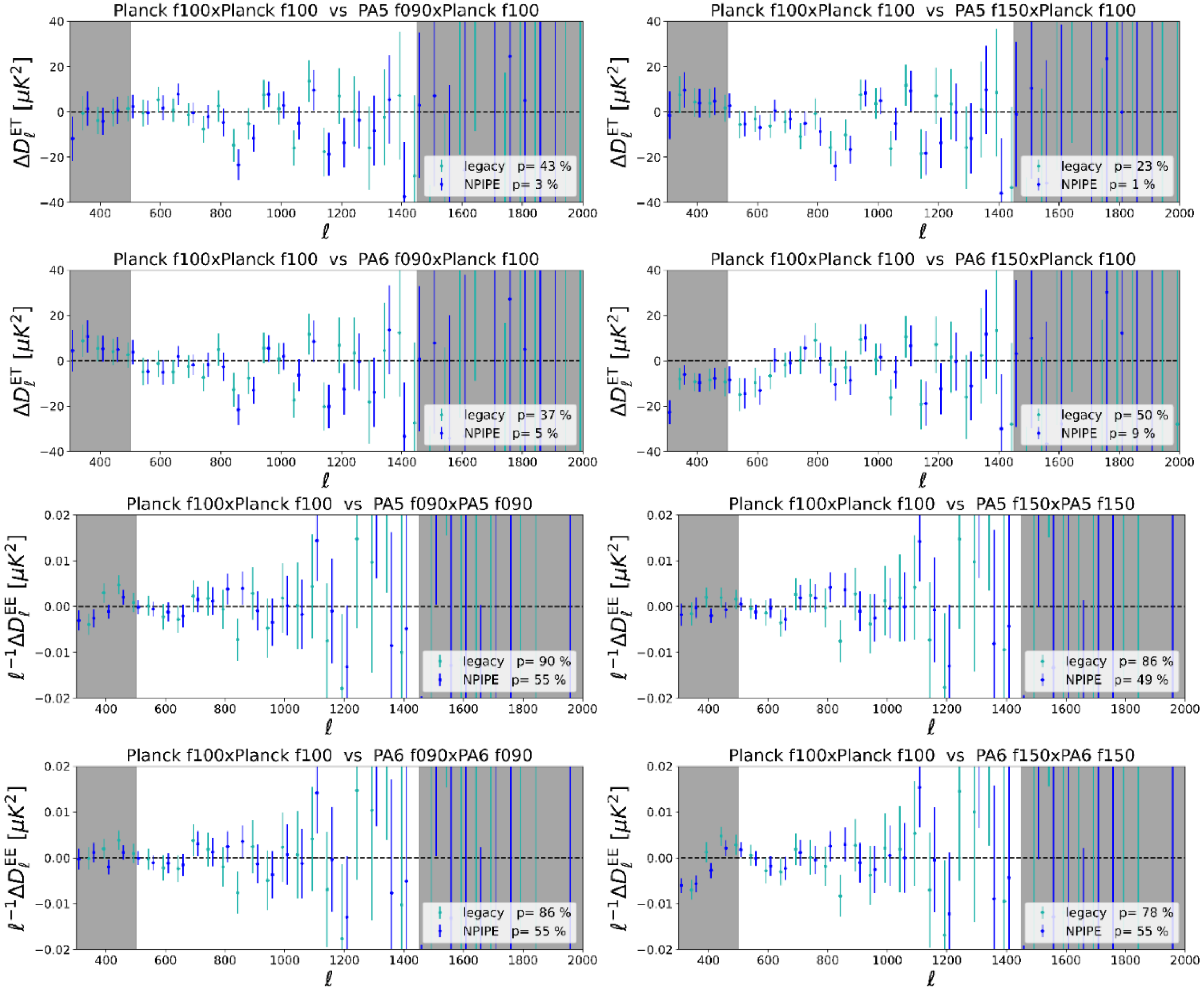

ACT and Planck on the same patch of the sky

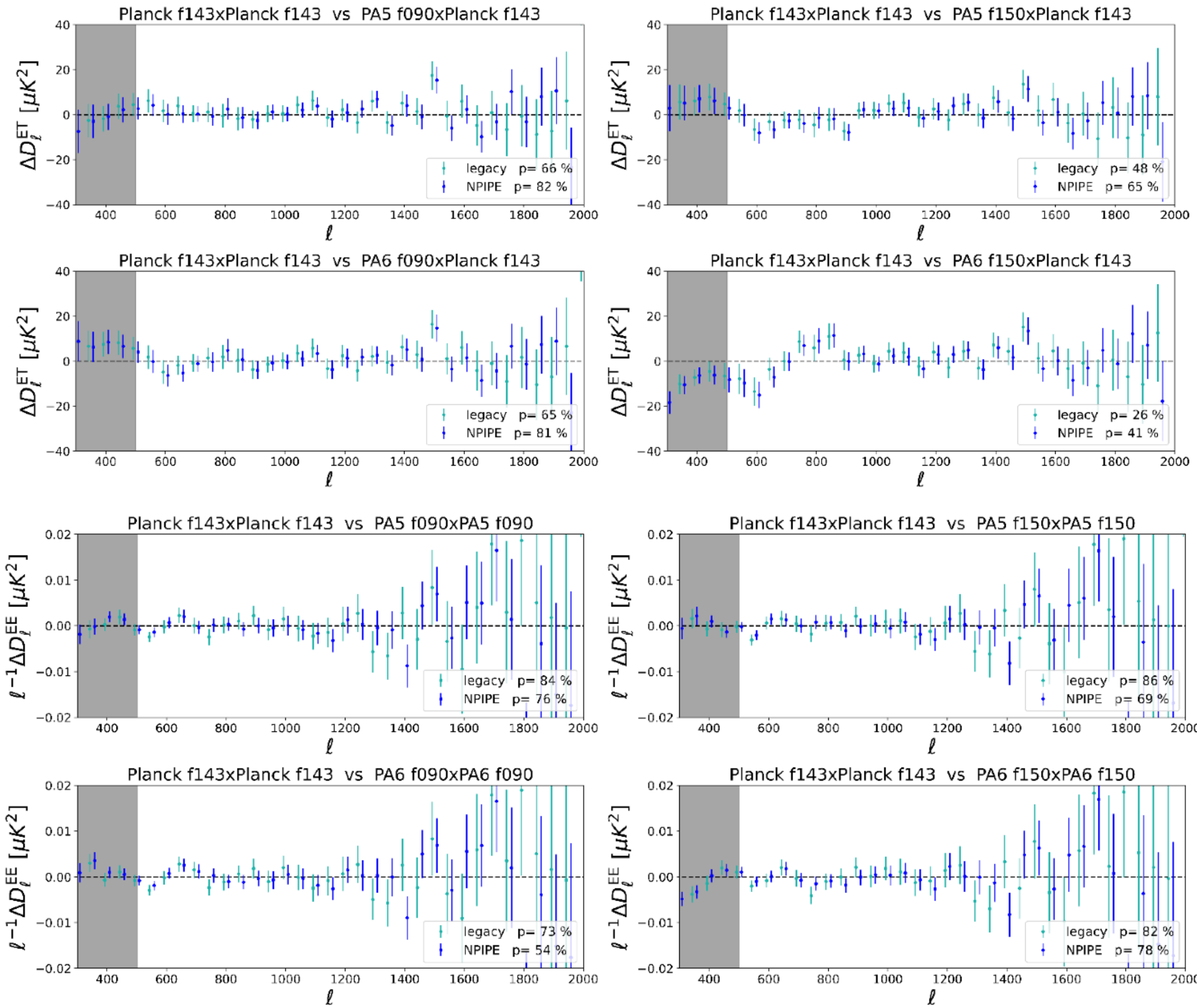

ACT and Planck on the same patch of the sky

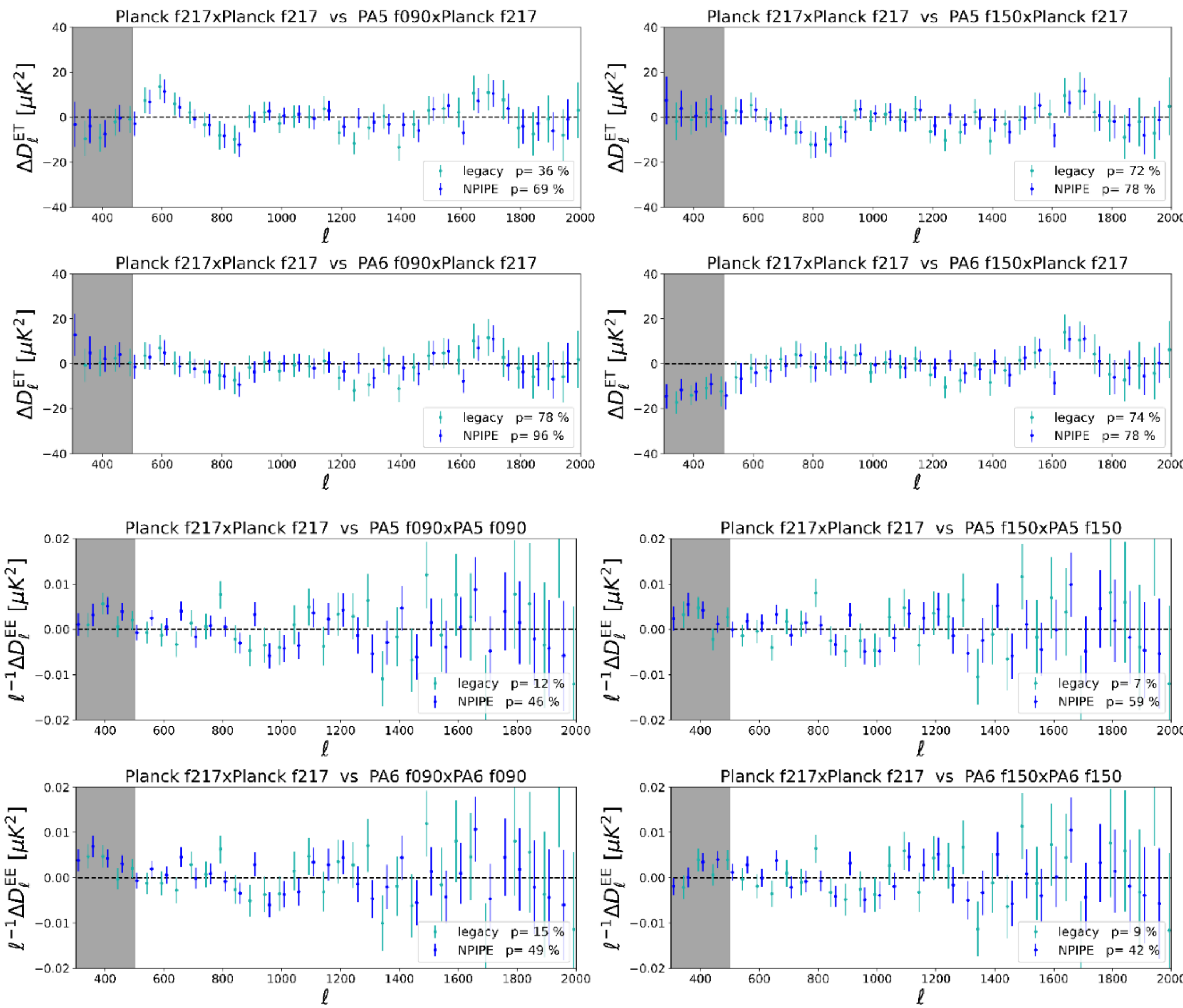

Comparison with Planck PR4 (NPIPE)

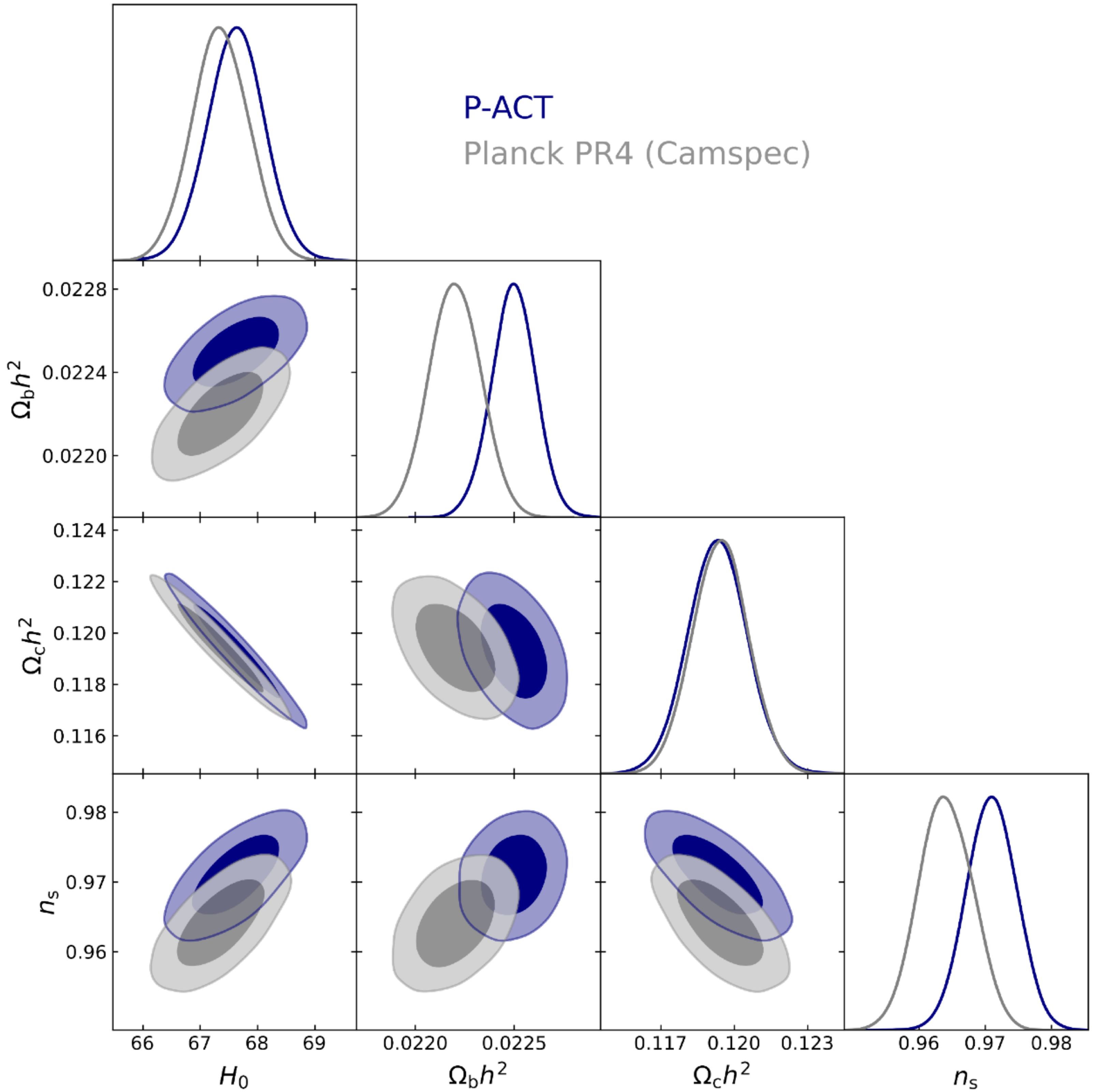

Birefringence

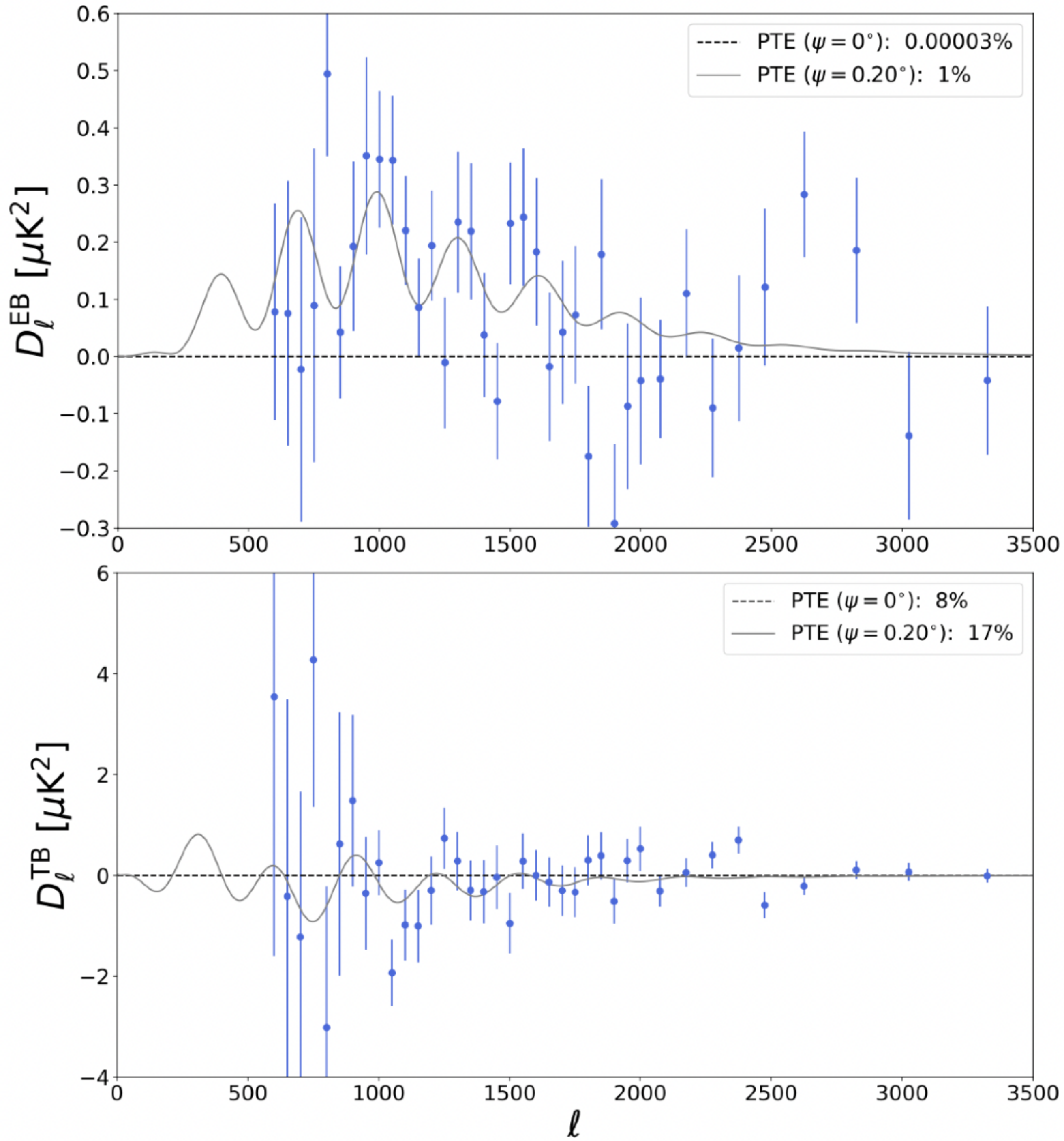
PTE ($\psi = 0^\circ$): 0.00003%
PTE ($\psi = 0.20^\circ$): 1%
D_ℓ^{EB} [μK^2]
PTE ($\psi = 0^\circ$): 8%
PTE ($\psi = 0.20^\circ$): 17%
D_ℓ^{TB} [μK^2]
ℓ

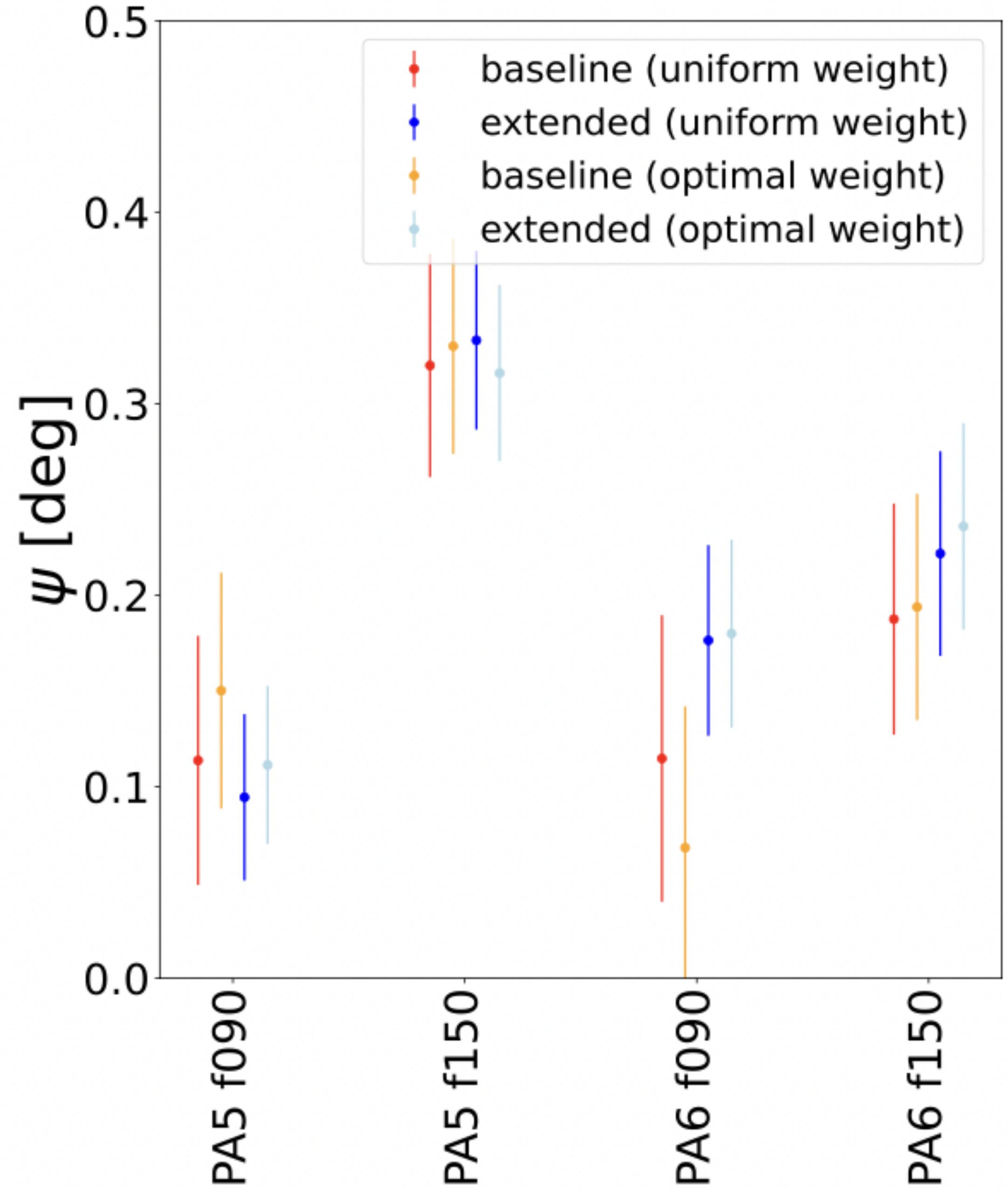
baseline (uniform weight)
extended (uniform weight)
baseline (optimal weight)
extended (optimal weight)
ψ [deg]
PA5 f090
PA5 f150
PA6 f090
PA6 f150

Post unblinding

Cosmo

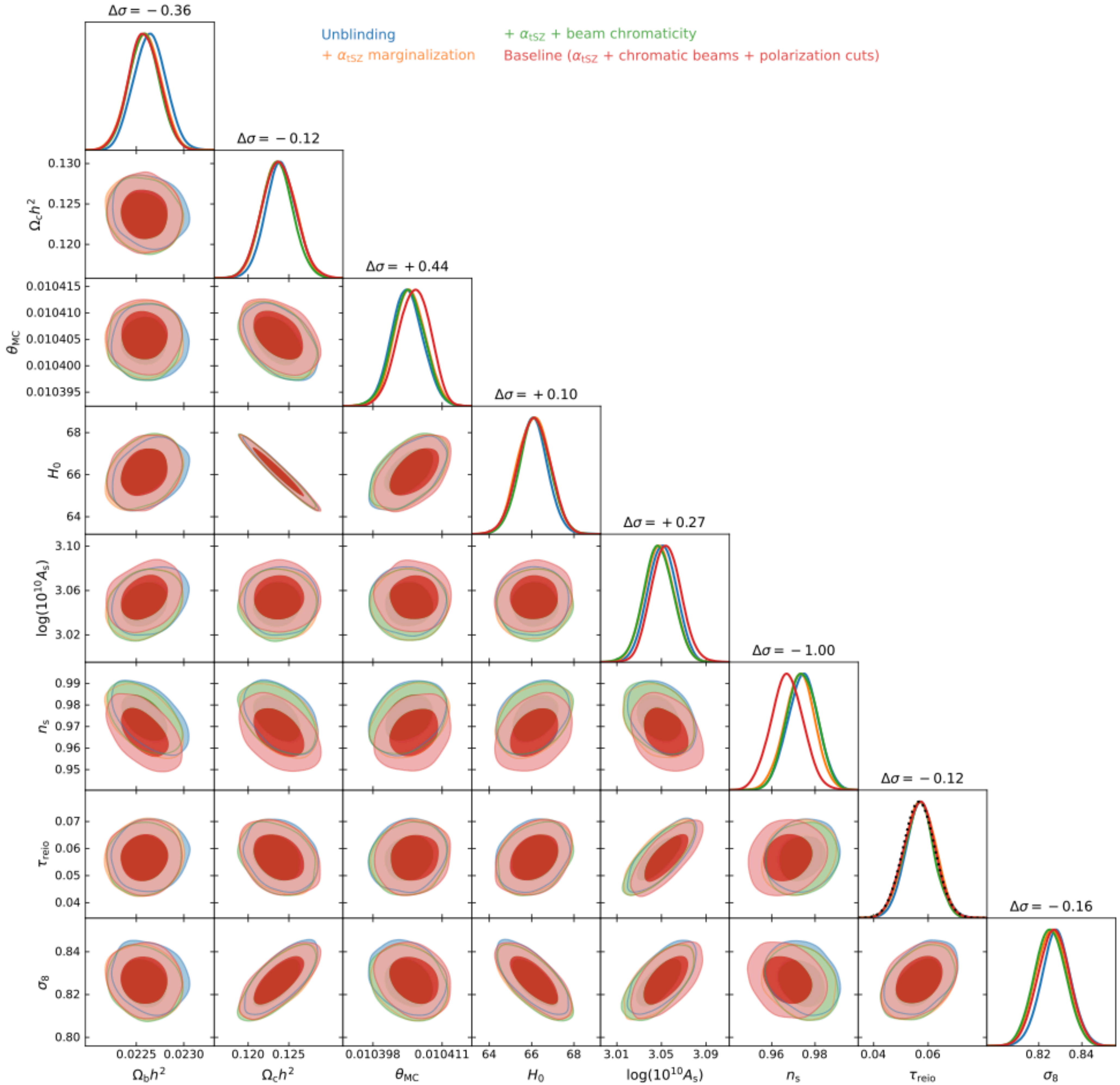

Unblinding
+ α_{tSZ} marginalization
+ α_{tSZ} + beam chromaticity
Baseline (α_{tSZ} + chromatic beams + polarization cuts)
$\Delta\sigma = -0.36$
$\Delta\sigma = -0.12$
$\Delta\sigma = +0.44$
$\Delta\sigma = +0.10$
$\Delta\sigma = +0.27$
$\Delta\sigma = -1.00$
$\Delta\sigma = -0.12$
$\Delta\sigma = -0.16$
$\Omega_b h^2$
$\Omega_c h^2$
θ_{MC}
H_0
$\log(10^{10}A_s)$
n_s
τ_{reio}
σ_8

Astrophysical foregrounds and instrument parameters

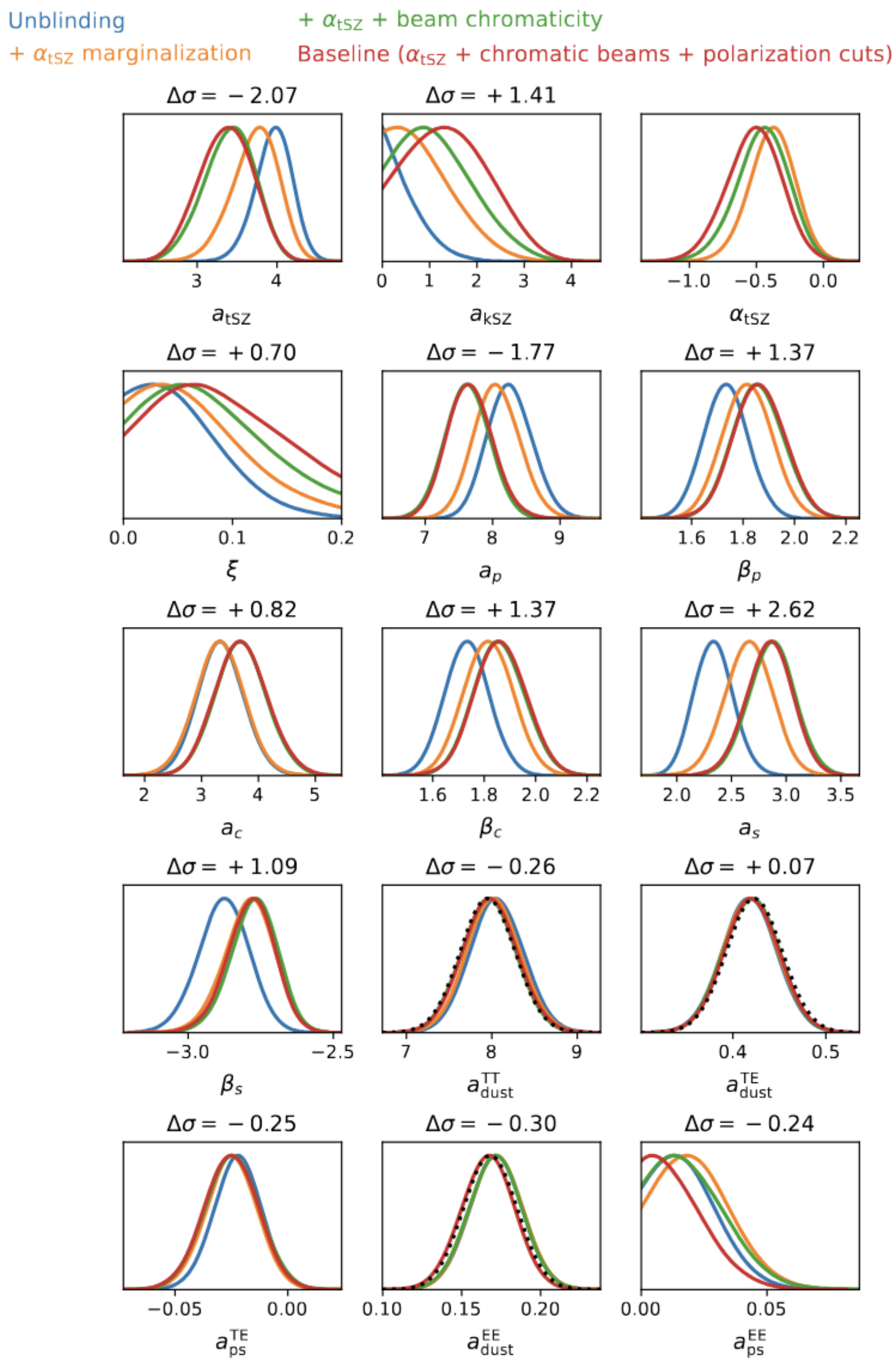

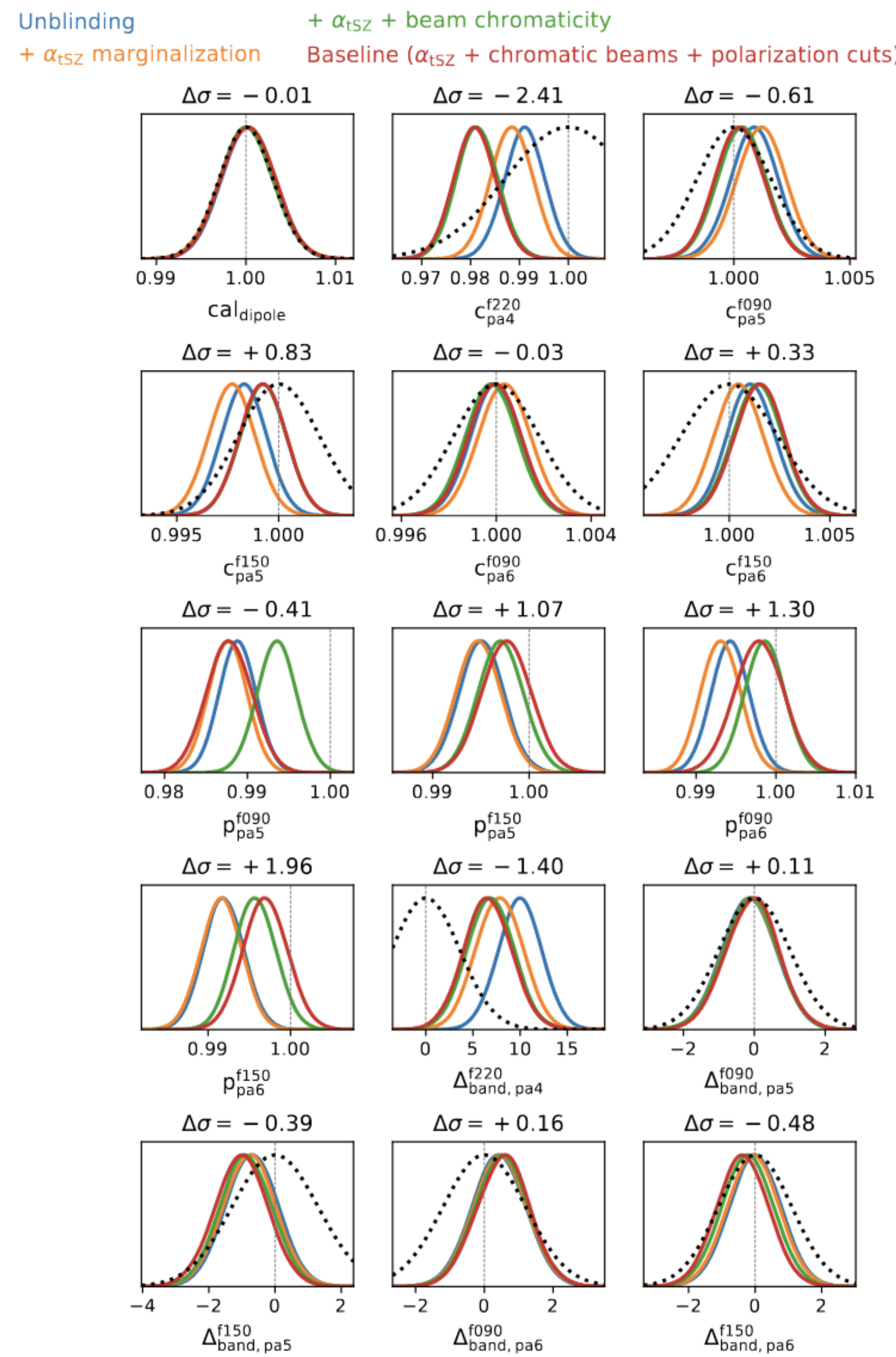

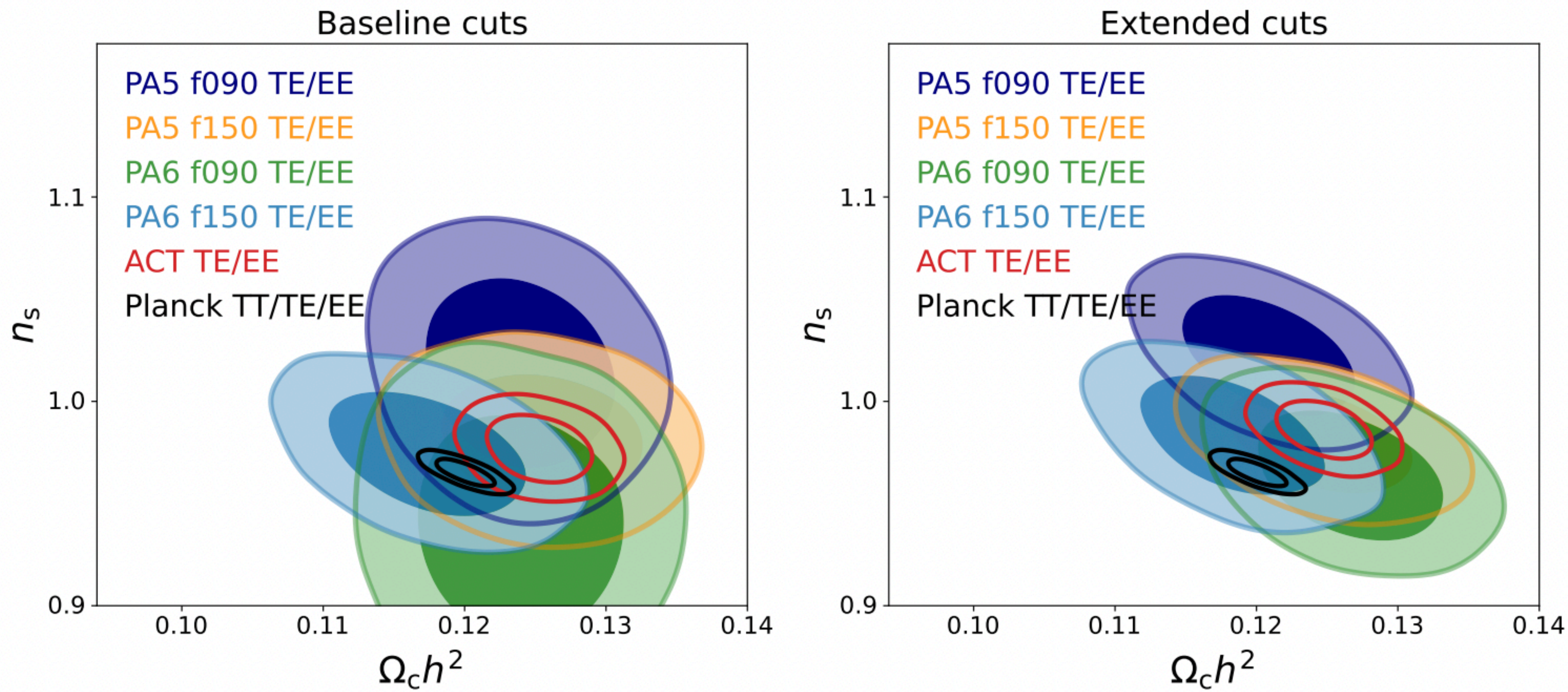

Baseline cuts
Extended cuts
PA5 f090 TE/EE
PA5 f150 TE/EE
PA6 f090 TE/EE
PA6 f150 TE/EE
ACT TE/EE
Planck TT/TE/EE
n_s
$\Omega_c h^2$
1.1
1.0
0.9
0.10
0.11
0.12
0.13
0.14

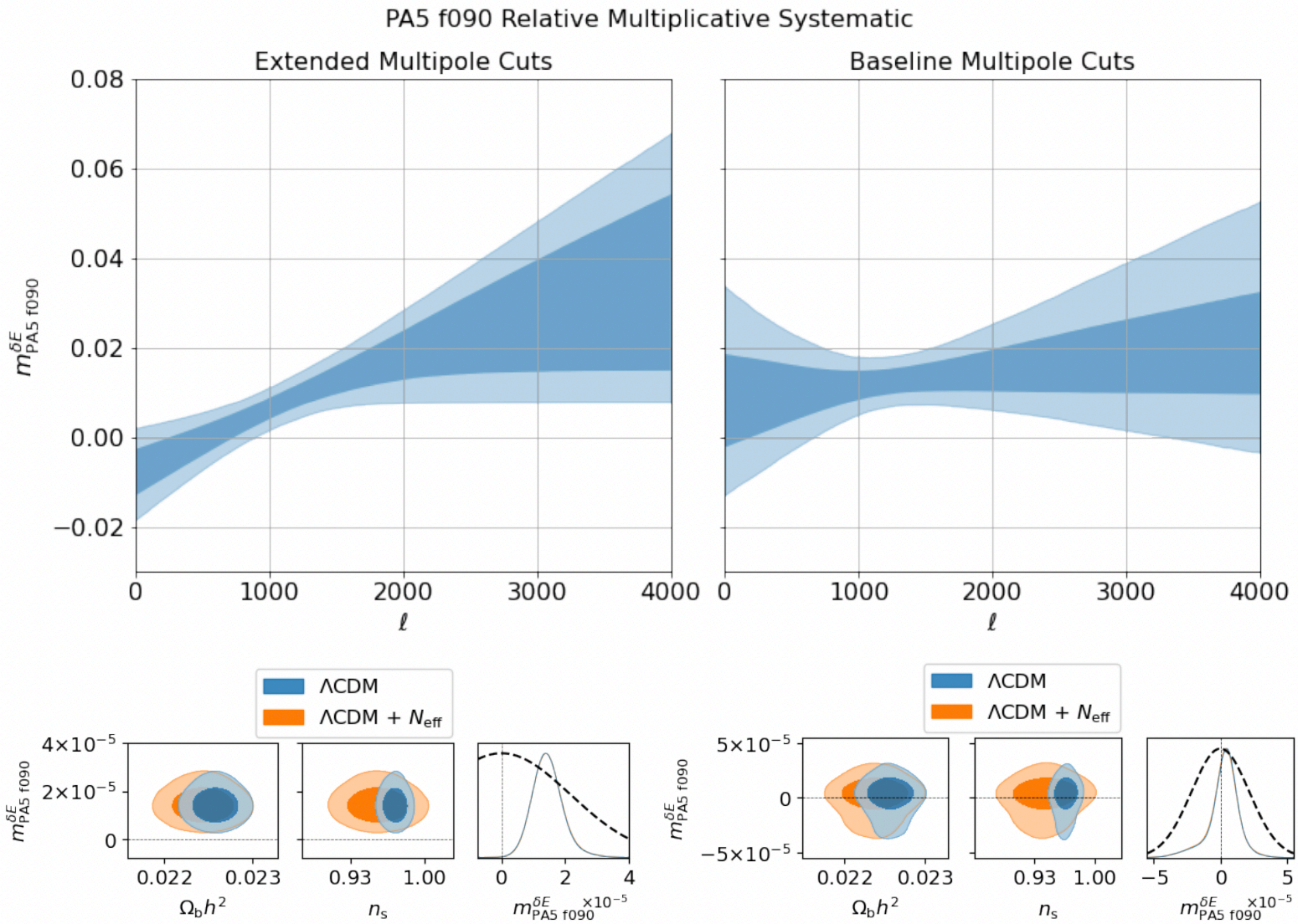

PA5 f090 Relative Multiplicative Systematic
Extended Multipole Cuts
Baseline Multipole Cuts
$m^{\delta E}_{\mathrm{PA5\ f090}}$
0.08
0.06
0.04
0.02
0.00
−0.02
0
1000
2000
3000
4000
ℓ
ΛCDM
ΛCDM + N_{eff}
4×10^{-5}
2×10^{-5}
5×10^{-5}
-5×10^{-5}
0.022
0.023
0.93
1.00
$\Omega_{\mathrm{b}}h^2$
n_{s}
$\times10^{-5}$

DR6 vs DR4

DR6 vs DR4 cosmology

- very good agreement between DR6 and DR4 baseline result obtained from ACT+WMAP
- some differences with DR4 ACT-alone cosmology
- mainly driven by TE data at multipoles <2000 (where residuals are mostly negative, disfavoring the DR6 LCDM cosmology)
- we speculate beam leakage modelling might be playing a role

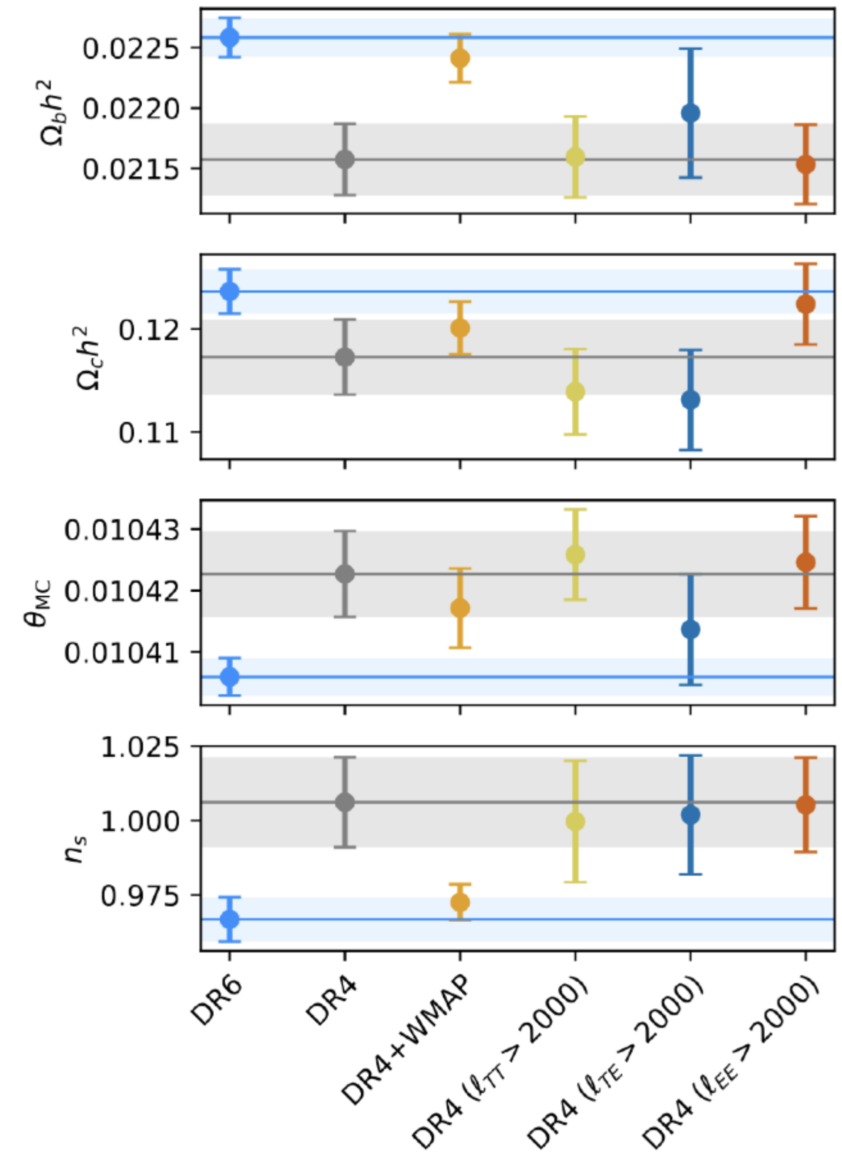

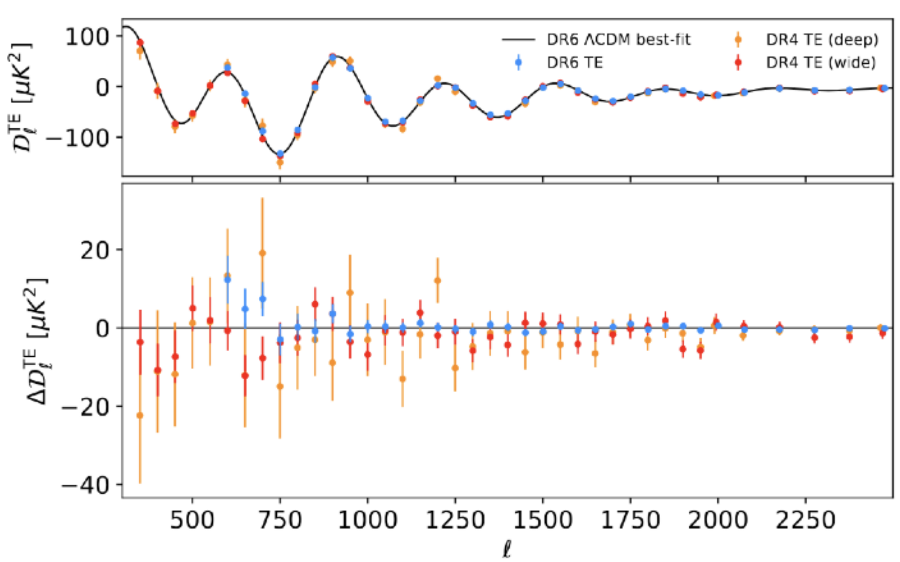

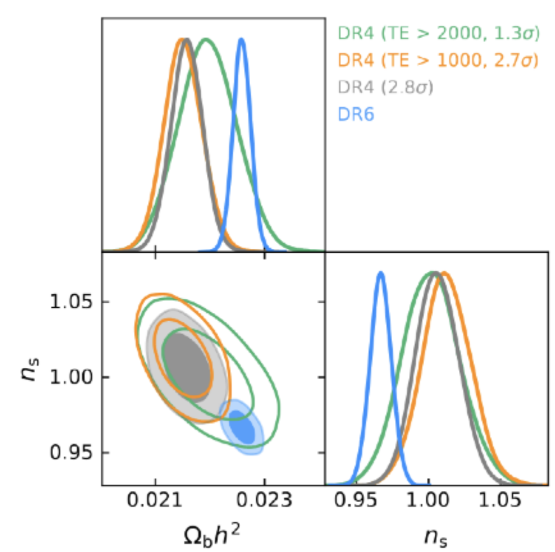

Pre- and modified recombination physics: DR4 vs. DR6 EDE constraints

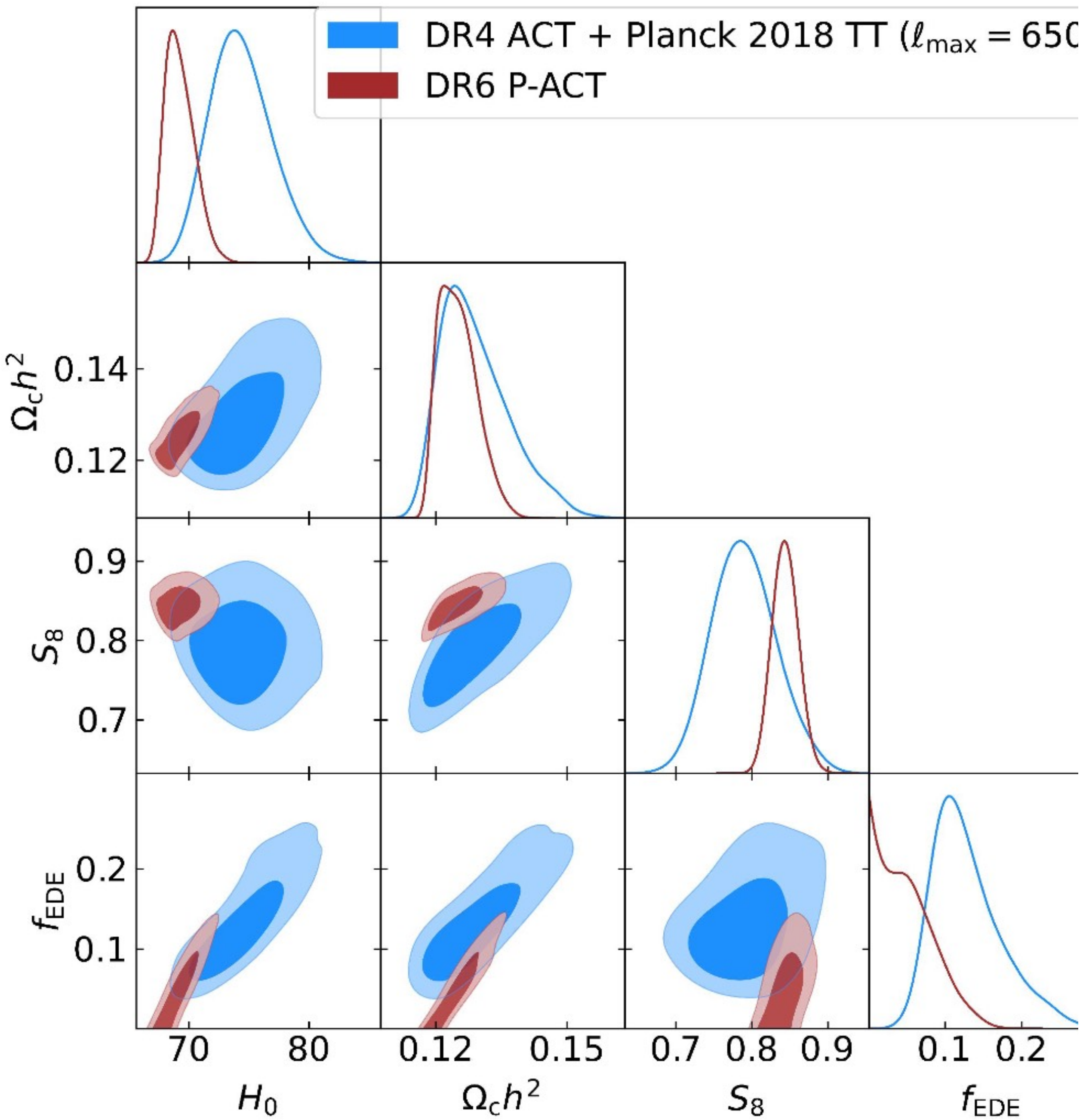

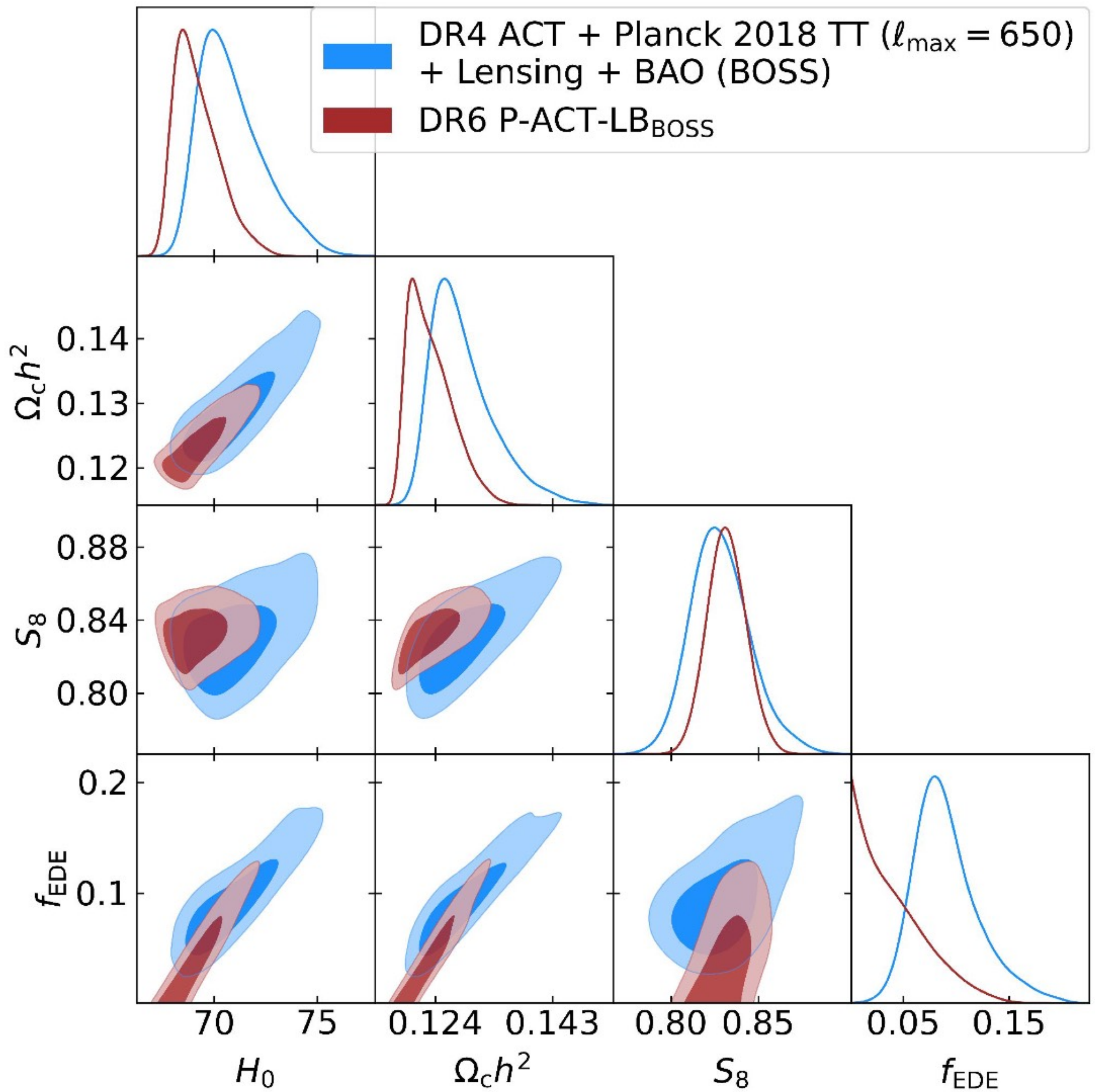

Dust in the DR6 patch

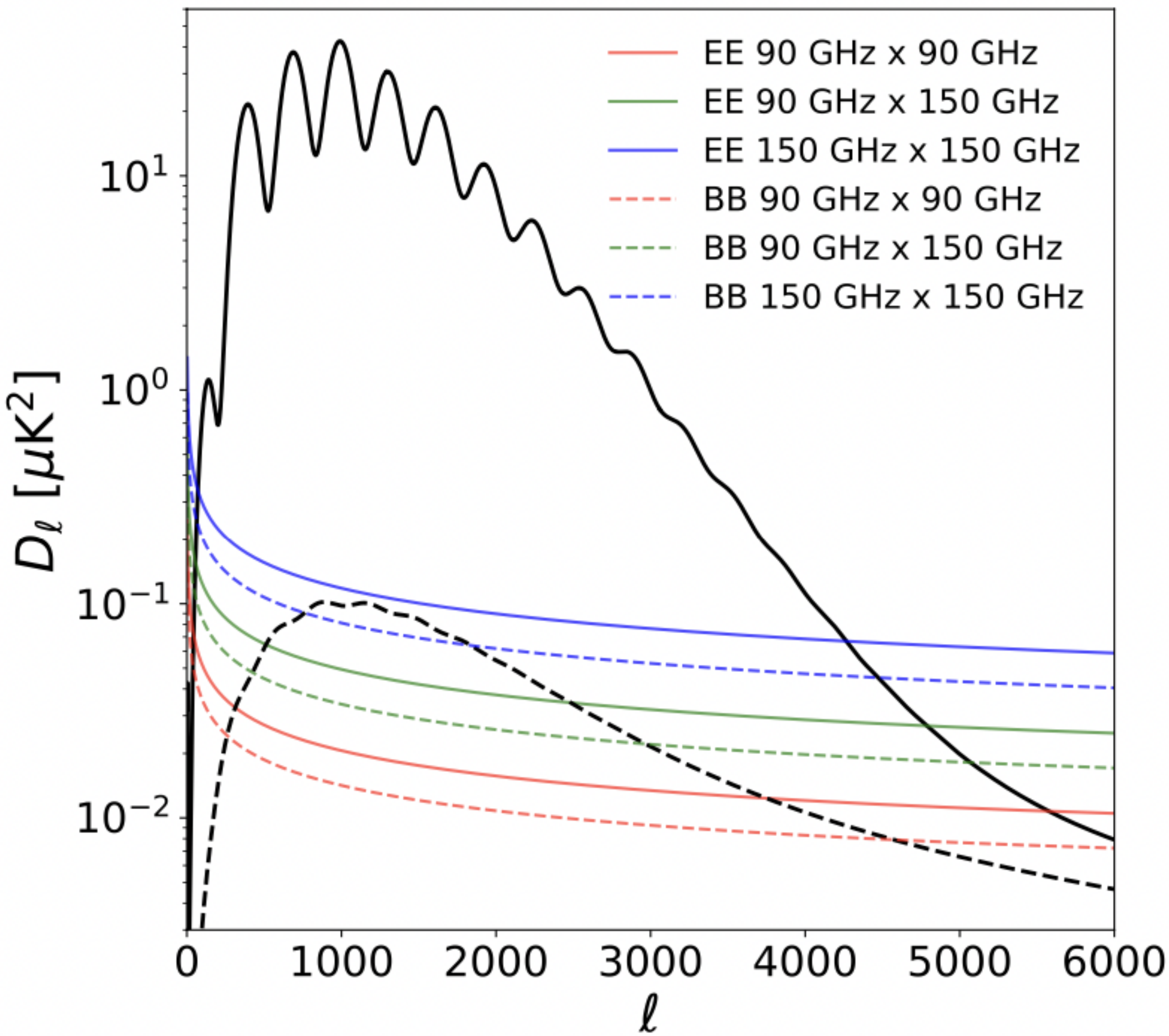

Independent constraints from ACT & WMAP

- Cosmological constraints from ACT DR6 and Planck are consistent (**1.6σ**)
- ACT + WMAP provides an independent and competitive dataset with e.g.

$\Omega_b h^2 = 0.02263 \pm 0.00012$
$H_0 = 66.78 \pm 0.68$ km/s/ Mpc

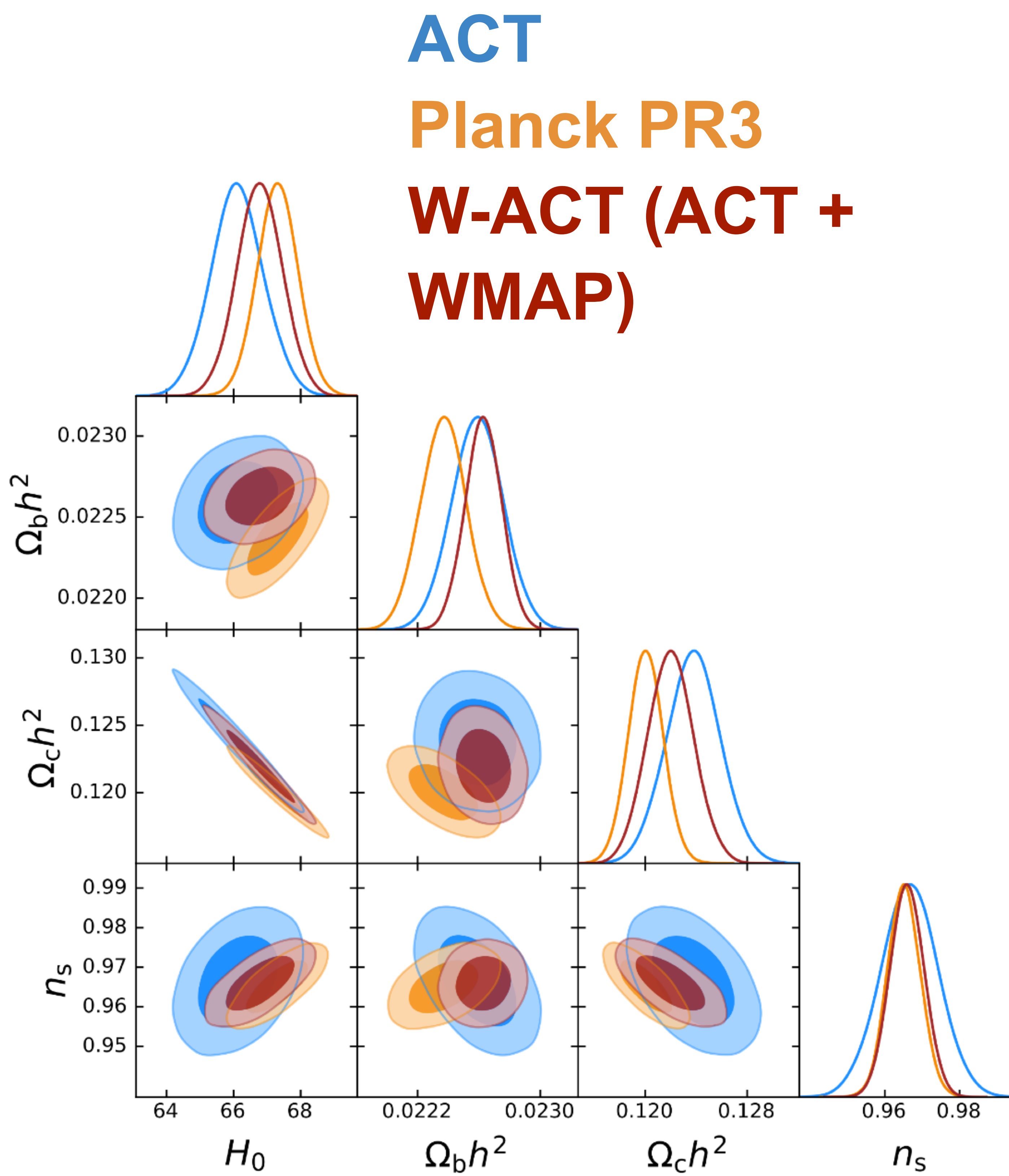

SPT post unblinding

https://arxiv.org/pdf/2411.06000 / SPT3G

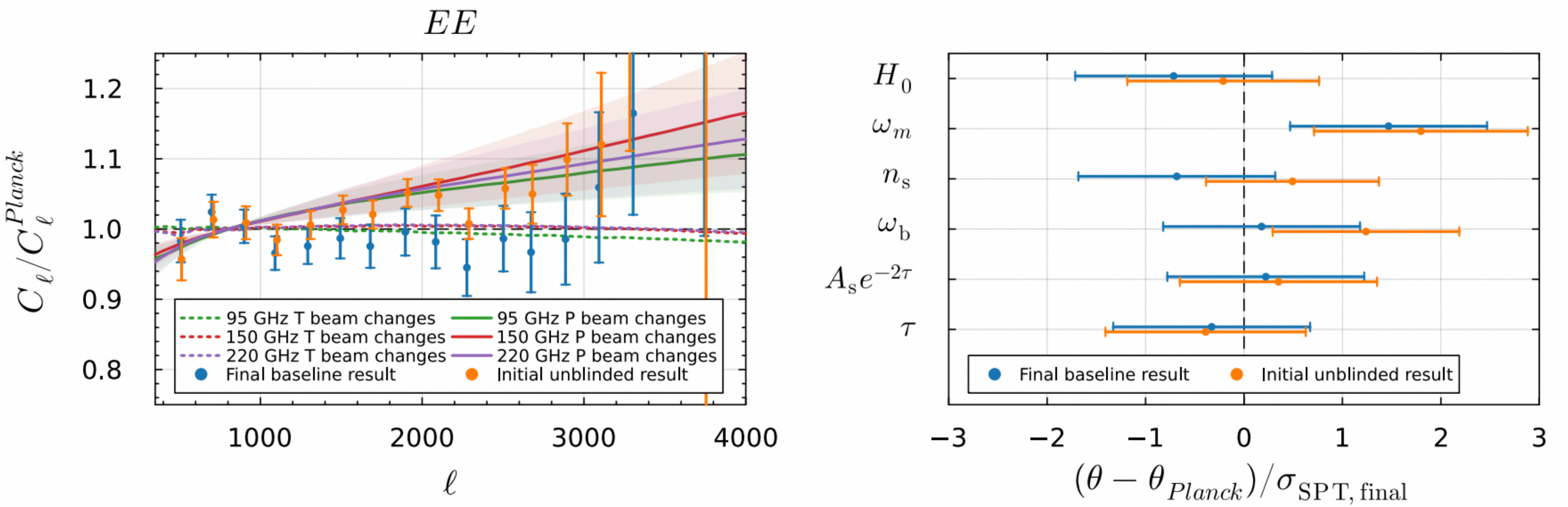

https://arxiv.org/pdf/2411.06000 / SPT3G

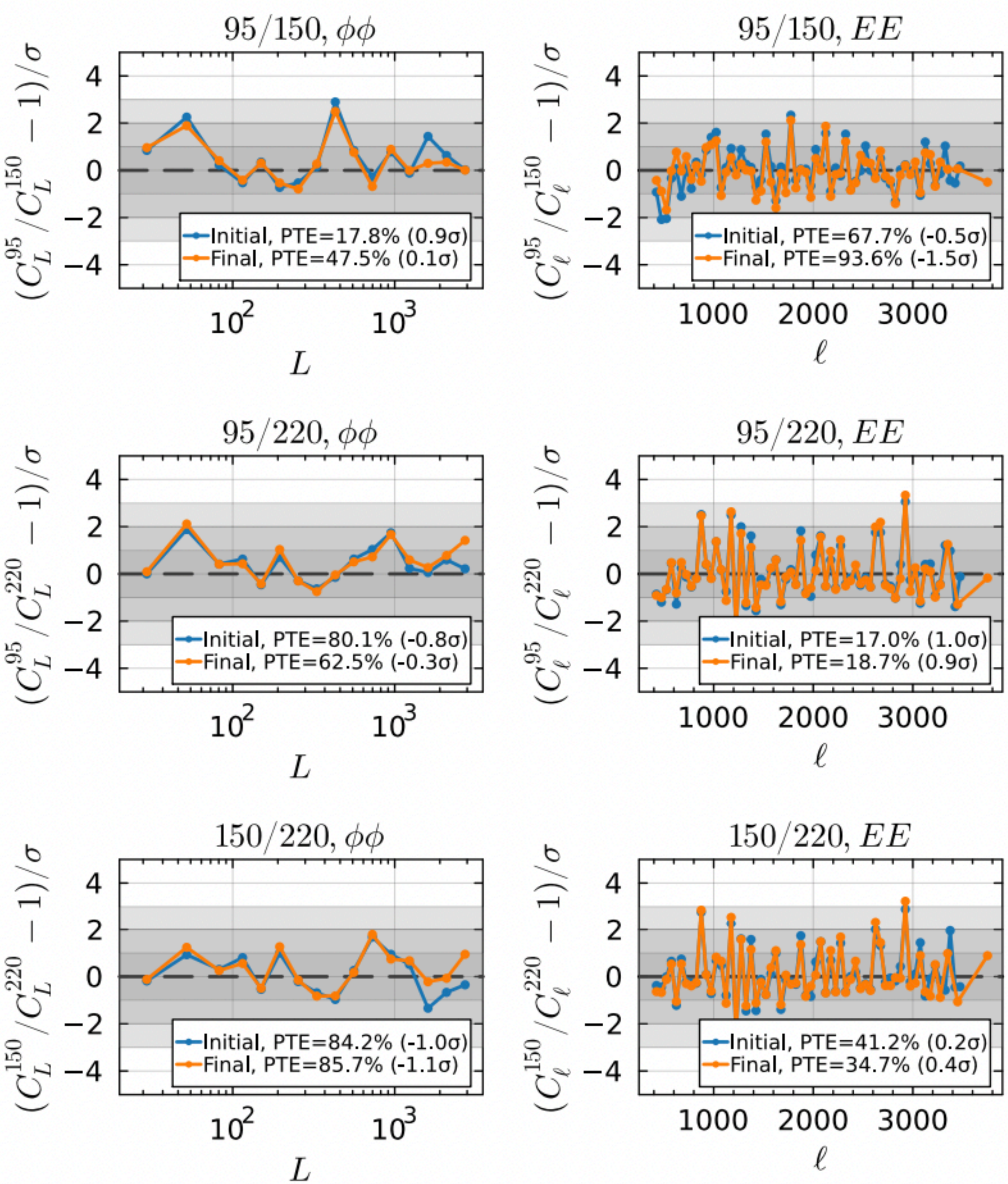

https://arxiv.org/pdf/2411.06000 / SPT3G

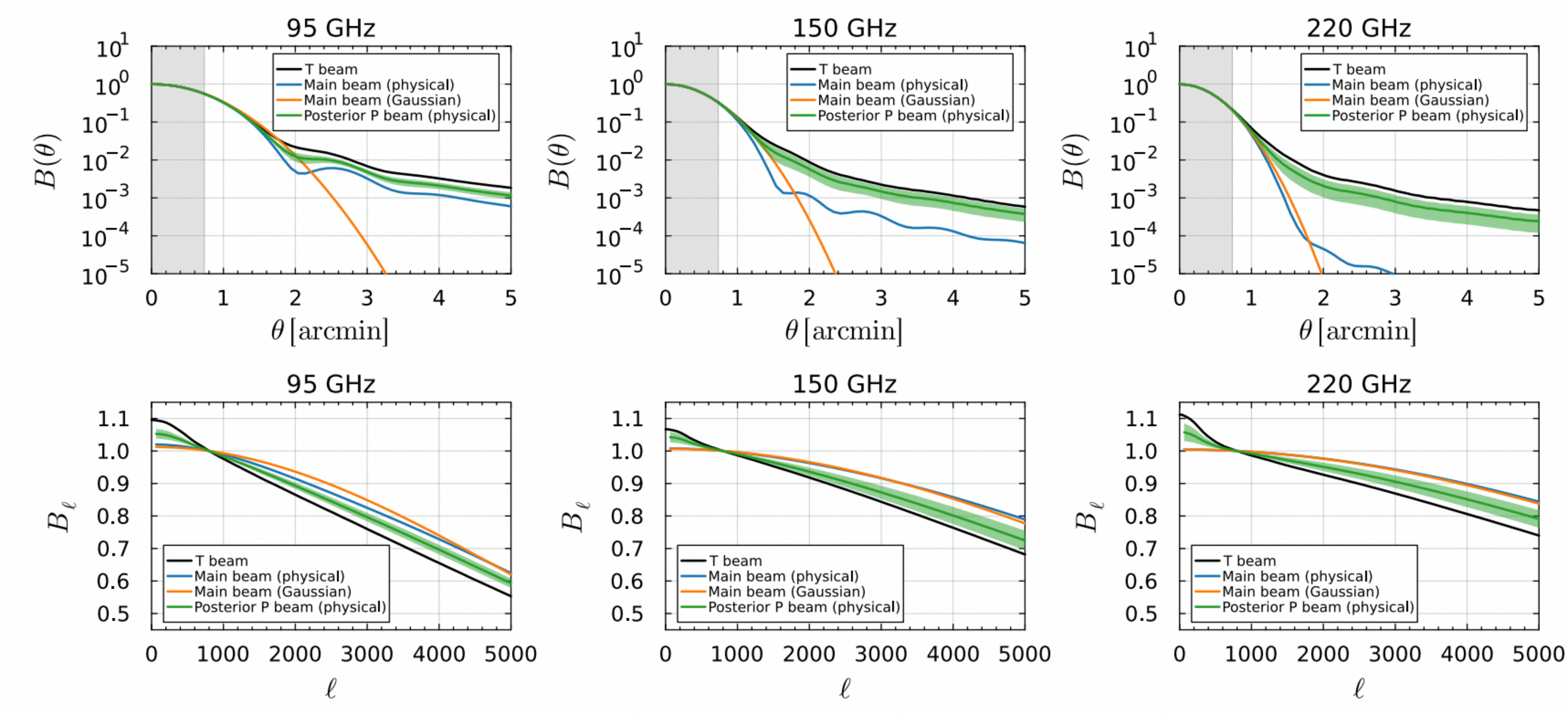

Posterior			
	95 GHz	150 GHz	220 GHz
$A^1_{\rm cal}$	0.8977±0.0074	0.9276±0.0074	0.8612±0.0084
$A^2_{\rm cal}$	0.8928±0.0072	0.9133±0.0071	0.864±0.0079
$A^3_{\rm cal}$	0.8861±0.0073	0.9399±0.0075	0.849±0.0083
$A^4_{\rm cal}$	0.8775±0.008	0.9272±0.0081	0.8405±0.0097
$100\,\epsilon^1_{\rm Q}$	0.291±0.025	0.319±0.021	0.492±0.059
$100\,\epsilon^2_{\rm Q}$	0.402±0.024	0.39±0.022	0.418±0.06
$100\,\epsilon^3_{\rm Q}$	0.555±0.025	0.838±0.021	2.096±0.066
$100\,\epsilon^4_{\rm Q}$	0.603±0.033	0.912±0.03	2.221±0.084
$100\,\epsilon^1_{\rm U}$	0.584±0.027	0.74±0.025	0.735±0.064
$100\,\epsilon^2_{\rm U}$	0.648±0.025	0.748±0.023	0.642±0.058
$100\,\epsilon^3_{\rm U}$	0.851±0.027	1.238±0.023	1.33±0.063
$100\,\epsilon^4_{\rm U}$	0.83±0.035	1.174±0.03	1.121±0.092
$\psi_{\rm pol}\,[^\circ]$	0.393±0.024	0.419±0.021	-0.188±0.079
$\beta_{\rm pol}$	0.44±0.20	0.60±0.28	0.51±0.26

Polar efficiencies

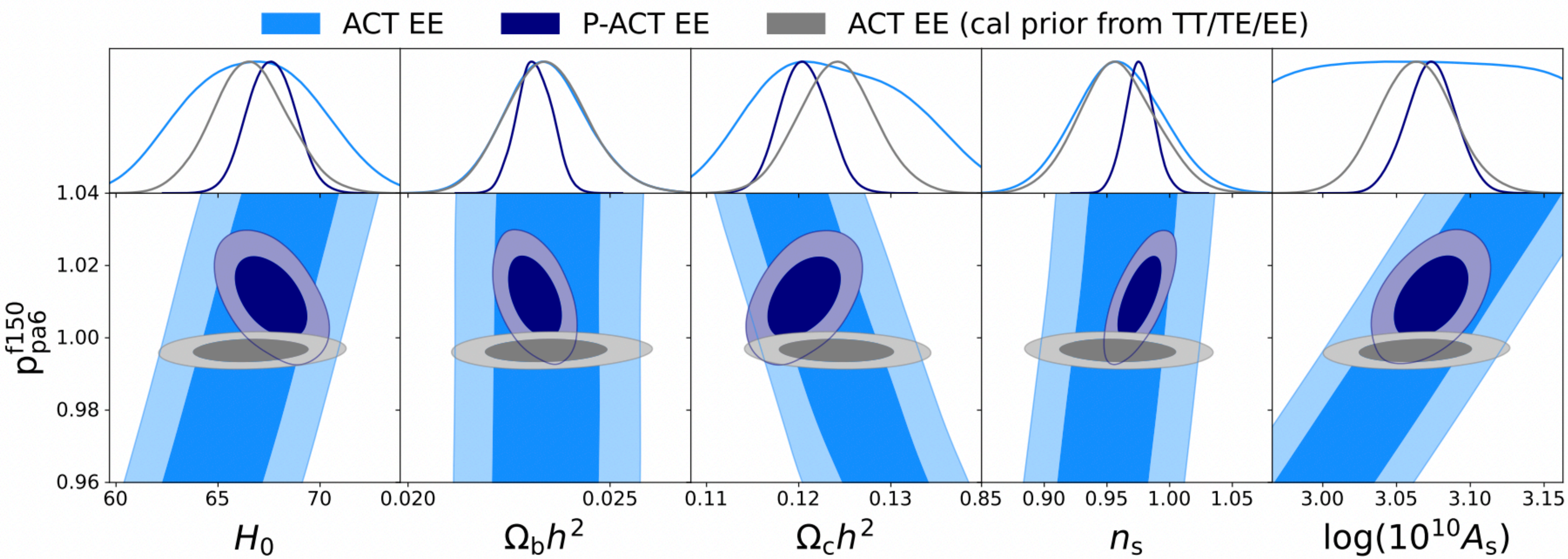

Figure 38. Marginalised posterior distributions of sampled parameters from EE, including the polarization efficiency for PA6 f150. We show constraints from ACT only (including the Sroll2 data to measure optical depth, light blue), P-ACT (dark blue) and ACT when using calibration and polarization efficiency priors from a full TT/TE/EE run (gray).

Telescopes

Telescope [edit]

The ACT is an off-axis Gregorian telescope. This off-axis configuration is beneficial to minimize artifacts in the point spread function. The telescope reflectors consist of a six-metre (236 in) primary mirror and a two-metre (79 in) secondary mirror. Both mirrors are composed of segments, consisting of 71 (primary) and 11 (secondary) aluminum panels. These panels follow the shape of an ellipsoid of revolution and are carefully aligned to form a joint surface.